

Aus dem Experimental and Clinical Research Center der Medizinischen
Fakultät Charité – Universitätsmedizin Berlin

DISSERTATION

Die kardiovaskuläre Magnetresonanztomographie in der
Diagnostik der Herzinsuffizienz mit erhaltener Ejektionsfraktion

zur Erlangung des akademischen Grades
Doctor medicinae (Dr. med.)

vorgelegt der Medizinischen Fakultät
Charité – Universitätsmedizin Berlin

von

Josephine Kermer
aus Leipzig

Datum der Promotion: 04.03.2022

Inhaltsverzeichnis

Abstrakt	4
Abstract	6
1. Einleitung.....	8
1.1. Herzinsuffizienz mit erhaltener Ejektionsfraktion und diastolische Dysfunktion.....	8
1.2. Die kardiovaskuläre Magnetresonanztomographie	9
1.3. Die kardiovaskuläre Magnetresonanztomographie in der Diagnostik der Herzinsuffizienz mit erhaltener Ejektionsfraktion.....	9
1.4. Zielstellung der Arbeit.....	11
2. Methodik	12
2.1. Vergleich verschiedener Techniken der kardiovaskulären Magnetresonanztomographie zur Beurteilung der diastolischen Funktion	12
2.1.1. Studiendesign und MRT-Scan-Protokoll	12
2.1.2. Bildanalyse.....	13
2.1.3. Statistik	15
2.2. Etablierung linksatrialer Normwerte.....	16
2.2.1. Studiendesign und MRT-Scan-Protokoll	16
2.2.2. Bildanalyse.....	16
2.2.3. Statistik	16
2.3. Vergleich unterschiedlicher Late Gadolinium Enhancement-Sequenzen	17
2.3.1. Studiendesign und MRT Scan-Protokoll	17
2.3.2. Bildanalyse.....	17
2.3.3. Statistik	18
3. Ergebnisse.....	18
3.1. Vergleich verschiedener Techniken der kardiovaskulären Magnetresonanztomographie zur Beurteilung der diastolischen Funktion.....	18
3.1.1. Vergleich linksventrikulärer und linksatrialer Dimensionen	18
3.1.2. Strainanalysen	22
3.1.3. Unterschiede intramyokardialer Geschwindigkeiten.....	22
3.1.4. Vergleich transmitraler Flussgeschwindigkeiten	22
3.2. Etablierung linksatrialer Normwerte.....	22
3.2.1. Vergleich der Parameter in Abhängigkeit von Feldstärke, Alter und Geschlecht	23
3.2.2. Unterschiede in Abhängigkeit der Phasendefinition	23
3.3. Vergleich unterschiedlicher Late Gadolinium Enhancement-Sequenzen	24
3.3.1. Unterschiede in der Aufnahmezeit	25

3.3.2. Vergleich der Bildqualität	25
3.3.3. Qualitative und quantitative LGE-Analyse.....	26
4. Diskussion	27
4.1. Linksatriale Dimensionen bei der Beurteilung der diastolischen Funktion.....	27
4.2. Transmitrale Fluss- und intramyokardiale Deformierungsparameter zur Beurteilung der diastolischen Funktion.....	28
4.3. Zeiteffiziente Gewebedifferenzierung	30
4.4. Zusammenfassung.....	32
5. Literaturverzeichnis	33
Eidesstattliche Versicherung	38
Anteilserklärung an den vorliegenden Publikationen	39
Publikationen	41
Lebenslauf	74
Publikationsliste	75
Danksagung	76

Abstrakt

Die Herzinsuffizienz ist eine der häufigsten Todesursachen in Deutschland. In mehr als 50% der Fälle liegt dabei eine Herzinsuffizienz mit erhaltener Pumpfunktion (HFpEF) vor. Innerhalb aktueller Leitlinien der Kardiologie gewinnt die kardiovaskuläre Magnetresonanztomographie (MRT) zunehmend an Bedeutung. In der Diagnostik der HFpEF spielt sie bisher jedoch eine untergeordnete Rolle. Grund dafür sind unter anderem lange Untersuchungszeiten, limitierende Untersuchungsbedingungen sowie fehlende, klinisch etablierte Parameter zur Beurteilung der diastolischen Funktion und entsprechende Referenzwerte.

Ziel dieser Arbeit ist es, Parameter der kardiovaskulären MRT zu identifizieren, welche am besten zur Evaluierung der diastolischen Funktion geeignet sind und darüber hinaus schnellere Methoden zu etablieren, welche insbesondere auch eine Untersuchung schwer kranker Patientinnen und Patienten ermöglichen.

Die diastolische Funktion von 50 Patientinnen und Patienten wurde anhand des echokardiographischen Verhältnisses aus E/E', des invasiv gemessenen, linksventrikulären enddiastolischen Drucks sowie des NT-proBNP- Serumspiegels (N-Terminal pro-brain Natriuretic Peptide) in normal, eingeschränkt und unklar eingeteilt. Anschließend wurden verschiedene MRT-Parameter zur Beurteilung linksventrikulärer Volumina, Funktion, Blutflussgeschwindigkeiten und intramyokardialer Deformierung hinsichtlich ihrer Übereinstimmung mit dieser Gruppeneinteilung analysiert (1).

Bei 203 gesunden Probandeninnen und Probanden wurden unter Anwendung zeiteffizienter Routineprotokolle linksatriale Volumina analysiert, um Normwerte zu generieren. Diese wurden bezüglich einer Abhängigkeit von Alter, Geschlecht und Feldstärke untersucht (2).

Darüber hinaus erfolgte der Vergleich zweier neuer, schneller Sequenzen zur Beurteilung myokardialer Fibrose mit einer Standardreferenzsequenz. Dafür wurden 312 Patientinnen und Patienten mit ischämischen und nicht-ischämischen Kardiomyopathien untersucht (3).

Verminderte basolaterale Deformierungseigenschaften sowie eine linksatriale Dilatation stellten die besten Diskriminierungsparameter zwischen Patientinnen bzw. Patienten mit normaler und eingeschränkter diastolischer Funktion dar (1).

Linksatriale Normwerte konnten bestimmt und eine altersabhängige Abnahme dieser Werte gezeigt werden. Geschlechtsabhängige Unterschiede waren nach Normierung auf Körperoberfläche oder Körperhöhe nicht mehr nachweisbar. Eine Abhängigkeit von der Feldstärke bestand nicht (2).

Verglichen mit der Standardreferenzsequenz benötigten neue *multi-slice* Sequenzen signifikant weniger Zeit zur Datenaufnahme und zeigten äquivalente Ergebnisse in der Beurteilung myokardialen Narbengewebes. Zudem konnte selbst unter Arrhythmien und verminderter Atemhaltekapazität eine ausgezeichnete Bildqualität verzeichnet werden (3).

Zusammenfassend können die Möglichkeit der Beurteilung der diastolischen Funktion und zeiteffizientere, Rhythmus- und Atemmuster-unabhängige Untersuchungsmethoden helfen, die kardiovaskuläre MRT als diagnostisches Mittel der HFpEF voranzubringen.

Abstract

Heart failure is one of the leading causes of death in Germany, while heart failure with preserved ejection fraction (HFpEF) is prevalent in more than 50% of affected patients. According to current cardiological guidelines cardiovascular magnetic resonance imaging (CMR) has become increasingly important. However, concerning the diagnosis of HFpEF CMR represents merely an adjunct. Long acquisition time, limiting examination conditions, a lack of valid clinical parameters to assess diastolic function and corresponding reference values are some of the reasons.

Aim of this work is to identify the best CMR-parameters to evaluate diastolic function and furthermore to establish less time-consuming methods to especially be able to perform investigations in severely ill patients.

Based on echocardiographic generated E/E', invasively measured left ventricular end-diastolic pressure and serum level of N-terminal pro brain natriuretic peptide, diastolic function of a 50 patients' cohort was graded in normal, impaired and uncertain. Different CMR-parameters for assessment of left ventricular volumes, function, blood flow velocities and intramyocardial deformation were quantified (1).

203 healthy volunteers were investigated to generate normal values of left atrial volumes using time efficient routine CMR-protocols. Dependence of sex, age and field strength was analysed (2). Furthermore, we compared the standard sequence for assessment of myocardial fibrosis with two new faster sequences. Therefor 312 patients with ischaemic and non-ischaemic cardiomyopathies were examined (3).

Reduced basolateral deformation and left atrial dilatation showed best discrimination between patients with and without diastolic dysfunction (1).

Left atrial reference values decreased with age. Sex-dependent differences disappeared after normalisation to body height or body surface area. Field strength did not show any influence (2).

In comparison new multi-slice sequences showed equivalent results in assessment of myocardial scarring to the reference sequence while data acquisition was significantly less time-consuming. Even in cases with arrhythmia or limited breathhold conditions, multi-slice sequences reached excellent image quality (2).

In conclusion, the possibility to assess diastolic function as well as using time-efficient, rhythm- and breathhold-independent examination methods might help to integrate CMR as a diagnostic feature of HFrEF.

1. Einleitung

1.1. Herzinsuffizienz mit erhaltener Ejektionsfraktion und diastolische Dysfunktion

Das Syndrom der Herzinsuffizienz ist eine der häufigsten Todesursachen in Deutschland (4). In mehr als 50% der Fälle liegt dabei eine Herzinsuffizienz mit erhaltener Pumpfunktion (*heart failure with preserved ejection fraction - HFpEF*) vor (5). Seit 2007 ist diese durch das Auftreten von Zeichen und/oder Symptomen der Herzinsuffizienz, einer linksventrikulären Ejektionsfraktion (LVEF) $\geq 50\%$, erhöhter Serumspiegel der natriuretischen Peptide BNP bzw. NT-proBNP (Brain Natriuretic Peptide/ N-terminales pro-BNP) sowie das Vorhandensein einer strukturellen Herzerkrankung oder diastolischen Dysfunktion definiert (6). Insbesondere aufgrund einer großen Zahl nach diesem Schema nicht ausreichend klassifizierbarer Patientinnen und Patienten, erschien 2019 ein aktualisiertes Konsensuspapier der *European Society of Cardiology* (7). Im Rahmen dessen wird ein schrittweises Herangehen zum Nachweis bzw. Ausschluss einer HFpEF empfohlen. Nach initialer „Routinediagnostik“ hilft ein Score-System basierend auf echokardiographischen Parametern und (NT-pro)BNP-Leveln bei der Diagnosestellung einer HFpEF. Im Falle fortbestehend uneindeutiger Befunde wird eine nicht-invasive bzw. invasive Stresstestung empfohlen. Abschließend wird die Abklärung der zugrundeliegenden Ätiologie - vor allem auch zur Einleitung gezielterer Therapieansätze - mehr in den Vordergrund gerückt.

Der diastolischen Dysfunktion liegen eine verminderte Relaxationsfähigkeit und eingeschränkte Compliance des linken Ventrikels (LV) zu Grunde. Die dadurch bedingte, verzögerte Mitralklappenöffnung und erhöhten enddiastolischen Druckbedingungen verursachen eine verminderte Füllung des LV. Um dennoch eine adäquate Ventrikelfüllung zu gewährleisten, steigt der linksatriale Druck und in diesem Zuge die Wandspannung des linken Vorhofs (LA), was wiederum zu einer Dehnung und Dilatation des LA-Myokards führt (8-10).

Goldstandard in der Diagnostik der diastolischen Dysfunktion stellen invasiv gemessene Druckvolumenkurven dar. Mittels Herzkatheter lässt sich zudem der LV enddiastolische Druck (LVEDP) ermitteln. Werte über 16mmHg weisen auf eine diastolische Dysfunktion hin (7, 11). In der klinischen Routine ist die Echokardiographie das wichtigste bildgebende diagnostische Verfahren. Es existieren zahlreiche echokardiographische Parameter zur Beurteilung der diastolischen Funktion. Insbesondere das Verhältnis der

frühdiastolischen Peaks aus transmitralem Fluss und Gewebedoppler E/E' gibt Anhalt für das Vorliegen einer diastolischen Funktionsstörung (12).

Das Spektrum der Pathogenese einer HFpEF ist breit. Die Ursache der HFpEF ist multifaktoriell und wird von verschiedenen Faktoren beeinflusst. Verglichen mit der Herzinsuffizienz mit reduzierter Pumpfunktion (HFrEF) sind Betroffene älter, eher weiblich und weisen in der Vorgeschichte häufiger eine arterielle Hypertonie, Vorhofflimmern oder einen Diabetes mellitus auf. Eine ischämische Genese tritt hingegen seltener auf. Die Mortalität von Patientinnen und Patienten mit HFpEF ist nur wenig geringer bis vergleichbar zu der von Patientinnen und Patienten mit reduzierter EF. Während die Sterblichkeit bei Erkrankten mit HFrEF über die letzten Jahrzehnte reduziert werden konnte, ist dies bei Patientinnen und Patienten mit HFpEF nicht der Fall (13, 14). Ein nicht zu vernachlässigender Aspekt dafür ist die häufige Fehldiagnose und Unterschätzung der Krankheit (7). Zudem konnte bisher keine der „gängigen“ Herzinsuffizienz-Behandlungen eine Verbesserung von Morbidität und Mortalität bei Betroffenen mit HFpEF zeigen, sodass Empfehlungen aktueller Guidelines lediglich auf symptom-kontrollierende Therapieansätze begrenzt sind (6).

1.2. Die kardiovaskuläre Magnetresonanztomographie

Die kardiovaskuläre Magnetresonanztomographie (MRT) ist eine nicht-invasive, auf nicht-ionisierender Strahlung basierende Bildgebung, welche es ermöglicht, Aufnahmen in jedweder topographischen Ebene durch den Körper zu erstellen (15). Sie gilt als Goldstandard in der Messung links- und rechtsventrikulärer Dimensionen und Funktion und stellt die bildgebende Methode der Wahl zur Darstellung myokardialer Fibrose dar (6, 16, 17). Mittels *Late Gadolinium Enhancement* (LGE) als Bestandteil eines multifaktoriellen Untersuchungsansatzes bietet sie die Möglichkeit der Differenzierung zwischen nicht-ischämischer und ischämischer Fibrosierung (6).

1.3. Die kardiovaskuläre Magnetresonanztomographie in der Diagnostik der Herzinsuffizienz mit erhaltener Ejektionsfraktion

Die kardiovaskuläre MRT spielt bereits eine tragende Rolle bei der Klärung der Pathogenese einer Herzinsuffizienz. Die LGE-Ausprägung trägt dabei dazu bei, zwischen einer ischämischen, entzündlichen, hypertrophen oder systemerkrankungsbedingten Kardiomyopathie zu unterscheiden (6, 18). Die standardmäßig angewandten, *phase-sensitiv inversion recovery* (PSIR)-basierten Sequenzen zur LGE-Beurteilung werden

typischer Weise in Form einer Schichtaufnahme pro Atemanhalte (*single-slice, single-breathhold*) generiert (19). Im Falle insuffizienter Atemanhalte oder Arrhythmien kann es zu relevanten Einschränkungen der Bildqualität mit unzureichender diagnostischer Aussagekraft kommen (20). Darüber hinaus sind bis zu 10 Minuten nötig, um das gesamte Herz abzubilden. Patientinnen und Patienten mit HFpEF leiden häufig an Dyspnoe, sodass die erforderlichen Atemkommandos nicht umgesetzt werden können und die zur Verfügung stehende Untersuchungszeit in flacher Rückenlage begrenzt ist. Mithilfe neuer *multi-slice* LGE-Sequenzen können die Scanzeit verkürzt und Aufnahmen in freier Atmung erzeugt werden. Bisher wurden diese Sequenzen überwiegend in kleinen Studien, welche sich auf ein Krankheitsbild fokussierten und Patientinnen und Patienten mit Arrhythmien ausschlossen, untersucht (21, 22).

Ein Teil der vorliegenden, kumulativen Doktorarbeit umfasst die Validierung neuer schneller *multi-slice* LGE-Sequenzen.

Die Beurteilung der diastolischen Funktion ist bisher kein Bestandteil der in der klinischen Routine durchgeführten, kardiovaskulären MRT. Es existieren verschiedene Forschungsansätze zur Evaluierung der diastolischen Funktion: Mittels Phasenkontrast (PC)-Messungen ist es möglich, transmitrale Flussmessungen durchzuführen. Ähnlich der Doppler-Echokardiographie können so früh- und spätdiastolische Spitzengeschwindigkeiten ermittelt werden (23). *Tissue Phase Mapping* (TPM) bietet die Möglichkeit, intramyokardiale Geschwindigkeiten zu untersuchen (24). *Tagging* dient der Analyse myokardialer Deformation. Dem Myokard wird durch bestimmte Impulse ein intrinsisches Gitter aufgeprägt, dessen Verformung während des Herzzyklus gemessen und im Rahmen von Strain- bzw. Strain Rate (SR)-Untersuchungen quantifiziert werden kann (25). Strainanalysen können seit kurzem auch anhand gängiger *cine*-Aufnahmen durchgeführt werden. Die dafür nötige post-processing Methode des *Tissue Trackings* basiert auf Voxel-bezogener Quantifizierung myokardialer Deformation (26).

Die Anwendbarkeit dieser Techniken zur Beurteilung der diastolischen Funktion bei Gesunden (24, 27) und Erkrankten (28-34) wurde in mehreren Studien belegt. Falls vorhanden, erfolgte der Vergleich der Daten in der Regel mit echokardiographischen Messungen oder zwischen verschiedenen Verfahren der kardiovaskulären MRT.

Ein weiterer Teil dieser Dissertation befasst sich mit der Untersuchung, welche der beschriebenen MRT-Methoden am besten zur Beurteilung der diastolischen Funktion dienen. Dabei wird sowohl auf bereits veröffentlichte Parameter zurückgegriffen als auch

neue Variablen eingeführt. Deren Aussagekraft wird dann anhand eines vorab publizierten Standards aus echokardiographischer, laborchemischer und invasiver Diagnostik gemessen.

Dass es durch erhöhte LV-Druckverhältnisse im Rahmen einer diastolischen Dysfunktion zur Vergrößerung des LA kommen kann, ist bekannt. In den echokardiographischen Empfehlungen gehört eine LA-Dilatation bereits zu den Diagnosekriterien einer diastolischen Dysfunktion (7, 11, 12). Normwerte zur Quantifizierung linksatrialer Dimensionen mittels kardiovaskulärer MRT wurden in mehreren Studien publiziert (35-37). Teilweise basieren die Messungen auf mehrschichtigen, den gesamten LA abfassenden Aufnahmen, welche zusätzlich zum Routine-Protokoll generiert werden müssten und so die Scanzeit verlängern.

Die Etablierung alters- und geschlechtsbezogener linksatrialer Normwerte basierend auf Routineaufnahmen der kardiovaskulären MRT ist ein weiterer Teil der vorliegenden Dissertation.

1.4. Zielstellung der Arbeit

Ziel dieser kumulativen Doktorarbeit ist es, die Einsatzfähigkeit der kardiovaskulären MRT in der Diagnostik der HFpEF voranzubringen. Der Fokus liegt dabei darauf, diejenigen Parameter zu identifizieren, welche am besten zwischen einer normalen und eingeschränkten diastolischen Funktion diskriminieren können.

2. Methodik

Im Mittelpunkt dieser Arbeit stand die Evaluierung unterschiedlicher Parameter der kardiovaskulären MRT hinsichtlich ihrer Eignung zur Beurteilung der diastolischen Funktion. Darüber hinaus wurden bereits etablierte Methoden, welche bezüglich ihrer Anwendung auf symptomatische Patientinnen und Patienten optimiert wurden, validiert.

2.1. Vergleich verschiedener Techniken der kardiovaskulären Magnetresonanztomographie zur Beurteilung der diastolischen Funktion

2.1.1. Studiendesign und MRT-Scan-Protokoll

Patientinnen und Patienten mit Indikation zur Durchführung einer Koronarangiographie und erhaltener systolischer Pumpfunktion ($LVEF>50\%$) wurden prospektiv eingeschlossen. Die Ausschlusskriterien sind in Abbildung 1 aufgeführt. Anhand des echokardiographisch ermittelten Verhältnisses aus E/E' , des invasiv gemessenen LVEDP und dem laborchemisch bestimmten NT-proBNP erfolgte gemäß den Empfehlungen von Paulus et al.(11) eine Einteilung in Patientinnen bzw. Patienten mit (DD+), ohne (DD-) oder fraglicher (DD±) diastolischer Dysfunktion (Abbildung 1) (1).

Bei allen Probandinnen und Probanden wurde eine kardiale Magnetresonanztomographie an einem 1,5T-Scanner (Avanto, Siemens Healthineers, Erlangen) durchgeführt. Zur Berechnung linksventrikulärer und linksatrialer Dimensionen wurden diese in drei langen Achsen (LAX) und je einem Kurzachsenpaket als standard *cine steady-state free precession* (SSFP) Aufnahmen dargestellt. Zur SR-Messung mittels *Tissue Tracking* und *Tagging* wurden je eine LAX im 4-Kammer-Blick sowie drei kurze Achsen (SAX) (basal, mittventrikulär und apikal) generiert. Zum Einsatz kamen dafür zeitlich hoch-auflösende *cine SSFP-* bzw. *SSFP spacial modulation of magnetisation* (SPAMM) und *complementary SPAMM Tagging*-Sequenzen. Aufnahmen einer *black blood prepared gradient echo* TPM-Sequenz dienten der Bestimmung intramyokardialer Geschwindigkeiten in drei SAX (basal, mittventrikulär und apikal). Auf Höhe der Mitralklappenspitzen während der Enddiastole und senkrecht zum transmitralen Einfluss wurden basale Phasenkontrast SAX-Aufnahmen erstellt, welche der Analyse transmitraler Flussgeschwindigkeiten dienten (1).

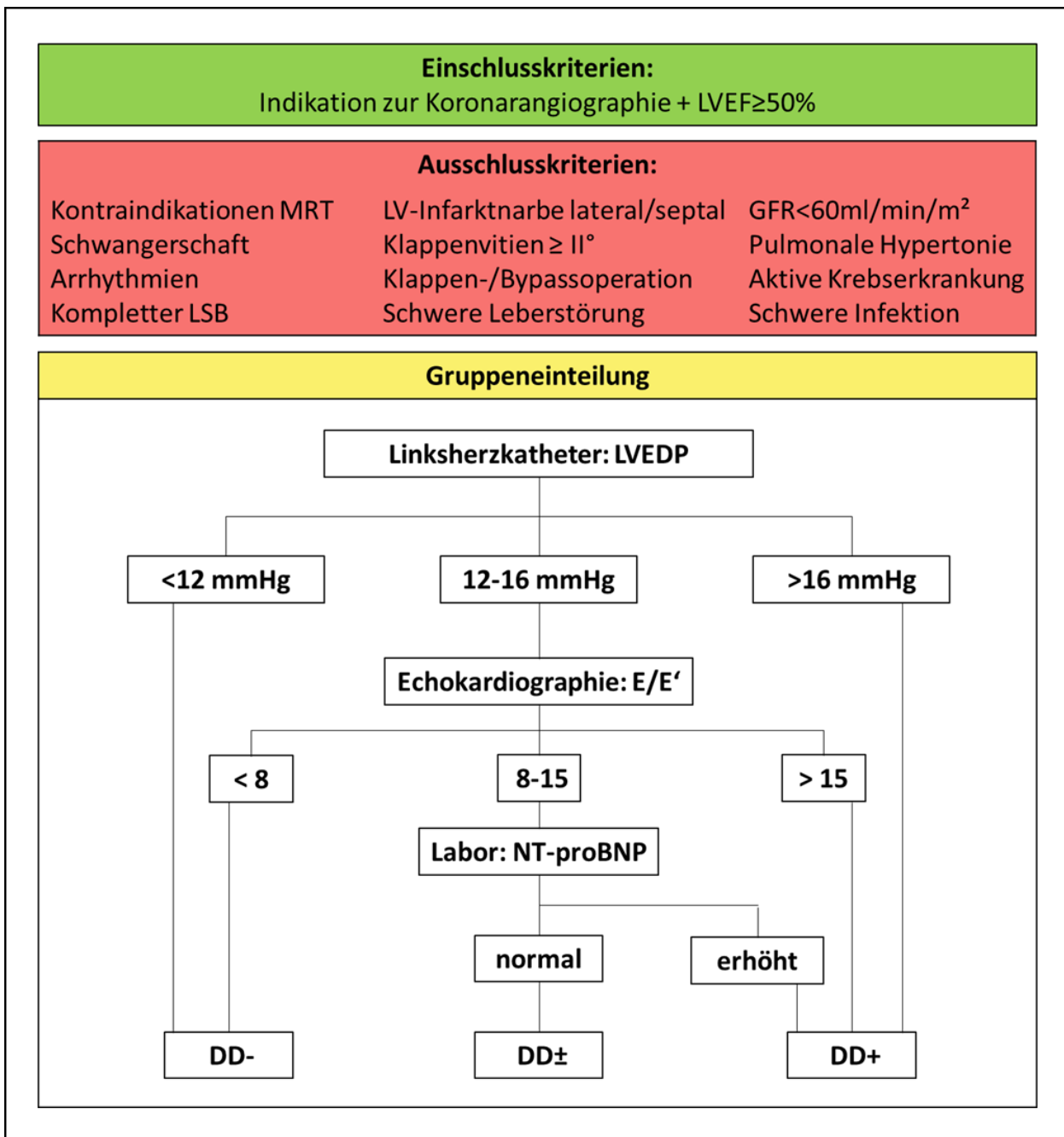


Abbildung 1 modifiziert nach Kermer et al. (1) (Lizenznummer: 5024240029746): Ein-/Ausschlusskriterien und Definition der Gruppeneinteilung in Patientinnen und Patienten mit (DD+), fraglicher (DD±) und ohne (DD-) diastolische Dysfunktion. Verwendete Abkürzungen: LVEF - linksventrikuläre Ejektionsfraktion, MRT - Magnetresonanztomographie, LSB - Linksschenkelblock, GFR - glomeruläre Filtrationsrate

2.1.2. Bildanalyse

Zur Quantifizierung der LV- und LA-Parameter wurde cvi42 Version 4.1.3 (Circle Cardiovascular Imaging Inc., Calgary, Kanada) verwendet. Enddiastolische und endsystolische endo- und epikardiale Konturen wurden manuell bestimmt. Die Zyklusphasen wurden dabei separat für LV und LA entsprechend der maximalen bzw.

minimalen Ausdehnung der jeweiligen Herzhöhle definiert. Masse und/oder Volumina wurden anhand der jeweiligen SAX-Pakete ermittelt. Die LAX-Aufnahmen dienten der Bestimmung maximaler LA-Diameter und -Flächen (1).

SR-Messungen via *Tissue Tracking* wurden mit dem cvi42 Prototyp 5.3.0 (Circle Cardiovascular Imaging Inc.) durchgeführt. Nach manueller Definition der enddiastolischen endo- und epikardialen Konturen erfolgte eine automatische Verformungsanalyse mit Bestimmung SAX-basierter radialer (Err) und circumferentieller (Ecc) sowie LAX-basierter longitudinaler (Ell) SR-Kurven. Die Definition der diastolischen Peaks ist in Abbildung 2 dargestellt (1).

Die *Tagging*-Aufnahmen wurden mittels CIM Tag2D Heart Deformation WIP20 (Heart Deformation post-processing prototyp 2.0, Auckland MRI Research Group, Auckland, Neuseeland) analysiert. Nach Konturierung von Endo- und Epikard erfolgte eine semi-automatische Markierung der Tag-Linien. SAX-basierte Ecc- sowie LAX-basierte Ell-SR-Kurven wurden berechnet. Als diastolischer SR-Peak wurde der erste Peak nach der Endsystole definiert (1).

TPM-Analysen wurden unter Anwendung der post-processing Software MATLAB (The Mathworks, Inc., Natick, MA, USA) durchgeführt. Zuerst wurden endo- und epikardiale Konturen für jede Schicht und in jeder Phase definiert. Anschließend erfolgte die Messung intramyokardialer Geschwindigkeiten, welche in Geschwindigkeit-Zeit-Diagrammen dargestellt wurden. Radiale (Vr) und longitudinale (Vz) diastolische Geschwindigkeitspeaks wurden daraus generiert (1).

Die Analysen von SR und intramyokardialen Geschwindigkeiten wurden sowohl auf Schicht- als auch auf Segmentebene durchgeführt. Die segmentbasierte Auswertung erfolgte bei *Tissue Tracking* und TPM anhand des 16-Segment-Modells gemäß der *American Heart Association* (AHA) (38). Für die Segmentanalyse der *Tagging*-Daten wurde Software-bedingt jede Schicht in 6 Segmente geteilt (1).

Zur Beurteilung des transmitralen Flusses wurde cvi42 Version 4.1.3 (Circle Cardiovascular Imaging Inc., Calgary, Kanada) verwendet. In der Schicht, in welcher die Mitralklappenöffnung visuell am besten zur Darstellung kam, wurden den transmitralen Blutfluss begrenzende *Regions Of Interest* (ROI) markiert und auf jede Phase übertragen. Darauf basierend wurden Flussgeschwindigkeit-Zeit-Kurven generiert, in welchen früh- (E) und spätdiastolische (A), maximale Flussgeschwindigkeiten abgelesen werden konnten (1).

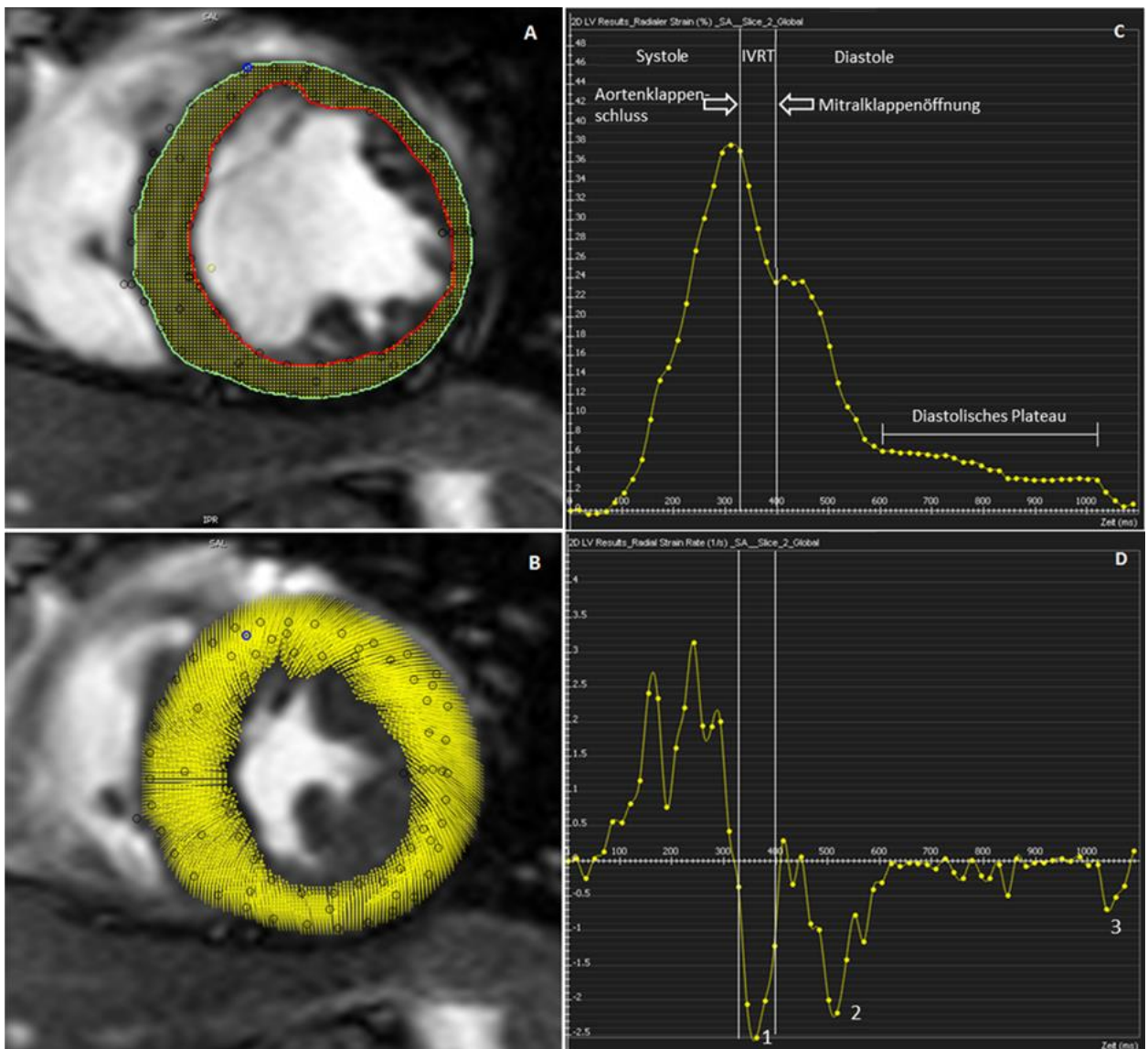


Abbildung 2 modifiziert nach Kermer et al. (1) (Lizenznummer: 5024240029746): Auswertung Tissue Tracking: A+B) mediale Kurze Achse mit A) Enddiastolischer Konturierung und Tissue Tracking; B) Endsystolischer Verformung; C+D) Kurven für globalen radialen Strain (C) und Strain Rate (D) für einen Herzzyklus. Die Phasen des Herzzyklus wurden wie folgt definiert: Endstole = Phase des Aortenklappenschluss; Isovolumetrische Relaxationszeit (IVRT) = Zeit zwischen Endstole und Mitralklappenöffnung; Enddiastole = Phase des Mitralklappenschluss. Die diastolischen Strain Rate Peaks wurden definiert als 1) preE = Peak innerhalb der IVRT; 2) E = Peak zwischen Mitralklappenöffnung und Beginn des diastolischen Plateaus; 3) A = Peak zwischen dem Ende des diastolischen Plateaus und der Endstole.

2.1.3. Statistik

Die statistische Auswertung beschränkte sich auf die Untersuchung der eindeutig zuzuordnenden Patientinnen bzw. Patienten mit oder ohne diastolische Dysfunktion. Zum Vergleich der Gruppen wurden Mittelwert und Standardabweichungen (SD) der

erhobenen Parameter berechnet. Unterschiede mit einem p-Wert <0,05 wurden als signifikant definiert. *Receiver Operating Characteristic* (ROC-) Kurven wurden erstellt, um Cut-off-Werte zu bestimmen (1). Für die statistischen Berechnungen wurde IBM SPSS Statistics Version 25 (IBM Corp., Armonk, NY, USA) genutzt.

2.2. Etablierung linksatrialer Normwerte

2.2.1. Studiendesign und MRT-Scan-Protokoll

Analysiert wurden MRT-Aufnahmen von 203 gesunden Probandinnen und Probanden, welche im Rahmen zweier zuvor abgeschlossener Studien prospektiv eingeschlossen worden waren. Aufnahmen mit inkompletter Darstellung des LA oder eingeschränkter Auswertbarkeit aufgrund von Überlagerungseffekten oder Artefakten wurden ausgeschlossen (2).

111 MRT-Untersuchungen wurden an einem 3T-Gerät (Magnetom Verio, Siemens Healthcare, Erlangen) durchgeführt, 92 weitere erfolgten mit 1,5T (Magnetom Avanto, Siemens Healthcare, Erlangen). Routinemäßige SSFP *cine*-Aufnahmen im 2- und 4-Kammerblick wurden generiert (2).

2.2.2. Bildanalyse

Zur Bildanalyse wurde cvi42 Version 5.1 (Circle Cardiovascular Imaging Inc., Calgary, Kanada) genutzt. Die Konturen des LA wurden manuell im 2- und 4-Kammerblick definiert. Dies erfolgte in LA-Enddiastole und -Endsystole. Die Phasen wurden zum einen - wie in der klinischen Routine gängig praktiziert - über die Endsystole und Enddiastole des LV definiert (LA-Diastole 1 bzw. LA-Systole 1), zum anderen anhand der tatsächlichen maximalen und minimalen LA-Ausdehnung (LA-Diastole 2 bzw. LA-Systole 2) bestimmt. Aus den biplanen Flächen konnten das enddiastolische Volumen (EDV), endsystolische Volumen (ESV), Schlagvolumen (SV) und die Ejektionsfraktion (EF) des LA, sowie deren Verhältnis zu Körperoberfläche (BSA) und Körperhöhe (H) berechnet werden (2).

2.2.3. Statistik

Mittelwert und Standardabweichung der LA-Volumina wurden kalkuliert und in Abhängigkeit von Geschlecht, Alter, Altersgruppe (Gruppe 1: 20-39 Jahre, Gruppe 2: 40-

59 Jahre, Gruppe 3: \geq 60 Jahre) und Feldstärke verglichen. Darüber hinaus wurde untersucht, ob die Definition der Zyklusphase (LA-Systole 1 vs. LA-Systole 2 bzw. LA-Diastole 1 vs. LA-Diastole 2) relevante Auswirkungen auf die Bestimmung der LA-Volumina hat (2). Für die statistische Auswertung wurde IBM SPSS Statistics Version 23 (IBM Corp., Armonk, NY, USA) verwendet.

2.3. Vergleich unterschiedlicher Late Gadolinium Enhancement-Sequenzen

2.3.1. Studiendesign und MRT Scan-Protokoll

Patientinnen und Patienten mit klinischer Indikation zur Durchführung einer kardialen MRT inklusive LGE-Darstellung wurden prospektiv eingeschlossen. Ausschlusskriterium stellte eine glomeruläre Filtrationsrate $<30\text{ml}/\text{min}/1,73\text{m}^2$ dar. Alle MRT-Untersuchungen erfolgten an einem 1,5T-Scanner (AvantoFit, Siemens Healthineers, Erlangen) und unter Anwendung körperegewichts-adaptierter Kontrastmittelgabe (Gadoteridol bzw. Gadopentetate 0,2mmol/kg i.v.). Zweidimensionale (2D) LGE-Aufnahmen wurden als den gesamten LV abdeckendes SAX-Packet erstellt. Dafür kamen 3 unterschiedliche LGE-Sequenzen zum Einsatz:

- I) eine segmentierte, *single-slice, single-breathhold 2D fast low angle shot* (FLASH) basierte PSIR (FLASH-PSIR) (Referenzstandard)
- II) eine *multi-slice 2D balanced SSFP* basierte *inversion recovery* Sequenz (bSSFP-IR)
- III) eine *multi-slice 2D bSSFP*-basierte PSIR Sequenz (bSSFP-PSIR)

Während alle Sequenzen in end-exspiratorischer Atemhalte aufgenommen wurden, erfolgten zusätzliche bSSFP-PSIR-Aufnahmen in freier Atmung. Die Reihenfolge der Sequenz-Aufnahmen war zufällig (3).

2.3.2 Bildanalyse

Für die Bildanalyse wurde cvi42 Version 5.6.2 (Circle Cardiovascular Imaging Inc., Calgary, Kanada) verwendet. Die Auswertung der LGE-Aufnahmen erfolgte verblindet und in zufälliger Reihenfolge. Für 30 Fälle wurde eine Intra- und Interobserver-Untersuchung durchgeführt.(3)

Alle LGE Sequenzen wurden zu Beginn visuell und mittels *Contrast-to-Noise-Ratio* (CNR) hinsichtlich ihrer Bildqualität bewertet. Anschließend erfolgte eine visuelle und

quantitative Beurteilung der LGE-Ausprägung. Für die quantitative Auswertung wurden epi- und endokardiale Konturen sowie ROI im gesunden und im LGE-aufweisenden Myokard markiert. Positive LGE-Areale wurden je nach Ausmaß der SD der Signalintensität vom gesunden Myokard derselben Schicht definiert. Bei Patientinnen bzw. Patienten mit abgelaufenem Myokardinfarkt galt dies für Regionen, deren Signalintensität 6 SD über dem Referenzmyokard lag. Im Falle einer hypertrophen Kardiomyopathie (HCM) oder entzündlicher Herzerkrankungen musste eine Abweichung von 3 SD über dem Vergleichsmyokard vorliegen. Anschließend wurde die Masse gesunden und vernarbten Gewebes für jedes Segment des AHA 16 Segment-Modells berechnet (3).

2.3.3. Statistik

Statistische Untersuchungen wurden mittels IBM SPSS Statistics 17.0 (IBM Corp., Armonk, NY, USA) durchgeführt. Zur quantitativen Analyse wurden Mittelwert und SD berechnet. Die LGE-Sequenzen wurden hinsichtlich ihrer Bildqualität und LGE-Größe verglichen (3).

3. Ergebnisse

3.1. Vergleich verschiedener Techniken der kardiovaskulären Magnetresonanztomographie zur Beurteilung der diastolischen Funktion

Von 59 eingeschlossenen Patientinnen und Patienten konnten 50 in die endgültige Analyse eingehen. Die Gruppenzuordnung ergab 26 DD-, 15 DD+ und 9 DD±. DD+ wies einen signifikant höheren *Body Mass Index* (BMI: DD- $26,7 \pm 3,0 \text{kg/m}^2$ vs. DD+ $29,7 \pm 3,2 \text{kg/m}^2$) auf. Darüber hinaus ergaben sich keine relevanten Unterschiede in Bezug auf die demographischen Eigenschaften (1).

3.1.1. Vergleich linksventrikulärer und linksatrialer Dimensionen

Die Ergebnisse der Analyse sind in Tabelle 1 dargestellt. Die linksventrikulären Dimensionen zeigten keine signifikanten Unterschiede zwischen DD+ und DD-. DD+ wies größere LA-Parameter auf. So waren LA-EDV und LA-Fläche sowohl als absolute Zahlen als auch normiert auf die Körpergröße signifikant erhöht. Die ROC-Kurvenanalyse

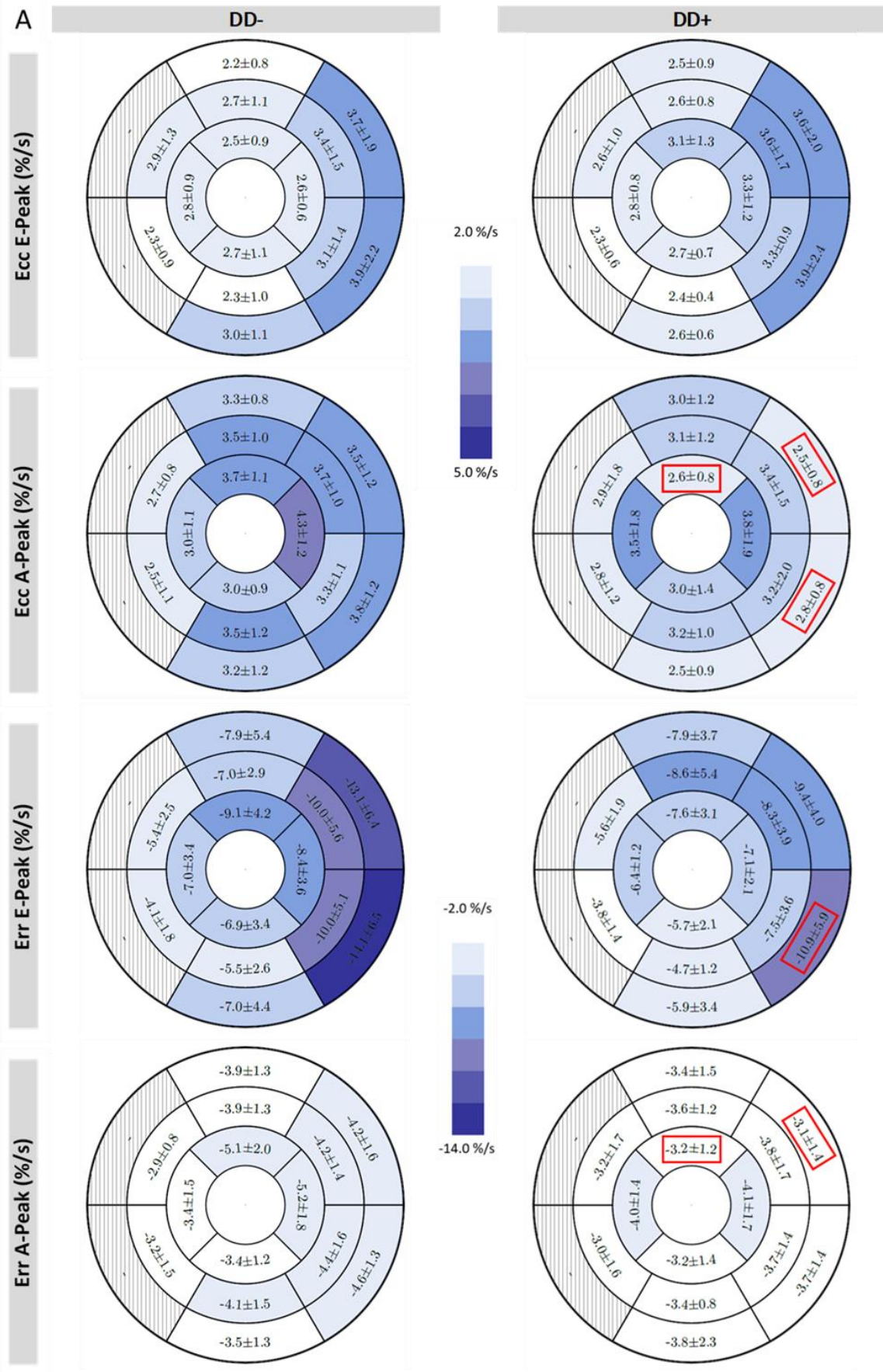
erbrachte die besten Resultate für LA-EDV/H. Der ermittelte Cut-off lag bei 52ml/cm (Sensitivität 0,71, Spezifität 0,84, *Area under the Curve* 0,75, Accuracy 0,75) (1).

Tabelle 1: Ergebnisse der Analyse linksventrikulärer und linksatrialer Dimensionen

	DD-	DD+	p-Wert
Linker Ventrikel			
LVEDV, ml	122.6 ± 34.3	130.5 ± 32.4	0.429
LVEDV/BSA, ml/m ²	63.7 ± 14.0	66.3 ± 14.9	0.639
LV-SV, ml	83.3 ± 21.3	86.0 ± 22.2	0.548
LV-EF, %	69.0 ± 7.6	66.0 ± 7.4	0.334
LVM, g	96.5 ± 29.9	110.2 ± 30.6	0.092
LVM/H, g/cm	0.6 ± 0.1	0.7 ± 0.2	0.050
LVM/BSA, g/m ²	49.9 ± 11.3	55.6 ± 12.3	0.079
LVRI, g/ml	0.8 ± 0.1	0.9 ± 0.2	0.412
Linker Vorhof - SAX-basierte Quantifikation (Volumen)			
LA-EDV, ml	74.4 ± 17.2	93.3 ± 26.2	0.014*
LA-EDV/H, ml/cm	0.4 ± 0.1	0.6 ± 0.1	0.010*
LA-EDV/ BSA, ml/m ²	39.2 ± 8.9	46.6 ± 12.0	0.069
LA-SV, ml	38.7 ± 8.4	41.2 ± 13.0	0.578
LA-EF, %	52.7 ± 7.4	45.7 ± 13.1	0.151
Linker Vorhof - LAX-basierte Quantifikation (Flächen)			
LA-Area4CV, mm ²	20.1 ± 6.2	22.1 ± 5.4	0.169
LA-Area4CV/H, mm ² /cm	0.12 ± 0.03	0.13 ± 0.03	0.188
LA-Area3CV, mm ²	18.6 ± 3.8	22.3 ± 5.9	0.033*
LA-Area3CV/H, mm ² /cm	0.11 ± 0.02	0.13 ± 0.03	0.026*
LA-Area2CV, mm ²	20.4 ± 5.5	24.8 ± 5.6	0.035*
LA-Area2CV/H, mm ² /cm	0.12 ± 0.03	0.15 ± 0.03	0.061
LA-Area-mean biplane, mm ²	20.2 ± 5.5	23.5 ± 4.8	0.084
LA-Area-mean biplane/ H, m ² /cm	0.12 ± 0.03	0.14 ± 0.03	0.079
LA-Area-mean triplane, mm ²	19.7 ± 4.6	23.1 ± 5.1	0.084
LA-Area-mean triplane/ H, m ² /cm	0.12 ± 0.03	0.13 ± 0.03	0.046*

modifiziert nach Kerner et al. (1) (Lizenznummer: 5024240029746)

Angaben in Mittelwert ± Standardabweichung; * markiert signifikante Unterschiede mit p-Wert <0,05



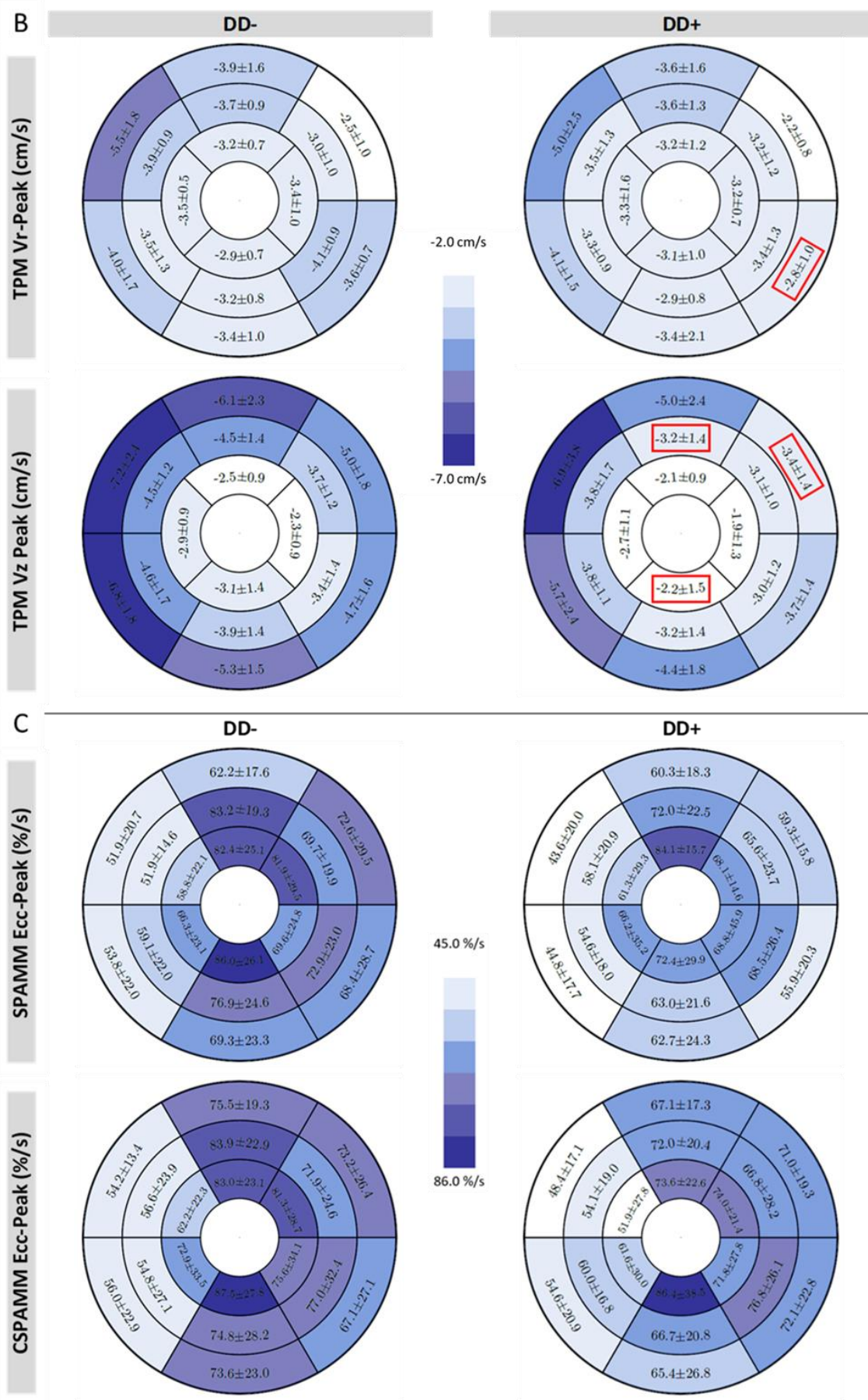


Abbildung 3 aus Kermer et al.(1) (Lizenznummer: 5024240029746):

Segmentale Unterschiede zwischen Patientinnen bzw. Patienten ohne (DD-) und mit (DD+) diastolischer Dysfunktion. Angaben in Mittelwert \pm Standardabweichung, signifikante Unterschiede mit $p<0,05$ sind rot umrahmt. A) Tissue Tracking SR-Ergebnisse mit signifikanten Unterschieden für Ecc A-Peak basal inferolateral ($p=0,007$) und apikal anterior ($p=0,014$) sowie Err E-Peak basal inferolateral ($p=0,030$), Err A-Peak basal inferolateral ($p=0,033$) und apikal anterior ($p=0,019$). B) TPM-Ergebnisse mit signifikanten Unterschieden für Vr basal inferolateral ($p=0,018$), Vz basal anterolateral ($p=0,007$) und Vz medial anterior ($p=0,044$). C) Tagging SR-Ergebnisse

3.1.2. Strainanalysen

Auf globaler Ebene konnten in den *Tissue Tracking* und CSPAMM-Analysen keine signifikanten Unterschiede gesehen werden. DD+ zeigte eine Reduktion des diastolischen Ell SR-Peaks der SPAMM-Analysen (DD-: $-16,5\pm12,0\%/\text{s}$ vs. DD+: $34,8\pm9,2\%/\text{s}$, $p=0,022$). *Tissue Tracking* basierte Ell SR-Kurven zeigten unglaubliche Verläufe, sodass auf eine weitere Analyse verzichtet wurde (1).

Die Ergebnisse der segmentalen Auswertungen sind in Abbildung 3(A+C) dargestellt. Mittels *Tissue Tracking* konnten in DD+ signifikant reduzierte Werte der früh- und spätdiastolischen SR-Peaks in den basal inferolateral, anterolateral und apikal anterioren Segmenten gemessen werden. Die regionale Auswertung der *Tagging*-Daten erbrachte keine signifikanten Unterschiede (1).

3.1.3. Unterschiede intramyokardialer Geschwindigkeiten

DD+ zeigte signifikant reduzierte diastolische Vz der apikalen Schicht (DD-: $-2,7\pm0,6\text{cm/s}$ vs. DD+: $-2,2\pm1,0\text{cm/s}$, $p=0,029$). Auf segmentaler Ebene erschienen Vz und Vr in DD+ basolateral vermindert. Die detaillierten Ergebnisse sind in Abbildung 3(B) dargestellt (1).

3.1.4. Vergleich transmitraler Flussgeschwindigkeiten

Die Auswertung der transmitralen Flussgeschwindigkeiten erbrachte keine signifikanten Unterschiede zwischen DD+ und DD- (1).

3.2. Etablierung linksatrialer Normwerte

Aufgrund unzureichender Darstellung des LA mussten 21 Fälle ausgeschlossen werden. Somit gingen die Daten von 182 Probandeninnen und Probanden in die Analyse ein, von denen 89 bei 3,0T und 93 bei 1,5T untersucht wurden (2).

3.2.1. Vergleich der Parameter in Abhängigkeit von Feldstärke, Alter und Geschlecht

Im Vergleich der absoluten LA-Volumina in Abhängigkeit von der Feldstärke konnten keine signifikanten Unterschiede gesehen werden (LA-EDV: 1,5T 68 ± 19 ml vs. 3,0T 64 ± 18 ml ($p=0,19$); LA-ESV: 1,5T 23 ± 9 ml vs. 3,0T 23 ± 9 ml ($p=0,6$)) (2).

Männer wiesen signifikant höhere endsystolische und enddiastolische LA-Volumina auf ($p \leq 0,01$). Dieser Unterschied konnte nach Normierung der Volumina auf Körpergröße und BSA nicht mehr nachgewiesen werden (siehe Tabelle 2) (2).

Mit zunehmendem Alter konnte eine signifikante Abnahme des LA-EDV/BSA ($p < 0,001$) gezeigt werden. Gleiches galt für die Normierung zur Körpergröße. Dies war unabhängig vom Geschlecht und spiegelte sich sowohl im Gruppen-basierten als auch im kontinuierlichen Altersvergleich wider (siehe Tabelle 2) (2).

Tabelle 2: Linksatriale Volumina und Funktion in Abhängigkeit von Alter und Geschlecht

Abhängigkeit vom Geschlecht		
	Männer (n=105)	Frauen (n=77)
LA-EDV (ml)	70 ± 19	$61 \pm 16^*$
LA-ESV (ml)	24 ± 9	$21 \pm 8^*$
LA-SV (ml)	46 ± 13	46 ± 9
LA-EF (%)	66 ± 7	66 ± 8
LA-EDV/H (ml/m)	36 ± 12	34 ± 12
LA-ESV/H (ml/m)	12 ± 5	12 ± 5
LA-EDV/BSA (ml/m ²)	34 ± 10	33 ± 9
LA-ESV/BSA (ml/m ²)	12 ± 4	11 ± 4

Abhängigkeit vom Alter			
	Gruppe 1	Gruppe 2	Gruppe 3
LA-EDV/H (ml/m)	38 ± 10	$34 \pm 11^{**}$	$31 \pm 12^{\dagger}$
LA-EDV/BSA (ml/m ²)	36 ± 8	$33 \pm 10^{**}$	$29 \pm 9^{\dagger}$

Darstellung in Mittelwert \pm Standardabweichung. Signifikante Unterschiede mit $p < 0,05$ sind markiert als: * im Vergleich Männer gegen Frauen, ** im Vergleich Gruppe 1 gegen Gruppe 2 und † im Vergleich Gruppe 2 gegen Gruppe 3

3.2.2. Unterschiede in Abhängigkeit der Phasendefinition

Endsystolische und Enddiastolische LA-Volumina unterschieden sich signifikant in Abhängigkeit des Zeitpunkts der Phasendefinition (LA-ESV: LA-Systole 1 38 ± 11 ml vs. LA-Systole 2 28 ± 8 ml ($p < 0,001$) und LA-EDV: LA-Diastole 1 92 ± 21 ml vs. LA-Diastole 2

$74 \pm 18 \text{ ml}$ ($p < 0,001$). Folglich kam es auch in der Berechnung der LA-EF zu signifikanten Unterschieden (LA-EF 1 $59 \pm 6\%$ vs. LA-EF 2 $63 \pm 7\%$ ($p < 0,001$)) (2).

3.3. Vergleich unterschiedlicher Late Gadolinium Enhancement-Sequenzen

312 Patientinnen und Patienten wurden eingeschlossen. 14 Fälle mussten aufgrund unvollständiger Untersuchungen ausgeschlossen werden, sodass die Daten von 203 Fällen mit chronischer Myokardischämie, 50 mit HCM und 45 mit inflammatorischer Herzerkrankung in die Analyse eingingen (3). Eine Übersicht repräsentativer LGE-SAX-Bilder für jede Studiengruppe und jede Sequenz ist in Abbildung 4 dargestellt.

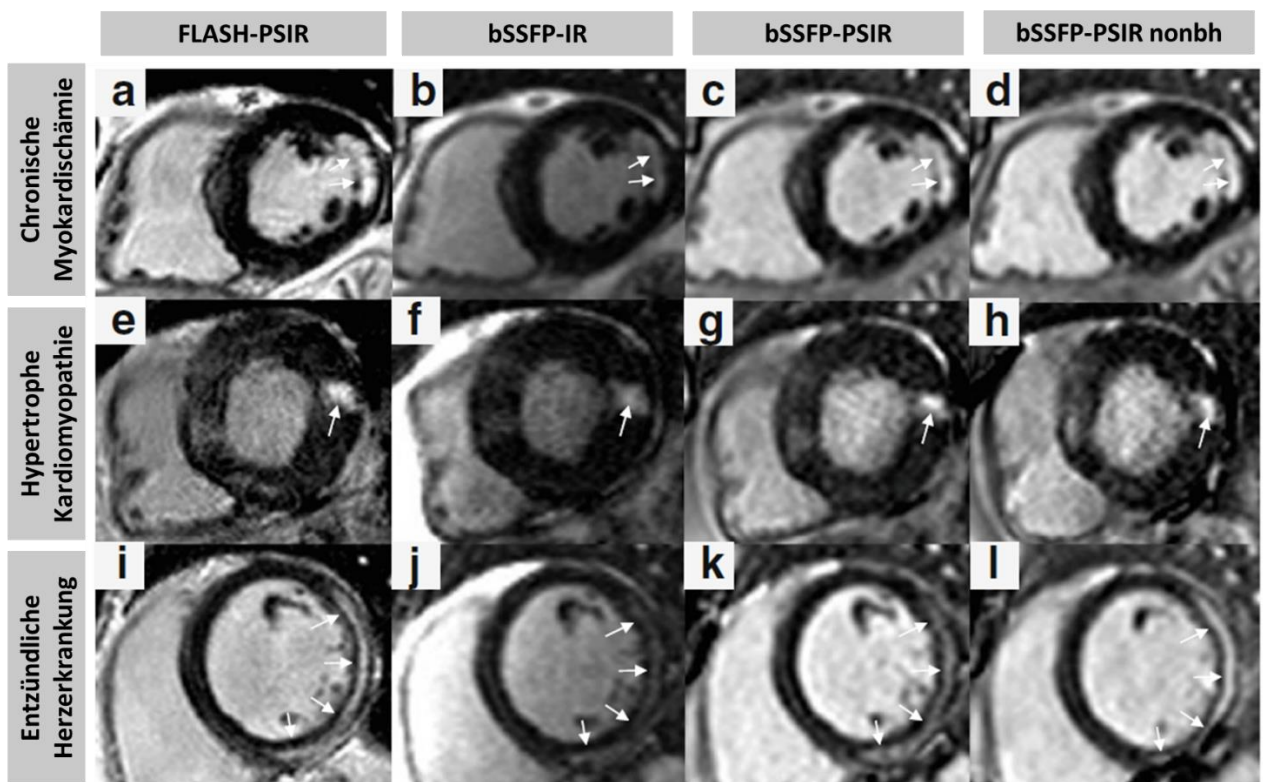


Abbildung 4 übersetzt nach Muehlberg et al.(3)

Repräsentative LGE-Aufnahmen von 3 ausgewählten Fällen mit chronischer Myokardischämie (a-d), hypertropher Kardiomyopathie (e-h) und akut entzündlicher Herzerkrankung (i-l) mit typischen LGE-Lokalisationen (weiße Pfeile). Zum Vergleich der Sequenzen wurde innerhalb der Fallbeispiele auf dieselbe Schicht zurückgegriffen. Nonbh bedeutet ohne Atemanhalte (non-breathhold).

3.3.1. Unterschiede in der Aufnahmezeit

Die Bildaufnahme mittels Referenzsequenz benötigte signifikant mehr Zeit als unter Anwendung der *multi-Slice* Sequenzen (Referenzsequenz FLASH-PSIR: $361,5 \pm 95,3$ s, bSSFP-IR: $23,4 \pm 7,2$ s ($p < 0,01$), bSSFP-PSIR: $21,9 \pm 6,4$ s ($p < 0,01$)) (3).

3.3.2. Vergleich der Bildqualität

Alle *multi-Slice* Sequenzen wiesen im Vergleich zur Referenzsequenz signifikante Unterschiede in der visuell beurteilten Bildqualität auf. Dabei konnte keine Abhängigkeit von der Krankheitsentität oder, im Falle der bSSFP-PSIR Sequenz, Atemvorgabe gesehen werden (3).

Während Arrhythmien die Bildqualität der *multi-Slice* Sequenzen nicht beeinflussten, wiesen 48,8% der Referenzsequenz-Bilder darunter eine schlechte oder nicht-auswertbare Qualität auf (3).

Insgesamt zeigte die bSSFP-PSIR sowohl im visuellen als auch CNR-Vergleich die beste Bildqualität (siehe Tabelle 3). Unter freier Atmung konnte eine leichte Abnahme der CNR verzeichnet werden. Verglichen mit der Referenzsequenz lagen die CNR-Werte der bSSFP-PSIR jedoch weiterhin über dem Standard ($p < 0,01$) (3).

Tabelle 3: Vergleich der Bildqualität in Abhängig von Grundrhythmus und Krankheitsbild

	Bildqualitätsscore		CNR-Vergleich			
	SR	Arrhyth.	alle Gruppen	Chron. MI	HCM	entzündliche Herzerkrankung
FLASH- PSIR	1,83	2,38*	65,9 $\pm 71,9$	67,9 $\pm 58,5$	80,4 $\pm 126,8$	37,0 $\pm 21,3$
bSSFP-IR	1,96 **	2,03	40,1 $\pm 26,8^\dagger$	43,2 $\pm 28,4^\dagger$	38,5 $\pm 19,9^\dagger$	31,5 $\pm 22,2^\dagger$
bSSFP- PSIR bh	1,57**	1,55	137,8 $\pm 103,7^\dagger$	149,8 $\pm 114,9^\dagger$	118,4 $\pm 66,9^\dagger$	95,7 $\pm 49,2^\dagger$
bSSFP- PSIR nbh	1,48**	1,37	125,9 $\pm 72,5^\dagger$	134,5 $\pm 72,5^\dagger$	101,7 $\pm 65,8^\dagger$	109,0 $\pm 73,4^\dagger$

modifiziert nach Muehlberg et al.(3)

Angaben in Mittelwert (\pm Standardabweichung); visueller Vergleich: mittlerer Bildqualitätscores aller Patientinnen und Patienten einer Gruppe, Score-System: 1=ausgezeichnete Qualität, keine Artefakte, 2=gute Qualität, minimale Artefakte, 3=moderate Qualität, einige Artefakte, welche die Diagnostik nicht beeinflussen, 4=schlechte Qualität, inakzeptable Artefakte, * $p < 0,05$ innerhalb der Sequenz, ** $p < 0,05$ verglichen mit FLASH-PSIR (Referenzsequenz)

CNR- (*Contrast-to-Noise*) Vergleich: t $p<0,05$ verglichen mit FLASH-PSIR innerhalb derselben Krankheitsentität. Folgende weitere Abkürzungen wurden verwendet: SR = Sinusrhythmus, Arrhyth. = Arrhythmie, chron. MI = chronische Myokardischämie, HCM = Hypertrophe Kardiomyopathie

3.3.3. Qualitative und quantitative LGE-Analyse

In den Referenzaufnahmen konnten insgesamt in 201 Fällen LGE-Läsionen nachgewiesen werden (davon 143 mit chronischer Myokardischämie, 31 mit HCM, 27 mit entzündlicher Herzerkrankung). Mittels bSSFP-IR-Aufnahmen konnten alle LGE-Fälle identifiziert werden. Unter Anwendung der bSSFP-PSIR-Sequenz kamen 2 kleine LGE-Läsionen (<1g) nicht zur Darstellung (3).

In der quantitativen Analyse der LGE-Ausdehnung konnten keine signifikanten Unterschiede zwischen den *multi-Slice* Sequenzen und der Referenzsequenz gesehen werden (siehe Tabelle 4). Die Ergebnisse waren zudem unabhängig von den Atemvorgaben (Aufnahme in Atemanhalte vs. freies Atmen). Bei Vorliegen von Arrhythmien ergaben sich im Rahmen der *multi-Slice*-Sequenz-Analysen keine signifikanten Unterschiede in der LGE Größe (bSSFP-IR: $7,6 \pm 6,1$ g, bSSFP-PSIR mit Atemanhalte: $7,7 \pm 5,6$ g, bSSFP-PSIR in freier Atmung: $7,4 \pm 5,6$ g). Die Referenzsequenz ging aufgrund der überwiegend nicht auswertbaren Bildqualität unter Arrhythmie nicht in die Analyse ein (3).

Im Intra- und Interobserver-Vergleich der LGE-Größe konnten gute Übereinstimmungen gezeigt werden (Pearson Koeffizient: Intraobserver aller Sequenzen >0,95, Interobserver bSSFP-PSIR in Atemanhalte 0,92 / ohne Atemanhalte 0,88).(3)

Tabelle 4: Quantitative Beurteilung der LGE-Ausdehnung

	alle Gruppen	chronische	Hypertrophe	entzündliche
		Myokardischämie	Kardiomyopathie	Herzerkrankung
FLASH-PSIR	$8,96 \pm 10,64$ g	$7,47 \pm 6,65$ g	$15,42 \pm 20,00$ g	$9,39 \pm 10,28$ g
bSSFP-IR	$8,69 \pm 10,75$ g	$7,26 \pm 7,03$ g	$15,31 \pm 20,02$ g	$8,67 \pm 9,66$ g
bSSFP-PSIR bh	$9,05 \pm 10,84$ g	$7,68 \pm 7,18$ g	$15,51 \pm 20,31$ g	$8,89 \pm 9,30$ g
bSSFP-PSIR nbh	$8,85 \pm 10,71$ g	$7,41 \pm 6,91$ g	$15,38 \pm 19,96$ g	$8,97 \pm 9,94$ g

modifiziert nach Muehlberg et al. (3)

Angabe der LGE-Größe in Gramm. bh bedeutet mit Atemanhalte (breathhold), nbh bedeutet ohne Atemanhalte (non breathhold)

4. Diskussion

Die vorliegenden Studien demonstrieren, dass die kardiovaskuläre MRT Möglichkeiten zur Beurteilung der diastolischen Funktion bei Patientinnen und Patienten mit HFrEF bietet. Darüber hinaus gewährleisten zeiteffizientere Methoden die Durchführung aussagekräftiger Untersuchungen auch im Falle schwer kranker Patientinnen und Patienten.

4.1. Linksatriale Dimensionen bei der Beurteilung der diastolischen Funktion

Patientinnen und Patienten mit diastolischer Dysfunktion wiesen eine signifikante Vergrößerung des LA auf. Als Cut-off konnte ein $LA-EDV/H \geq 0,52\text{ml/cm}$ definiert werden (1). Sowohl in der 2007 veröffentlichten Konsens-Erklärung der *Heart Failure and Echocardiography Association of the European Society of Cardiology* (11) als auch in den 2016 erschienen Empfehlungen der *American Society of Echocardiography* und *European Society of Cardiovascular Imaging* (12) und dem aktuellen Konsensuspapier der *European Society of Cardiovascular Imaging* (7) stellt die LA-Dilatation ein Diagnosekriterium der diastolischen Dysfunktion dar. Als echokardiographischer Parameter wird in allen drei Stellungnahmen das maximale LA-Volumen im Verhältnis zur BSA herangezogen. In unseren Messungen zeigte LA-EDV/BSA keine signifikanten Unterschiede zwischen DD+ und DD-. Grund dafür könnte sein, dass DD+ einen signifikant erhöhten BMI aufwies. Patel et al. berichteten von einer Unterschätzung der LA-Dimensionen durch LA-EDV/BSA bei übergewichtigen Patientinnen und Patienten, während eine Normierung zu H vom Grad der Übergewichtigkeit unberührt blieb (39). Verglichen mit den empfohlenen Cut-off-Werten der Echokardiographie von 40 bzw. 34ml/m^2 (7, 11, 12), lagen in unserer Studie in beiden Gruppen grenzwertige bis erhöhte Mittelwerte vor (DD-: $39,2 \pm 8,9\text{ml/m}^2$ vs. DD+: $46,6 \pm 12,0\text{ml/m}^2$) (1). Es ist bekannt, dass die LA-Volumina mittels kardiovaskulärer MRT systematisch größer gemessen werden als in der Echokardiographie (40). Daher sind methodenspezifische Normwerte unerlässlich.

Um eine möglichst kurze Untersuchungszeit zu gewährleisten, veröffentlichten wir LA-Normwerte basierend auf biplaner Volumenmessung anhand routinemäßig generierter Aufnahmen. In der geschlechtsabhängigen Analyse konnte gesehen werden, dass zwischen Männern und Frauen keine Unterschiede vorliegen, sobald die Parameter ins Verhältnis zu BSA oder H gesetzt werden. Maceira et al. fanden ebenfalls heraus, dass

sich das LA-Volumen nach Normierung zu BSA zwischen den Geschlechtern nicht mehr relevant unterscheidet (35). Hudsmith et al. wiesen einen geschlechtsabhängigen Unterschied der LA-Volumina nach, untersuchten die Parameter jedoch nicht in Abhängigkeit zu BSA oder H (36).

In unseren Auswertungen konnte gezeigt werden, dass LA-EDV/H bzw. LA-EDV/BSA im Alter signifikant abnimmt (2). Maceira et al. stellten keinen altersabhängigen Unterschied des LA-Volumens fest. Allerdings zeigten LA-Diameter eine altersbedingte Abnahme, während die LA-Fläche mit dem Alter zunahm (35). Sievers et al. konnten ebenfalls keine altersabhängigen Unterschiede im LA-Volumen feststellen, wobei der Vergleich zwischen Patientinnen und Patienten unter bzw. über 50 Jahren erfolgte (37). Ausgehend von unseren Daten ist anzunehmen, dass eine feinere Abstufung der Altersgruppen möglicherweise ebenfalls altersabhängige Unterschiede zum Vorschein gebracht hätte. Die Feldstärke scheint keinen Einfluss auf die erhobenen Parameter zu haben, was sich mit vorherigen Untersuchungen zum Einfluss der Feldstärke auf LV-Dimensionen deckt (41).

Die Beurteilung der LA-Dimensionen ist nicht nur für die Diagnostik einer diastolischen Dysfunktion relevant. So gilt eine LA-Vergrößerung als Risikofaktor für die Entwicklung von Vorhofflimmern (42), eines Schlaganfalls (43) oder kardiovaskulärer Ereignisse (44), geht mit einer erhöhten Mortalität und schlechterem klinischen Outcome bei Patientinnen und Patienten mit dilatativer Kardiomyopathie einher (45) und ist Bestandteil der Empfehlungen der *European Society of Cardiology* zur Risikostratifizierung des plötzlichen Herztodes bei HCM (46). Allerdings tritt eine Dilatation des LA sowohl bei systolischer als auch bei diastolischer Funktionsstörung auf und kann somit nicht als alleiniges Diagnosekriterium einer HFpEF fungieren (47).

4.2. Transmitrale Fluss- und intramyokardiale Deformierungsparameter zur Beurteilung der diastolischen Funktion

Die kardiovaskuläre MRT bietet eine Fülle klinisch etablierter und experimenteller Untersuchungsmethoden zur Beurteilung verschiedenster Fragestellungen. Mittels Phasenkontrast-Aufnahmen ist es möglich, Geschwindigkeiten des Blutflusses zu messen. Zur Graduierung diastolischer Funktionsstörungen werden in der Echokardiographie unter anderem früh- (E) und spätdiastolische (A) Peaks transmitraler Flussgeschwindigkeiten angewandt (12). Äquivalente Flussmessung können so auch mittels kardiovaskulärer MRT erfolgen und zeigten eine gute Übereinstimmung zwischen

den Methoden mit allgemeiner Unterschätzung transmitraler Flussparameter durch die MRT (23). In unseren Untersuchungen waren E, A und das Verhältnis E/A nicht geeignet, um zwischen DD+ und DD- zu unterscheiden. Eine Graduierung diastolischer Funktionseinschränkung war nicht Bestandteil unseres Studienkonzeptes, sodass diesbezüglich keine Aussagen gemacht werden konnten (1).

Die diastolische Dysfunktion hat ihren Ursprung auf zellulärer Ebene und es existieren mehrere Erklärungsansätze für die Entstehung der verminderten Elastizität des Herzmuskels. Wünschenswert wäre daher, die diastolische Funktion direkt durch Parameter intramyokardialer Eigenschaften beurteilen zu können. Eine diastolische Funktionsstörung könnte so ggf. bereits vor Auftreten möglicher Folgen - wie eine atriale Dilatation oder veränderte Flussprofile - erkannt und frühzeitiger behandelt werden.

Mittels Strain- und SR-Analysen kann die Verformung des Myokards über den Herzzyklus hinweg evaluiert werden. In der Echokardiographie kommen Messungen der *global* Ell SR zur Beurteilung der diastolischen und systolischen Funktion zum Einsatz (12). Ell SR war in unseren *Tagging* SPAMM-Analysen bei DD+ signifikant reduziert. Aufgrund technischer Limitationen konnte *Tissue Tracking* nicht zur Auswertung von Ell SR-Daten genutzt werden (1).

Die *Tagging*-Analysen frühdiastolischer Ecc SR-Peaks erbrachten keine Unterschiede zwischen den Gruppen (1). Andere Studien konnten hingegen eine Reduktion des Ecc SR-Peaks bei Patientinnen und Patienten mit HCM (33) oder LV Hypertrophie (32) nachweisen. Ein Grund für die diskrepanten Ergebnisse könnten Unterschiede in der Studienpopulation und Krankheitsausprägung sein. Verglichen mit unserer DD+ Gruppe wiesen die Gruppen der Erkrankten der beiden anderen Studien eine deutlich stärkere Hypertrophie mit ggf. daraus resultierender, ausgeprägterer Einschränkung der diastolischen Funktion auf. Ein direkter Vergleich, inwieweit die erhobenen SR-Ergebnisse mit der Einschätzung der diastolischen Funktion durch klinisch etablierte Methoden korrelieren, geht aus beiden Studien nicht hervor.

In den SR-Analysen mittels *Tissue Tracking* fiel insbesondere eine Peakreduktion in den basolateralen Segmenten der DD+ Gruppe auf (1). Ein Vergleich dieser Ergebnisse mit anderen Studien war limitiert, da sich die meisten Untersuchungen auf systolische Analysen fokusstieren, unterschiedliche Auswertesoftwaren verwendet und Parameter uneinheitlich definiert wurden (27, 28, 48). Kuetting et al. untersuchte frühdiastolische und maximale Ecc-SR-Peaks auf mittventrikulärer Schichtebene bei Patientinnen und Patienten mit echokardiographisch diagnostizierter, diastolischer Dysfunktion und

gesunden Probandinnen und Probanden. Beide Parameter erschienen bei den Erkrankten signifikant erniedrigt (28). Diese Ergebnisse konnten wir nicht reproduzieren, was daran liegen könnte, dass der Altersunterschied zwischen den Gruppen in unserer Studie deutlich geringer ausfiel und die frühdiastolische Ecc SR grundsätzlich mit dem Alter abnimmt (27).

Auch in unseren TPM-Analysen konnten verminderte Peak-Geschwindigkeiten der basolateralen Segmente in der DD+ Gruppe nachgewiesen werden (1). Von Knobelsdorff et al. (31) und Foell et al.(29) fanden ebenfalls reduzierte diastolische Vz und Vr Peak-Geschwindigkeiten bei Patientinnen und Patienten mit hypertensiver Herzkrankung im Vergleich zu gesunden Probandinnen und Probanden. Die signifikanten Unterschiede gingen in beiden Studien jedoch über die Region der basolateralen Wand hinaus. In unserer Studie stand keine gesunde Kontrollgruppe zur Verfügung, da eine Durchführung invasiver Messungen an gesunden Probandinnen und Probanden nicht in Betracht gezogen wurde. Es wurden ausschließlich Patientinnen und Patienten mit studienunabhängiger Indikation zur Herzkatheteruntersuchung eingeschlossen. Der Vergleich erfolgte zwischen Patientinnen und Patienten mit und ohne diastolischer Dysfunktion. Verglichen mit den Kontrollgruppen der anderen Studien waren DD+ und DD- durch ein höheres Lebensalter und ein überwiegendes Vorhandensein einer arteriellen Hypertonie charakterisiert. Sowohl zunehmendes Alter (24) als auch eine hypertensive Herzkrankheit (29, 31) gehen nachweislich mit einer Reduktion diastolischer Vz und Vr Peaks einher. Möglicherweise liegt in der DD- Gruppe daher bereits eine gewisse, klinisch nicht zur Diagnose einer diastolischen Dysfunktion führende Einschränkung der diastolischen Funktion vor, welche die Unterschiede zwischen DD- und DD+ reduziert. Die verminderten diastolischen Peak-Geschwindigkeiten der basolateralen Wand könnten hingegen eine Rolle in der Diskriminierung altersbedingter Relaxationsstörung von pathologischer diastolischer Dysfunktion spielen. Auf globaler Ebene konnten signifikant reduzierte Vz Peaks der apikalen Schicht gesehen werden. Diese Ergebnisse konnten in der segmentalen Analyse jedoch nur teilweise reproduziert werden (1).

4.3. Zeiteffiziente Gewebedifferenzierung

In unserer Studie zur Identifizierung kardiovaskulärer MRT-Parameter zur Beurteilung der diastolischen Funktion war vor allem eine Reduktion myokardialer Verformung in der basolateralen LV-Region auffällig. Interessanterweise gehen verschiedene Formen von

Kardiomyopathien (49-52) überwiegend mit Fibrosierungen in der inferolateralen Wand einher. Das Auftreten fokaler und diffuser Fibrosen wurde darüber hinaus bereits bei Patientinnen und Patienten mit HFpEF nachgewiesen (53). Für unser Studienprotokoll benötigten wir im Schnitt 45min. Eine Erweiterung um zusätzliche LGE-Aufnahmen wäre den Probandinnen und Probanden grundsätzlich und insbesondere im Falle vorliegender Symptome einer Herzinsuffizienz schwer zumutbar gewesen. Umso wichtiger erscheint die Etablierung zeiteffizienter LGE-Sequenzen.

Alle von uns getesteten *multi-slice* LGE-Sequenzen benötigten weniger Zeit für die Bildakquise als die segmentierte Standardsequenz. Unabhängig von der zugrunde liegenden Krankheit ermöglichen *multi-slice* Sequenz-Aufnahmen eine ebenso gute visuelle Detektion, Ausdehnungsbeurteilung und Quantifizierung von LGE-Läsionen wie unter Anwendung der Referenzsequenz (3). Unsere Ergebnisse decken sich mit früheren Studien zur Anwendung *multi-slice* basierter LGE-Sequenzen bei HCM oder ischämischer Herzerkrankung. Die Studien konzentrierten sich jedoch stets auf eine Krankheitsentität, wiesen kleinere Studienpopulationen auf und schlossen Fälle mit Arrhythmien aus (21, 22).

Optimale MRT-Bilder werden in der Regel bei stabilem Sinusrhythmus und suffizienter Atemhalte generiert. Dies gilt auch für die LGE-Standardsequenz. Bei Patientinnen und Patienten mit Herzinsuffizienz ist es nicht unüblich, dass sie Arrhythmien aufweisen oder, je nach Ausprägung der Symptomatik, den Atem nicht ausreichend anhalten können. In unserer Studie war die Referenzsequenz im Falle von Arrhythmien aufgrund eines Großteils diagnostisch nicht verwertbarer Bildaufnahmen nicht anwendbar. Die *multi-slice* Sequenzen zeigten hingegen eine gute bis ausgezeichnete Bildqualität unter Arrhythmien (3). Rosendhal et al. konnten ebenfalls einen Vorteil *multi-slice* basierter gegenüber segmentierten Sequenzen bei Vorliegen von Arrhythmien nachweisen. Es handelte sich dabei um andere als die in unserer Studie angewandten *multi-slice* Sequenzen (54).

Mittels bSSFP-PSIR war es zudem möglich, Patientinnen und Patienten auch ohne Atemkommandos adäquat zu untersuchen. Ob der Atem angehalten wurde oder Aufnahmen in freier Atmung generiert wurden, hatte keine Auswirkung auf die LGE-Erkennung und -Quantifizierung (3).

Zwei kleine Fibrosen, welche mittels Referenzsequenz detektiert wurden, konnten in den bSSPF-PSIR-Aufnahmen nicht nachgewiesen werden. Die absolute LGE-Masse war in beiden Fällen mit weniger als 1 Gramm sehr gering. Bei grundlegend guter Bildqualität

können Partial-Volumen-Effekte oder Schichtpositionsverschiebungen durch Atembewegungen als Ursache angenommen werden. Nichtsdestotrotz ist nicht auszuschließen, dass sehr kleine Läsionen mittels *multi-slice* bSSFP-PSIR nicht dargestellt oder übersehen werden (3).

Basierend auf den vorliegenden Ergebnissen kann eine Anwendung *multi-slice* basierter LGE-Sequenzen im Falle bekannter oder vermuteter myokardialer Narben, bei Vorliegen von Arrhythmien oder insuffizienter Atemhalte empfohlen werden. Im Falle unklarer Kardiomyopathien und bei diffuseren Läsionen wie bei HCM oder inflammatorischen Herzerkrankungen sollte auf die segmentierte FLASH-PSIR zurückgegriffen werden, vorausgesetzt es liegt ein konstanter Sinusrhythmus und ausreichende Atemhaltemöglichkeit vor.

Neben den von uns dargestellten Sequenzoptimierungen gibt es weitere Methoden, um zeiteffiziente kardiovaskuläre MRT-Untersuchungen bei symptomatischen Patientinnen und Patienten durchzuführen. So konnten mittels bewegungskorrigierten (*Motion Correction* = MOCO) LGE-Aufnahmen ohne Atemhalte eine bessere Bildqualität und kürzere Scanzeiten als unter Anwendung segmentierter LGE-Sequenzen nachgewiesen werden (55, 56).

4.4. Zusammenfassung

In mehr als der Hälfte der Fälle von Herzinsuffizienz liegt eine HFpEF vor. Anders als bei der HFrEF ist es bisher jedoch nicht gelungen, eine sterblichkeitsminimierende Behandlung zu etablieren. Grundvoraussetzung für eine adäquate Therapieeinleitung ist die korrekte Diagnosestellung. Die kardiovaskuläre MRT spielte bisher nur eine untergeordnete Rolle in der Diagnostik der HFpEF. Grund dafür sind u.a. fehlende eindeutige, klinisch etablierte Parameter zur Beurteilung der diastolischen Funktion, entsprechende Referenzwerte, lange Untersuchungszeiten und eingeschränkte Anwendbarkeit bei Vorliegen von Arrhythmien oder verminderter Atemhaltekapazität. Die vorliegenden, dissertationsrelevanten Studien tragen dazu bei, die diastolische Funktion mithilfe der kardiovaskulären MRT zu beurteilen. Zum einen konnten Parameter zur Evaluierung der diastolischen Funktion identifiziert werden. Vergrößerungen des LA und verminderte diastolische SR- und intramyokardiale Geschwindigkeitspeaks der basolateralen LV-Wand stehen dabei im Vordergrund. Es wurden zudem linksatriale Normwerte veröffentlicht, welche keine, über ein Routineprotokoll hinausreichende Aufnahmen nötig machen. Zum anderen bieten neue *multi-slice* LGE-Aufnahmen die

Möglichkeit, insbesondere auch schwer kranke Patientinnen und Patienten schneller und ohne Einschränkung durch Herzrhythmus oder Atemanhaltekapazitäten zu untersuchen, wodurch u.a. die Genese einer HFpEF weiter abgeklärt werden kann.

Insgesamt werden die beschriebenen Studien helfen, die Diagnostik der HFpEF mittels kardiovaskulärer MRT voranzubringen.

5. Literaturverzeichnis

1. Kermer J, Traber J, Utz W, Hennig P, Menza M, Jung B, Greiser A, Barckow P, von Knobelsdorff-Brenkenhoff F, Töpper A, Blaszczyk E, Schulz-Menger J. Assessment of diastolic dysfunction: comparison of different cardiovascular magnetic resonance techniques. *ESC Heart Failure*. 2020;7(5):2637-49.
2. Funk S, Kermer J, Doganguezel S, Schwenke C, von Knobelsdorff-Brenkenhoff F, Schulz-Menger J. Quantification of the left atrium applying cardiovascular magnetic resonance in clinical routine. *Scandinavian cardiovascular journal : SCJ*. 2018;1-8.
3. Muehlberg F, Arnhold K, Fritschi S, Funk S, Prothmann M, Kermer J, Zange L, von Knobelsdorff-Brenkenhoff F, Schulz-Menger J. Comparison of fast multi-slice and standard segmented techniques for detection of late gadolinium enhancement in ischemic and non-ischemic cardiomyopathy – a prospective clinical cardiovascular magnetic resonance trial. *Journal of cardiovascular magnetic resonance : official journal of the Society for Cardiovascular Magnetic Resonance*. 2018;20.
4. Statistisches Bundesamt, Sterbefälle (absolut, Sterbeziffer, Ränge, Anteile) für die 10 häufigsten Todesursachen (ab 1998). [Tabelle im Internet]. www.gbe-bund.de [updated 19.05.2020]. Available from: https://www.gbe-bund.de/gbe/!pkg_olap_tables.prc_set_orientation?p_uid=gastd&p_aid=43395886&p_sprache=D&p_help=2&p_indnr=516&p_ansnr=35490688&p_version=4&D.000=1&D.001=3&D.002=3&D.003=3.
5. van Riet EE, Hoes AW, Wagenaar KP, Limburg A, Landman MA, Rutten FH. Epidemiology of heart failure: the prevalence of heart failure and ventricular dysfunction in older adults over time. A systematic review. *European journal of heart failure*. 2016;18(3):242-52.
6. Ponikowski P, Voors AA, Anker SD, Bueno H, Cleland JG, Coats AJ, Falk V, Gonzalez-Juanatey JR, Harjola VP, Jankowska EA, Jessup M, Linde C, Nihoyannopoulos P, Parissis JT, Pieske B, Riley JP, Rosano GM, Ruilope LM, Ruschitzka F, Rutten FH, van der Meer P. [2016 ESC Guidelines for the diagnosis and treatment of acute and chronic heart failure]. *Kardiologia polska*. 2016;74(10):1037-147.
7. Pieske B, Tschöpe C, de Boer RA, Fraser AG, Anker SD, Donal E, Edelmann F, Fu M, Guazzi M, Lam CSP, Lancellotti P, Melenovsky V, Morris DA, Nagel E, Pieske-Kraigher E, Ponikowski P, Solomon SD, Vasan RS, Rutten FH, Voors AA, Ruschitzka F, Paulus WJ, Seferovic P, Filippatos G. How to diagnose heart failure with preserved ejection fraction: the HFA-PEFF diagnostic algorithm: a consensus recommendation from the Heart Failure Association (HFA) of the European Society of Cardiology (ESC). *European heart journal*. 2019;40(40):3297-317.
8. Kindermann M, Reil JC, Pieske B, van Veldhuisen DJ, Bohm M. Heart failure with normal left ventricular ejection fraction: what is the evidence? *Trends Cardiovasc Med*. 2008;18(8):280-92.

9. Tsang TS, Barnes ME, Gersh BJ, Bailey KR, Seward JB. Left atrial volume as a morphophysiologic expression of left ventricular diastolic dysfunction and relation to cardiovascular risk burden. *The American journal of cardiology*. 2002;90(12):1284-9.
10. Greenberg B, Chatterjee K, Parmley WW, Werner JA, Holly AN. The influence of left ventricular filling pressure on atrial contribution to cardiac output. *Am Heart J*. 1979;98(6):742-51.
11. Paulus WJ, Tschope C, Sanderson JE, Rusconi C, Flachskampf FA, Rademakers FE, Marino P, Smiseth OA, De Keulenaer G, Leite-Moreira AF, Borbely A, Edes I, Handoko ML, Heymans S, Pezzali N, Pieske B, Dickstein K, Fraser AG, Brutsaert DL. How to diagnose diastolic heart failure: a consensus statement on the diagnosis of heart failure with normal left ventricular ejection fraction by the Heart Failure and Echocardiography Associations of the European Society of Cardiology. *European heart journal*. 2007;28(20):2539-50.
12. Nagueh SF, Smiseth OA, Appleton CP, Byrd BF, 3rd, Dokainish H, Edvardsen T, Flachskampf FA, Gillebert TC, Klein AL, Lancellotti P, Marino P, Oh JK, Popescu BA, Waggoner AD. Recommendations for the Evaluation of Left Ventricular Diastolic Function by Echocardiography: An Update from the American Society of Echocardiography and the European Association of Cardiovascular Imaging. *Journal of the American Society of Echocardiography : official publication of the American Society of Echocardiography*. 2016;29(4):277-314.
13. The survival of patients with heart failure with preserved or reduced left ventricular ejection fraction: an individual patient data meta-analysis. *European heart journal*. 2012;33(14):1750-7.
14. Owan TE, Hodge DO, Herges RM, Jacobsen SJ, Roger VL, Redfield MM. Trends in prevalence and outcome of heart failure with preserved ejection fraction. *N Engl J Med*. 2006;355(3):251-9.
15. Hundley WG, Bluemke DA, Finn JP, Flamm SD, Fogel MA, Friedrich MG, Ho VB, Jerosch-Herold M, Kramer CM, Manning WJ, Patel M, Pohost GM, Stillman AE, White RD, Woodard PK. ACCF/ACR/AHA/NASCI/SCMR 2010 expert consensus document on cardiovascular magnetic resonance: a report of the American College of Cardiology Foundation Task Force on Expert Consensus Documents. *Journal of the American College of Cardiology*. 2010;55(23):2614-62.
16. Bellenger NG, Burgess MI, Ray SG, Lahiri A, Coats AJ, Cleland JG, Pennell DJ. Comparison of left ventricular ejection fraction and volumes in heart failure by echocardiography, radionuclide ventriculography and cardiovascular magnetic resonance; are they interchangeable? *European heart journal*. 2000;21(16):1387-96.
17. Grothues F, Smith GC, Moon JC, Bellenger NG, Collins P, Klein HU, Pennell DJ. Comparison of interstudy reproducibility of cardiovascular magnetic resonance with two-dimensional echocardiography in normal subjects and in patients with heart failure or left ventricular hypertrophy. *The American journal of cardiology*. 2002;90(1):29-34.
18. Gonzalez JA, Kramer CM. Role of Imaging Techniques for Diagnosis, Prognosis and Management of Heart Failure Patients: Cardiac Magnetic Resonance. *Current heart failure reports*. 2015;12(4):276-83.
19. Kellman P, Arai AE, McVeigh ER, Aletras AH. Phase-sensitive inversion recovery for detecting myocardial infarction using gadolinium-delayed hyperenhancement. *Magnetic resonance in medicine*. 2002;47(2):372-83.
20. Sievers B, Rehwald WG, Albert TS, Patel MR, Parker MA, Kim RJ, Judd RM. Respiratory motion and cardiac arrhythmia effects on diagnostic accuracy of myocardial delayed-enhanced MR imaging in canines. *Radiology*. 2008;247(1):106-14.

21. Viallon M, Jacquier A, Rotaru C, Delattre BM, Mewton N, Vincent F, Croisille P. Head-to-head comparison of eight late gadolinium-enhanced cardiac MR (LGE CMR) sequences at 1.5 tesla: from bench to bedside. *Journal of magnetic resonance imaging* : JMRI. 2011;34(6):1374-87.
22. Morita K, Utsunomiya D, Oda S, Komi M, Namimoto T, Hirai T, Hashida M, Takashio S, Yamamuro M, Yamashita Y. Comparison of 3D phase-sensitive inversion-recovery and 2D inversion-recovery MRI at 3.0 T for the assessment of late gadolinium enhancement in patients with hypertrophic cardiomyopathy. *Academic radiology*. 2013;20(6):752-7.
23. Rathi VK, Doyle M, Yamrozik J, Williams RB, Caruppannan K, Truman C, Vido D, Biederman RW. Routine evaluation of left ventricular diastolic function by cardiovascular magnetic resonance: a practical approach. *Journal of cardiovascular magnetic resonance* : official journal of the Society for Cardiovascular Magnetic Resonance. 2008;10(1):36.
24. Foll D, Jung B, Schilli E, Staehle F, Geibel A, Hennig J, Bode C, Markl M. Magnetic resonance tissue phase mapping of myocardial motion: new insight in age and gender. *Circulation Cardiovascular imaging*. 2010;3(1):54-64.
25. Ibrahim el SH. Myocardial tagging by cardiovascular magnetic resonance: evolution of techniques--pulse sequences, analysis algorithms, and applications. *Journal of cardiovascular magnetic resonance* : official journal of the Society for Cardiovascular Magnetic Resonance. 2011;13:36.
26. Ortega M, Triedman JK, Geva T, Harrild DM. Relation of left ventricular dyssynchrony measured by cardiac magnetic resonance tissue tracking in repaired tetralogy of fallot to ventricular tachycardia and death. *The American journal of cardiology*. 2011;107(10):1535-40.
27. Andre F, Steen H, Mattheis P, Westkott M, Breuninger K, Sander Y, Kammerer R, Galuschky C, Giannitsis E, Korosoglou G, Katus HA, Buss SJ. Age- and gender-related normal left ventricular deformation assessed by cardiovascular magnetic resonance feature tracking. *Journal of cardiovascular magnetic resonance* : official journal of the Society for Cardiovascular Magnetic Resonance. 2015;17:25.
28. Kuettling D, Sprinkart AM, Doerner J, Schild H, Thomas D. Comparison of magnetic resonance feature tracking with harmonic phase imaging analysis (CSPAMM) for assessment of global and regional diastolic function. *Eur J Radiol*. 2015;84(1):100-7.
29. Foell D, Jung B, Germann E, Staehle F, Bode C, Markl M. Hypertensive heart disease: MR tissue phase mapping reveals altered left ventricular rotation and regional myocardial long-axis velocities. *European radiology*. 2013;23(2):339-47.
30. Jung B, Foll D, Bottler P, Petersen S, Hennig J, Markl M. Detailed analysis of myocardial motion in volunteers and patients using high-temporal-resolution MR tissue phase mapping. *Journal of magnetic resonance imaging* : JMRI. 2006;24(5):1033-9.
31. von Knobelsdorff-Brenkenhoff F, Hennig P, Menza M, Dieringer MA, Foell D, Jung B, Schulz-Menger J. Myocardial dysfunction in patients with aortic stenosis and hypertensive heart disease assessed by MR tissue phase mapping. *Journal of magnetic resonance imaging* : JMRI. 2015.
32. Edvardsen T, Rosen BD, Pan L, Jerosch-Herold M, Lai S, Hundley WG, Sinha S, Kronmal RA, Bluemke DA, Lima JA. Regional diastolic dysfunction in individuals with left ventricular hypertrophy measured by tagged magnetic resonance imaging--the Multi-Ethnic Study of Atherosclerosis (MESA). *Am Heart J*. 2006;151(1):109-14.
33. Ennis DB, Epstein FH, Kellman P, Fananapazir L, McVeigh ER, Arai AE. Assessment of regional systolic and diastolic dysfunction in familial hypertrophic cardiomyopathy using MR tagging. *Magnetic resonance in medicine*. 2003;50(3):638-42.

34. Moody WE, Taylor RJ, Edwards NC, Chue CD, Umar F, Taylor TJ, Ferro CJ, Young AA, Townend JN, Leyva F, Steeds RP. Comparison of magnetic resonance feature tracking for systolic and diastolic strain and strain rate calculation with spatial modulation of magnetization imaging analysis. *Journal of magnetic resonance imaging : JMRI*. 2015;41(4):1000-12.
35. Maceira AM, Cosin-Sales J, Roughton M, Prasad SK, Pennell DJ. Reference left atrial dimensions and volumes by steady state free precession cardiovascular magnetic resonance. *Journal of cardiovascular magnetic resonance : official journal of the Society for Cardiovascular Magnetic Resonance*. 2010;12:65.
36. Hudsmith LE, Petersen SE, Francis JM, Robson MD, Neubauer S. Normal human left and right ventricular and left atrial dimensions using steady state free precession magnetic resonance imaging. *Journal of cardiovascular magnetic resonance : official journal of the Society for Cardiovascular Magnetic Resonance*. 2005;7(5):775-82.
37. Sievers B, Kirchberg S, Franken U, Bakan A, Addo M, John-Puthenveettil B, Trappe HJ. Determination of normal gender-specific left atrial dimensions by cardiovascular magnetic resonance imaging. *Journal of cardiovascular magnetic resonance : official journal of the Society for Cardiovascular Magnetic Resonance*. 2005;7(4):677-83.
38. Cerqueira MD, Weissman NJ, Dilsizian V, Jacobs AK, Kaul S, Laskey WK, Pennell DJ, Rumberger JA, Ryan T, Verani MS. Standardized myocardial segmentation and nomenclature for tomographic imaging of the heart. A statement for healthcare professionals from the Cardiac Imaging Committee of the Council on Clinical Cardiology of the American Heart Association. *Circulation*. 2002;105(4):539-42.
39. Patel DA, Lavie CJ, Gilliland Y, Shah S, Ventura H, Milani R. Abstract 712: Left Atrial Volume and Mortality Prediction: Does the Method of Indexing Matter? *Circulation*. 2009;120(Suppl 18):S382-S.
40. Madueme PC, Mazur W, Hor KN, Germann JT, Jefferies JL, Taylor MD. Comparison of area-length method by echocardiography versus full-volume quantification by cardiac magnetic resonance imaging for the assessment of left atrial volumes in children, adolescents, and young adults. *Pediatric cardiology*. 2014;35(4):645-51.
41. Hudsmith LE, Petersen SE, Tyler DJ, Francis JM, Cheng AS, Clarke K, Selvanayagam JB, Robson MD, Neubauer S. Determination of cardiac volumes and mass with FLASH and SSFP cine sequences at 1.5 vs. 3 Tesla: a validation study. *Journal of magnetic resonance imaging : JMRI*. 2006;24(2):312-8.
42. Vaziri SM, Larson MG, Benjamin EJ, Levy D. Echocardiographic predictors of nonrheumatic atrial fibrillation. The Framingham Heart Study. *Circulation*. 1994;89(2):724-30.
43. Xu Y, Zhao L, Zhang L, Han Y, Wang P, Yu S. Left Atrial Enlargement and the Risk of Stroke: A Meta-Analysis of Prospective Cohort Studies. *Frontiers in Neurology*. 2020;11(26).
44. Tsang TS, Barnes ME, Gersh BJ, Takemoto Y, Rosales AG, Bailey KR, Seward JB. Prediction of risk for first age-related cardiovascular events in an elderly population: the incremental value of echocardiography. *Journal of the American College of Cardiology*. 2003;42(7):1199-205.
45. Gulati A, Ismail TF, Jabbour A, Ismail NA, Morarji K, Ali A, Raza S, Khwaja J, Brown TD, Lioudakis E, Baksi AJ, Shakur R, Guha K, Roughton M, Wage R, Cook SA, Alpendurada F, Assomull RG, Mohiaddin RH, Cowie MR, Pennell DJ, Prasad SK. Clinical utility and prognostic value of left atrial volume assessment by cardiovascular magnetic resonance in non-ischaemic dilated cardiomyopathy. *European journal of heart failure*. 2013;15(6):660-70.

46. Elliott PM, Anastasakis A, Borger MA, Borggrefe M, Cecchi F, Charron P, Hagege AA, Lafont A, Limongelli G, Mahrholdt H, McKenna WJ, Mogensen J, Nihoyannopoulos P, Nistri S, Pieper PG, Pieske B, Rapezzi C, Rutten FH, Tillmanns C, Watkins H. 2014 ESC Guidelines on diagnosis and management of hypertrophic cardiomyopathy: the Task Force for the Diagnosis and Management of Hypertrophic Cardiomyopathy of the European Society of Cardiology (ESC). *European heart journal*. 2014;35(39):2733-79.
47. Upadhyay B, Taffet GE, Cheng CP, Kitzman DW. Heart failure with preserved ejection fraction in the elderly: scope of the problem. *Journal of Molecular and Cellular Cardiology*. 2015;83:73-87.
48. Taylor RJ, Moody WE, Umar F, Edwards NC, Taylor TJ, Stegemann B, Townend JN, Hor KN, Steeds RP, Mazur W, Leyva F. Myocardial strain measurement with feature-tracking cardiovascular magnetic resonance: normal values. *European heart journal cardiovascular Imaging*. 2015;16(8):871-81.
49. Mahrholdt H, Wagner A, Deluigi CC, Kispert E, Hager S, Meinhardt G, Vogelsberg H, Fritz P, Dippon J, Bock CT, Klingel K, Kandolf R, Sechtem U. Presentation, patterns of myocardial damage, and clinical course of viral myocarditis. *Circulation*. 2006;114(15):1581-90.
50. Schmacht L, Traber J, Grieben U, Utz W, Dieringer MA, Kellman P, Blaszczyk E, von Knobelsdorff-Brenkenhoff F, Spuler S, Schulz-Menger J. Cardiac Involvement in Myotonic Dystrophy Type 2 Patients With Preserved Ejection Fraction: Detection by Cardiovascular Magnetic Resonance. *Circulation Cardiovascular imaging*. 2016;9(7).
51. Blaszczyk E, Grieben U, von Knobelsdorff-Brenkenhoff F, Kellman P, Schmacht L, Funk S, Spuler S, Schulz-Menger J. Subclinical myocardial injury in patients with Facioscapulohumeral muscular dystrophy 1 and preserved ejection fraction - assessment by cardiovascular magnetic resonance. *Journal of cardiovascular magnetic resonance : official journal of the Society for Cardiovascular Magnetic Resonance*. 2019;21(1):25.
52. Mavrogeni S, Papavasiliou A, Skouteli E, Magoutas A, Dangas G. Cardiovascular magnetic resonance imaging evaluation of two families with Becker muscular dystrophy. *Neuromuscular disorders : NMD*. 2010;20(11):717-9.
53. Kanagala P, Cheng ASH, Singh A, Khan JN, Gulsin GS, Patel P, Gupta P, Arnold JR, Squire IB, Ng LL, McCann GP. Relationship Between Focal and Diffuse Fibrosis Assessed by CMR and Clinical Outcomes in Heart Failure With Preserved Ejection Fraction. *JACC Cardiovascular imaging*. 2019;12(11 Pt 2):2291-301.
54. Rosendahl L, Ahlander BM, Björklund PG, Blomstrand P, Brudin L, Engvall JE. Image quality and myocardial scar size determined with magnetic resonance imaging in patients with permanent atrial fibrillation: a comparison of two imaging protocols. *Clinical physiology and functional imaging*. 2010;30(2):122-9.
55. Captur G, Lobascio I, Ye Y, Culotta V, Boubertakh R, Xue H, Kellman P, Moon JC. Motion-corrected free-breathing LGE delivers high quality imaging and reduces scan time by half: an independent validation study. *The international journal of cardiovascular imaging*. 2019;35(10):1893-901.
56. Piehler KM, Wong TC, Puntil KS, Zareba KM, Lin K, Harris DM, Deible CR, Lacomis JM, Czeyda-Pommersheim F, Cook SC, Kellman P, Schelbert EB. Free-breathing, motion-corrected late gadolinium enhancement is robust and extends risk stratification to vulnerable patients. *Circulation Cardiovascular imaging*. 2013;6(3):423-32.

Eidesstattliche Versicherung

„Ich, Josephine Kermer, versichere an Eides statt durch meine eigenhändige Unterschrift, dass ich die vorgelegte Dissertation mit dem Thema: „Die kardiovaskuläre Magnetresonanztomographie in der Diagnostik der Herzinsuffizienz mit erhaltener Ejektionsfraktion“ selbstständig und ohne nicht offengelegte Hilfe Dritter verfasst und keine anderen als die angegebenen Quellen und Hilfsmittel genutzt habe.

Alle Stellen, die wörtlich oder dem Sinne nach auf Publikationen oder Vorträgen anderer Autoren/innen beruhen, sind als solche in korrekter Zitierung kenntlich gemacht. Die Abschnitte zu Methodik (insbesondere praktische Arbeiten, Laborbestimmungen, statistische Aufarbeitung) und Resultaten (insbesondere Abbildungen, Graphiken und Tabellen) werden von mir verantwortet.

Ich versichere ferner, dass ich die in Zusammenarbeit mit anderen Personen generierten Daten, Datenauswertungen und Schlussfolgerungen korrekt gekennzeichnet und meinen eigenen Beitrag sowie die Beiträge anderer Personen korrekt kenntlich gemacht habe (siehe Anteilserklärung). Texte oder Textteile, die gemeinsam mit anderen erstellt oder verwendet wurden, habe ich korrekt kenntlich gemacht.

Meine Anteile an etwaigen Publikationen zu dieser Dissertation entsprechen denen, die in der untenstehenden gemeinsamen Erklärung mit dem/der Erstbetreuer/in, angegeben sind. Für sämtliche im Rahmen der Dissertation entstandenen Publikationen wurden die Richtlinien des ICMJE (International Committee of Medical Journal Editors; www.icmje.org) zur Autorenschaft eingehalten. Ich erkläre ferner, dass ich mich zur Einhaltung der Satzung der Charité – Universitätsmedizin Berlin zur Sicherung Guter Wissenschaftlicher Praxis verpflichte.

Weiterhin versichere ich, dass ich diese Dissertation weder in gleicher noch in ähnlicher Form bereits an einer anderen Fakultät eingereicht habe.

Die Bedeutung dieser eidesstattlichen Versicherung und die strafrechtlichen Folgen einer unwahren eidesstattlichen Versicherung (§§156, 161 des Strafgesetzbuches) sind mir bekannt und bewusst.“

Datum

Unterschrift

Anteilserklärung an den vorliegenden Publikationen

Josephine Kermer hatte folgende Anteile an den vorliegenden Publikationen:

Publikation 1: **Kermer J**, Traber J, Utz W, Hennig P, Menza M, Jung B, Greiser A, Barckow P, von Knobelsdorff-Brenkenhoff F, Töpper A, Blaszczyk E, Schulz-Menger J. Assessment of diastolic dysfunction: comparison of different cardiovascular magnetic resonance techniques. ESC Heart Failure. 2020;7(5):2637-49.

Beitrag:

- Literaturrecherche
- Beteiligung an der Konzeption
- Ausarbeitung und Einreichung des Ethikantrags in Zusammenarbeit mit den Betreuern Prof. Dr. Jeanette Schulz-Menger, Dr. Julius Traber und dem Statistiker Dr. Carsten Schwenke
- Beteiligung an der Durchführung von Testläufen und Weiterentwicklung des Untersuchungsablaufs
- Komplettes Screening und überwiegende Rekrutierung (ca. 95%) der Probandinnen und Probanden
- Organisation der klinischen Untersuchungen (Echokardiographie, NT-proBNP- und LVEDP-Messung)
- Durchführung des 6 Minute-Walk-Tests
- Mitentwicklung des Auswerteprozesses basierend auf Literaturrecherche, Softwaremöglichkeiten und interdisziplinären Diskussionsrunden
- Etablierung der Auswertemethode und komplett Datenauswertung (Auswertung aller Daten zu linksatrialen bzw. linksventrikulären Dimensionen und Funktion sowie transmitralen Flussgeschwindigkeiten, aller Tagging-, Tissue Tracking- und Tissue Phase Mapping Daten)
- Kommunikation mit den entsprechenden Ansprechpartnern und Management von Problemen bezüglich der post-processing Software
- Statistische Auswertung und Interpretation der Daten
- Entwurf des kompletten Manuskripts, aller Tabellen (Tbl. 1-2 im Paper sowie Tbl. S1-S2 in den *Supporting Information*) und aller Abbildungen (Abb. 1-4)
- Diskussion mit den Koautoren
- Revision von Manuskript, Tabellen und Abbildungen

Publikation 2: Funk S, **Kermer J**, Doganguezel S, Schwenke C, von Knobelsdorff-Brenkenhoff F, Schulz-Menger J. Quantification of the left atrium applying cardiovascular magnetic resonance in clinical routine. Scandinavian cardiovascular journal : SCJ. 2018;1-8.

Beitrag:

- Beteiligung an der Konzeption der Auswertungsmethoden
- Auswertung des kompletten Datensatzes
- Diskussion unklarer Fälle
- Kritische Revision der Manuskriptentwürfe, Tabellen und Abbildungen

Publikation 3: Muehlberg F, Arnhold K, Fritschi S, Funk S, Prothmann M, **Kermer J**, Zange L, von Knobelsdorff-Brenkenhoff F, Schulz-Menger J. Comparison of fast multi-slice and standard segmented techniques for detection of late gadolinium enhancement in ischemic and non-ischemic cardiomyopathy – a prospective clinical cardiovascular magnetic resonance trial. Journal of cardiovascular magnetic resonance : official journal of the Society for Cardiovascular Magnetic Resonance. 2018;20.

Beitrag:

- Auswertung eines Teils der Daten als Interobserver (30 Fälle)
- Diskussion unklarer Fälle im Rahmen der Interobserverauswertung
- Kritische Revision der Manuskriptentwürfe, Tabellen und Abbildungen

Datum und Unterschrift der betreuenden Hochschullehrerin

Datum und Unterschrift der Doktorandin

Assessment of diastolic dysfunction: comparison of different cardiovascular magnetic resonance techniques

Josephine Kermer¹, Julius Traber¹, Wolfgang Utz¹, Pierre Hennig¹, Marius Menza², Bernd Jung³, Andreas Greiser⁴, Philipp Barckow⁵, Florian von Knobelsdorff-Brenkenhoff^{1,6}, Agnieszka Töpper^{1,7}, Edyta Blaszczyk^{1,8} and Jeanette Schulz-Menger^{1,8,9*}

¹Charité—Universitätsmedizin Berlin, corporate member of Freie Universität Berlin, Humboldt-Universität zu Berlin, and Berlin Institute of Health, Working Group on Cardiovascular Magnetic Resonance, Experimental and Clinical Research Center, a joint cooperation between the Charité Medical Faculty and the Max Delbrück Center for Molecular Medicine, Lindenberger Weg 80, Berlin, 13125, Germany; ²Department of Radiology, Medical Physics, Medical Center—University of Freiburg, Faculty of Medicine, University of Freiburg, Freiburg, Germany; ³Institute of Diagnostic, Interventional and Paediatric Radiology, University Hospital Bern, Bern, Switzerland; ⁴Siemens Healthineers GmbH, Erlangen, Germany; ⁵Circle Cardiovascular Imaging Inc., Calgary, Alberta, Canada; ⁶Department of Cardiology, Clinic Agatharied, Academic Teaching Hospital of the Ludwig-Maximilians-University of Munich, Munich, Germany; ⁷Zentrum für Innere Medizin, Kardiologie, Angiologie und Notfallambulanz, Johanniter-Krankenhaus Genthin-Stendal, Akut- und Schwerpunktkrankenhaus, Akademisches Lehrkrankenhaus Otto-von-Guericke-Universität Magdeburg, Stendal, Germany; ⁸DZHK (German Centre for Cardiovascular Research), partner site Berlin, Berlin, Germany; ⁹Department of Cardiology and Nephrology, HELIOS-Kliniken Berlin-Buch, Schwanebecker Chaussee 50, Berlin, 13125, Germany

Abstract

Aims Heart failure with preserved ejection fraction is still a diagnostic and therapeutic challenge, and accurate non-invasive diagnosis of left ventricular (LV) diastolic dysfunction (DD) remains difficult. The current study aimed at identifying the most informative cardiovascular magnetic resonance (CMR) parameters for the assessment of LVDD.

Methods and results We prospectively included 50 patients and classified them into three groups: with DD (DD+, $n = 15$), without (DD−, $n = 26$), and uncertain (DD±, $n = 9$). Diagnosis of DD was based on echocardiographic E/E', invasive LV end-diastolic pressure, and N-terminal pro-brain natriuretic peptide. CMR was performed at 1.5 T to assess LV and left atrial (LA) morphology, LV diastolic strain rate (SR) by tissue tracking and tagging, myocardial peak velocities by tissue phase mapping, and transmural inflow profile using phase contrast techniques. Statistics were performed only on definitive DD+ and DD− (total number 41). DD+ showed enlarged LA with LA end-diastolic volume/height performing best to identify DD+ with a cut-off value of ≥ 0.52 mL/cm (sensitivity = 0.71, specificity = 0.84, and area under the receiver operating characteristic curve = 0.75). DD+ showed significantly reduced radial (inferolateral E peak: DD−: $-14.5 \pm 6.5\%$ /s vs. DD+: $-10.9 \pm 5.9\%$ /s, $P = 0.04$; anterolateral A peak: DD−: $-4.2 \pm 1.6\%$ /s vs. DD+: $-3.1 \pm 1.4\%$ /s, $P = 0.04$) and circumferential (inferolateral A peak: DD−: $3.8 \pm 1.2\%$ /s vs. DD+: $2.8 \pm 0.8\%$ /s, $P = 0.007$; anterolateral A peak: DD−: $3.5 \pm 1.2\%$ /s vs. DD+: $2.5 \pm 0.8\%$ /s, $P = 0.048$) SR in the basal lateral wall assessed by tissue tracking. In the same segments, DD+ showed lower peak myocardial velocity by tissue phase mapping (inferolateral radial peak: DD−: -3.6 ± 0.7 ms vs. DD+: -2.8 ± 1.0 ms, $P = 0.017$; anterolateral longitudinal peak: DD−: -5.0 ± 1.8 ms vs. DD+: -3.4 ± 1.4 ms, $P = 0.006$). Tagging revealed reduced global longitudinal SR in DD+ (DD−: $45.8 \pm 12.0\%$ /s vs. DD+: $34.8 \pm 9.2\%$ /s, $P = 0.022$). Global circumferential and radial SR by tissue tracking and tagging, LV morphology, and transmural flow did not differ between DD+ and DD−.

Conclusions Left atrial size and regional quantitative myocardial deformation applying CMR identified best patients with DD.

Keywords Diastolic dysfunction; Cardiovascular magnetic resonance; Tissue tracking; Left atrium; Myocardial deformation; Heart failure with preserved ejection fraction

Received: 29 December 2019; Revised: 9 May 2020; Accepted: 1 June 2020

*Correspondence to: Jeanette Schulz-Menger, Charité—Universitätsmedizin Berlin, corporate member of Freie Universität Berlin, Humboldt-Universität zu Berlin, and Berlin Institute of Health, Working Group on Cardiovascular Magnetic Resonance, Experimental and Clinical Research Center, a joint cooperation between the Charité Medical Faculty and the Max Delbrück Center for Molecular Medicine, Lindenberger Weg 80, 13125 Berlin, Germany. Tel: +49 30 450 553 746; Fax: +49 30 450 553 949. Email: jeanette.schulz-menger@charite.de

Introduction

Heart failure (HF) with preserved ejection fraction (HFpEF) is prevalent in up to 50% of HF patients.¹ According to the 2016 European Society of Cardiology guidelines for the diagnosis and treatment of acute and chronic HF, HFpEF is defined as the presence of symptoms or signs of HF combined with left ventricular ejection fraction (LVEF) $\geq 50\%$ and evidence of left ventricular (LV) diastolic dysfunction (DD).² In contrast to HF with reduced ejection fraction, survival of HFpEF could not be improved in the last decades, although mortality is comparable between both groups.¹ The causes are complex and still subject of active research. In 2007, it was recommended to diagnose DD based on either invasive quantification of LV end-diastolic pressure or echocardiographic evaluation of LV diastolic function using the ratio (E/E') of early transmitral flow velocity (E) assessed by blood flow Doppler to tissue Doppler-derived early diastolic lengthening velocities (E') or by combination of echocardiographic parameters and N-terminal pro-brain natriuretic peptide as HF biomarker.² The non-invasive diagnosis remains challenging, even though different innovative parameters were introduced applying echocardiography³ as well as cardiovascular magnetic resonance (CMR).

CMR has the capability to identify and differentiate myocardial injury already in preserved ejection fraction as reflected in the recent guidelines of chronic HF.⁴ It is also known as the gold standard for assessment of LV volume and function and offers various techniques to characterize the myocardium. Assessment of DD applying CMR is not yet a clinical routine. Different approaches were evaluated and mostly compared with echocardiography as the diagnostic standard.^{5,6}

Similar to Doppler echocardiography, CMR is able to quantify transmitral flow using phase contrast (PC) imaging techniques. Early and late diastolic flow velocity peaks can be quantified and used for evaluation of LV diastolic function.⁷ CMR tissue phase mapping (TPM) offers the possibility to assess velocities of myocardial deformation.⁸ CMR tagging allows the quantification of myocardial strain based on an intrinsic tissue grid generated by magnetization saturation of specific myocardial localizations.⁹ Tissue tracking is a recently introduced post-processing method to quantify myocardial strain. It is based on voxel-related quantification of myocardial deformation using standard cine CMR images.¹⁰

Several studies have demonstrated the applicability of these techniques to evaluate diastolic LV function in both healthy^{8,11} and diseased patients,^{12–18} using different comparators.

The aim of our study was to evaluate the capability of different CMR parameters and techniques to detect DD.

Methods

Study population

Patients aged between 18 and 85 years with indication for elective left heart catheterization including coronary angiography were screened and prospectively enrolled into the study. Inclusion criterion was a preserved LVEF $\geq 50\%$. Exclusion criteria included common contraindications for CMR, pregnancy, cardiac arrhythmia, left bundle branch block, previously known infarction scars located at the lateral or septal LV wall, pericardial disease, moderate to severe valvular heart disease, history of valvular or bypass surgery, severe liver disease, impaired renal function (estimated glomerular filtration rate <60 mL/min/m²), severe pulmonary disease (\geq COPD GOLD II), pulmonary arterial hypertension, active cancer, or severe infections.

We identified patients with (DD+), without (DD−), or uncertain (DD±) DD according to Paulus *et al.*² by quantification of echocardiographic E/E', invasive LV end-diastolic pressure, and N-terminal pro-brain natriuretic peptide (Figure 1A). A 6 min walk test was performed to objectify functional exercise capacity according to the guidelines of the American Thoracic Society. We aimed at completing the whole study protocol within 24 h (Figure 1B).

Written informed consent was obtained from all patients. The study was approved by the institutional ethical board and complies with the Declaration of Helsinki.

Cardiovascular magnetic resonance

CMR was performed on a clinical 1.5 T MR scanner (Avanto, Siemens Healthineers, Erlangen, Germany) using a 12-channel phased-array coil. Image data were acquired electrocardiogram-gated and in end-expiratory breath-hold.

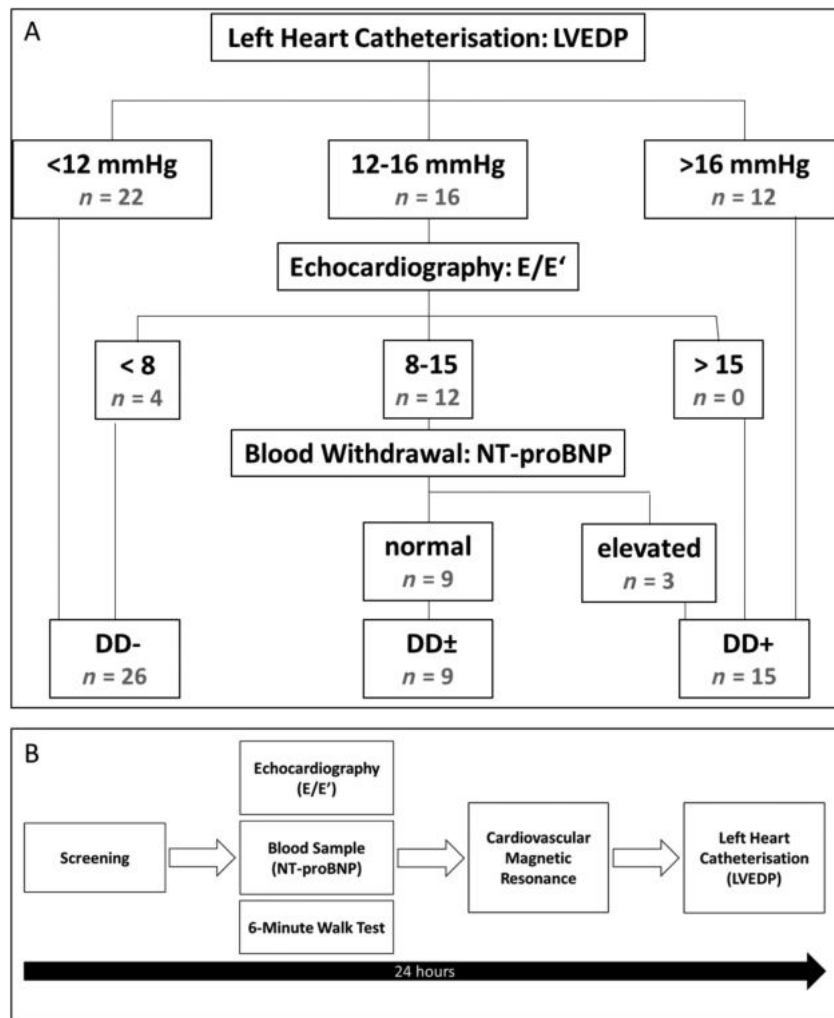
Assessment of the left ventricle and the left atrium

To assess LV and left atrial (LA) morphology and function, we acquired three long-axis (LAX) planes in two-chamber, three-chamber, and four-chamber views of the LV as well as two stacks of short-axis (SAX) views covering the entire LV or LA, respectively, using standard cine steady-state free precession (SSFP) sequences [temporal resolution 34.7 ms; echo time (TE) 1.2 ms; field of view (FOV) 292 × 360 mm²; LAX: slice thickness 6 mm and matrix 156 × 192//LV SAX: slice thickness 7 mm, spacing 3 mm, and matrix 208 × 256; and LA SAX: slice thickness 5 mm, no gap¹⁹].

Left ventricular cine images for tissue tracking

Cine SSFP images in LAX four-chamber views and three SAX slices (basal, midventricular, and apical) were acquired with a high temporal resolution of 13.8 ms (TE 1.2 ms, 64 phases,

Figure 1 (A) Study group definition and number of patients. (B) Study protocol. LVEDP, left ventricular end-diastolic pressure; NT-proBNP, N-terminal pro-brain natriuretic peptide.



matrix 208×256 , FOV 325×400 mm 2 , slice thickness 8 mm, and in-plane resolution 1.6×1.6 mm 2) to evaluate diastolic strain rate (SR) by tissue tracking.

Tagging

LAX four-chamber views and three SAX slices (basal, midventricular, and apical) were used to perform SSFP spatial modulation of magnetization (SPAMM) tagging and complementary SPAMM (CSPAMM) tagging for evaluation of diastolic SR (temporal resolution SPAMM/CSPAMM 21.1 ms/42.3 ms, TE 1.3 ms, matrix 256×256 , FOV 300×300 mm 2 , slice thickness 6 mm, flip angle 20°, tag spacing 7 mm, and one slice per breath-hold).²⁰

Tissue phase mapping

TPM imaging of three SAX slices (basal, midventricular, and apical) was acquired to assess myocardial peak velocities

using a black blood prepared gradient echo TPM sequence [temporal resolution of 17.1 ms, TE 3.9 ms, matrix 120×160 , FOV 255×340 mm 2 , slice thickness 8 mm, velocity encoding (VENC) in-plane 15 cm/s, VENC through plane 25 cm/s, and one slice per breath-hold].¹⁵

Phase contrast—transmural flow

We performed PC imaging in basal SAX positioned at the level of the mitral valve tips during end-diastole and perpendicular to the transmural inflow to analyse transmural flow velocities (temporal resolution of 17.4 ms, TE 2.4 ms, 64 phases, matrix 176×256 , FOV 220×320 mm 2 , slice thickness 5.5 mm, in-plane resolution 1.3×1.3 mm 2 , and VENC 120 cm/s). Two more SAX slices were acquired above and below this slice without gap. Each acquisition was repeated a second time.

Post-processing analysis

Assessment of the left ventricle and the left atrium

Analysis of LV and LA morphology was performed with commercially available software (cv42 Version 4.1.3, Circle Cardiovascular Imaging Inc., Calgary, Canada). LV epicardial and endocardial contours were traced manually in end-systole and end-diastole to assess LV mass (LVM), LV end-diastolic volume (LVEDV) and LV end-systolic volume, LV stroke volume, LVEF, and LV remodelling index as the ratio of LVEDV and LVM.^{21,22} Papillary muscles were traced separately.

The stack of LA SAX was analysed similarly. LA systole and LA diastole were defined as phases of minimal or maximal LA dimensions. Pulmonary veins and atrial appendage were excluded.²³ LA minimal and maximum volumes (LA-EDV), LA stroke volume, and LA ejection fraction were assessed. Normalization to body surface area (BSA) and body height (H) was performed for LVM, LVEDV, LV end-systolic volume, and the volumetric LA parameters.

LA area was measured in the LAX cine SSFP images in the two-chamber, three-chamber, and four-chamber views. Pulmonary veins were excluded, and LA appendage was included.¹⁹ Longitudinal and transversal diameters were defined in two-chamber and four-chamber views as well.¹⁹

Tissue tracking

Two-dimensional tissue tracking was performed using cv42 prototype 5.3.0 (Circle Cardiovascular Imaging Inc.). End-diastolic contours of LV endocardium and epicardium were defined in all slices excluding papillary muscles. For regional analysis, a basal SAX reference point was set at the anterior insertion of the right ventricle. The deformation analysis was performed automatically. Radial (Err) and circumferential (Ecc) myocardial deformation were evaluated based on SAX analysis, LAX four-chamber view was used to assess longitudinal (Ell) strain parameters. Global preE, E, and A peaks of diastolic SR were defined as shown in *Figure 2C*. SR peaks were determined manually for each slice and each direction of movement.

The analysis was performed both per slice and per segment to identify regional differences. The segmentation was based on the 16-segment model according to the American Heart Association.²⁴ We excluded the assessment of preE in the regional evaluation but determined the maximum peak (Ecc max and Err max) during the whole diastolic phase (time between aortic valve closure and mitral valve closure). In case of undefinable E and A, only maximum peaks during the whole diastole were assessed.

Tagging

Tagging images were analysed using CIM Tag2D Heart Deformation WIP20 (Heart Deformation post-processing prototype 2.0, Auckland MRI Research Group, University of Auckland, Auckland, New Zealand). LV endocardium and epicardium as

well as insertions of the right ventricle were defined in end-diastole. Myocardial tags were contoured semi-automatically in all phases of each slice. To achieve a maximum accordance of image tag lines and overlaid analysing grid, the model stripes were adapted every second (CSPAMM) to fourth (SPAMM) frame using additional guide points.¹⁸ We generated Ecc SR from SAX and Ell SR out of LAX four-chamber view images. Peak diastolic SR was defined as first peak after end-systole. Global and segmental (six segments per slice) analyses were performed.

Tissue phase mapping

Post-processing analysis was performed using MATLAB (The MathWorks, Inc., Natick, MA, USA). Epicardial and endocardial contours were defined semi-automatically for each phase of each slice before starting myocardial velocity measurements as described recently.¹⁵ Peak diastolic radial (Vr) and longitudinal (Vz) velocities were assessed for global and segmental analysis. Regional analysis was based on the 16-segment model according to the American Heart Association.²⁴

Phase contrast—transmural flow

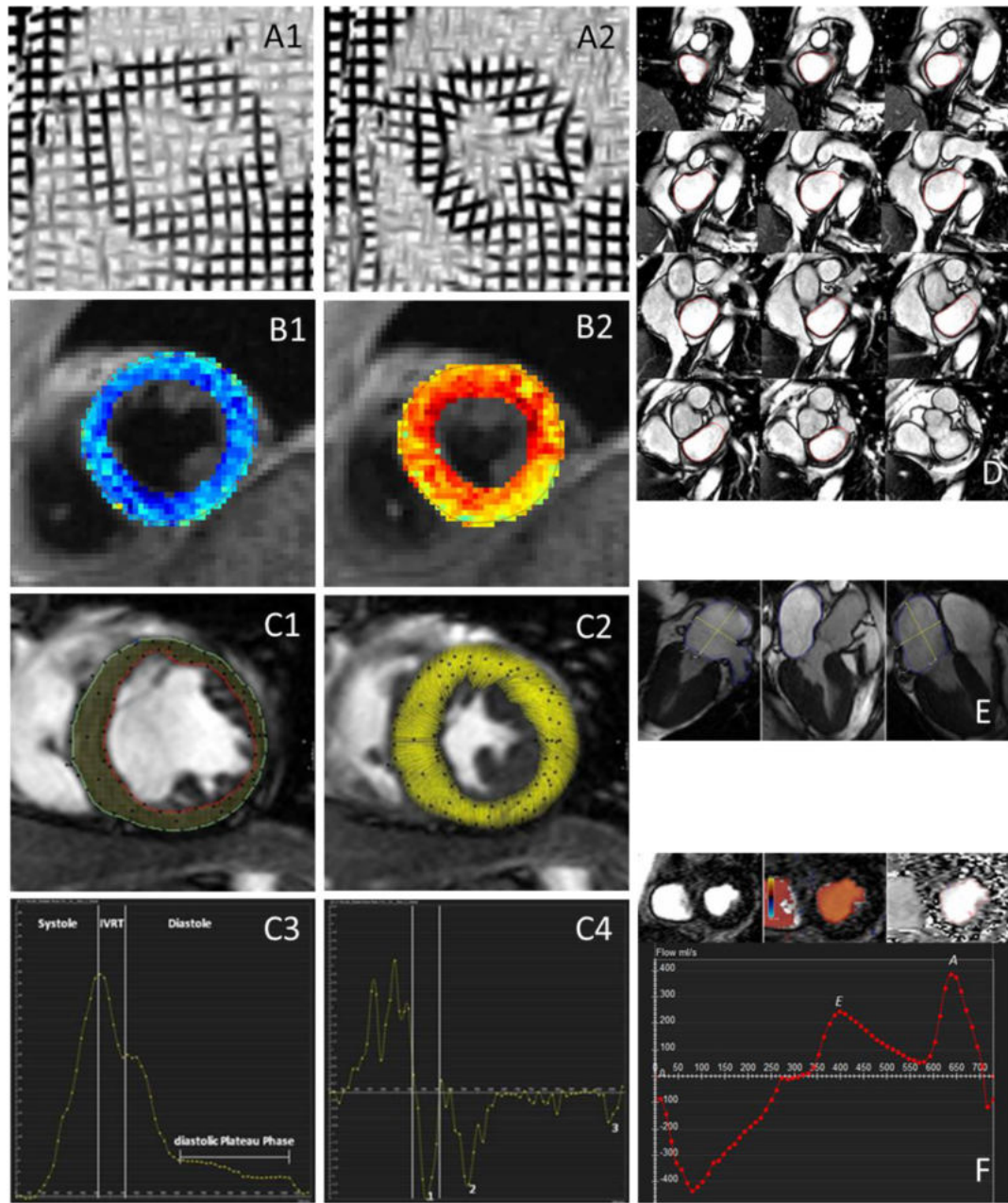
cv42 (Version 4.1.3, Circle Cardiovascular Imaging Inc.) was used to perform post-processing analysis of PC velocity measurements. The slice showing best the mitral valve tip separation was chosen. Regions of interest were set semi-automatically based on colour-coded display of transmural blood flow. Early (E) and late (A) diastolic peak velocities were derived from transmural flow velocity curves. For statistical analysis, we used mean values of repeated measurements of E, A, and the ratio E/A.

Non-diagnostic images due to breath-hold artefacts or malpositioning were excluded.

Statistical analysis

Statistical analyses were performed by relying only on DD+ ($n = 15$) and DD- ($n = 26$, i.e. in total 41 patients) groups as our aim was to identify a CMR parameter, which would best meet the published criteria to identify definite DD. Data are shown as mean \pm standard deviation. Statistical tests were performed using IBM SPSS Statistics 25 (IBM Corp., Armonk, NY, USA). Mann–Whitney *U* test was used for analysis of group differences, whereas significance was stated at $P < 0.05$. Correlation analysis was performed using the Spearman correlation coefficient. Receiver operating characteristic (ROC) curve analyses were established to define cut-off values. As the aim of this study was the identification of parameters with discriminatory power, no formal sample size calculation was performed.

Figure 2 Overview cardiovascular magnetic resonance techniques. Left ventricular–midventricular short-axis view of myocardial deformation via tagging in (A1) end-diastole and (A2) end-systole. Left ventricular–midventricular short-axis view of colour-encoded myocardial velocity tissue phase mapping in (B1) end-diastole and (B2) end-systole. Assessment of cardiovascular magnetic resonance tissue tracking: (C1) end-diastolic contouring and tissue tracking and (C2) end-systolic myocardial deformation. (C3) Radial strain and (C4) strain rate: the graphs show phases of one cardiac cycle. The definitions were as follows: end-systole = phase of aortic valve closure; isovolumetric relaxation time (IVRT) = time between end-systole and mitral valve opening; and end-diastole = phase of mitral valve closure. Peaks of myocardial strain rate were defined as follows: (i) preE = peak within IVRT; (ii) E = peak between mitral valve opening and start of diastolic plateau phase; and (iii) A = peak between end of diastolic plateau phase and end-diastole. (D) Stack of short-axis views of left atrial (LA) and contouring in LA diastolic phase. (E) Measurement of LA plane and diameters in long-axis two-chamber, three-chamber, and four-chamber views. (F) Assessment of phase contract transmural flow velocities: basal short-axis views with and without colour-encoded visualization and contouring of the mitral annulus; transmural flow velocity curve with early (E) and late (A) diastolic peak velocities.



Results

Study population

We screened 741 patients with an indication for LV catheterization between May 2013 and June 2014. Fifty-nine met our criteria and were included, with 39% having their first invasive procedure due to suspected coronary artery disease and 61% having suspicion of progression of their known coronary artery disease. Nine out of these 59 patients dropped out because of arrhythmia, EF < 50% as defined by CMR, claustrophobia, aortic stenosis, or increased LVEDV index, resulting in $n = 50$ as the final sample. We finally identified 26 DD–, 15 DD+, and 9 DD±. DD+ showed significant higher body mass index compared with DD–. For detailed demographics, see Table 1. In 40 out of 50 cases, examinations could be performed within 24 h (mean 25.4 h; range 16.3–91.1 h). Walking distance did not differ significantly between DD+ and DD– ($P = 0.129$). ROC curve analyses showed an area under the ROC curve (AUC) of 0.663 (Figure 3).

Cardiovascular magnetic resonance analysis

Data analysis was performed in all patients. Detailed data are given in Supporting Information, Tables S1 and S2.

Assessment of the left ventricle and the left atrium

Two cases had to be excluded. Results are given in Table 2. LV volumes and LVM did not show significant differences between DD+ and DD–.

Left atrial size was larger in DD+ with significantly higher LA-EDV and LA area. The difference remained significant

when normalizing to body height. ROC curve analysis (Figure 3) showed best results for LA-EDV/H with a cut-off value of ≥ 0.52 mL/cm (sensitivity = 0.71, specificity = 0.84, AUC = 0.75, and accuracy = 0.75) to differentiate between DD+ and DD–.

Tissue tracking

Five cases had to be excluded. Global analysis did not show significant differences. Results of regional analysis are shown in Figure 4A. In 53 out of 992 segments, only maximum peaks during the whole diastole were assessed. DD+ presented impaired E and A with significant reductions in basal inferolateral, anterolateral, and apical anterior segments. Furthermore, Err max of DD+ was significantly lower in the basal anterolateral segment (DD–: $-16.5 \pm 7.94\%$ /s vs. DD+: $-9.8 \pm 3.85\%$ /s, $P = 0.011$).

Tagging

We had to exclude 18 out of 666 segments in SPAMM data and 24 out of 630 segments in CSPAMM data. SPAMM showed reduced global EII SR in DD+ (DD–: $45.8 \pm 12.0\%$ /s vs. DD+: $34.8 \pm 9.2\%$ /s, $P = 0.022$). Further global and segmental amplitude of Ecc and EII diastolic SR did not differ significantly between DD+ and DD– (Figure 4C).

Tissue phase mapping

Forty-four out of 560 mostly apical located segments had to be excluded. The amount of global diastolic peak velocities reached statistical significance in apical Vz (DD–: -2.7 ± 0.6 cm/s vs. DD+: -2.2 ± 1.0 cm/s, $P = 0.029$). Results of segmental evaluation are visualized in Figure 4B. Vz and Vr differ significantly in the basolateral segments.

Table 1 Characteristics of the study population

	Study groups		
	Without diastolic dysfunction (DD–)	Uncertain diastolic function (DD±)	With diastolic dysfunction (DD+)
Sample size (n)	26	9	15
Sex (male female)	16 10	9 0	9 6
Age (years)	66.6 ± 8.9	68.0 ± 7.3	70.5 ± 7.4
BMI (kg/m ²)	26.7 ± 3.0	28.6 ± 4.7	$29.7 \pm 3.2^*$
6MWD (m)	509 ± 76	487 ± 114	446 ± 122
LVEDP (mmHg)	8 ± 3	$14 \pm 1^*$	$20 \pm 5^{\dagger}$
E/E'	8.5 ± 2.0	$10.8 \pm 1.4^*$	$10.1 \pm 2.0^*$
NT-proBNP (ng/mL)	184 ± 151	157 ± 107	447 ± 422
Heart rate (b.p.m.)	68 ± 11	70 ± 11	64 ± 8
Arterial hypertension (%)	84.6	100.0	93.3
Coronary artery disease (%)	88.5	100.0	80.0
One-vessel disease (%)	23.1	33.3	26.7
Two-vessel disease (%)	34.6	55.6	20.0
Three-vessel disease (%)	30.8	11.1	33.3
Diabetes mellitus (%)	34.6	11.1	33.3
Hyperlipoproteinemia (%)	38.5	66.7	60.0

6MWD, 6 min walking distance; BMI, body mass index; E/E', ratio of early transmural flow velocity (E) and early diastolic lengthening velocity (E'); LVEDP, left ventricular end-diastolic pressure; NT-proBNP, N-terminal pro-brain natriuretic peptide.

Data are shown as mean \pm standard deviation.

*For $P < 0.05$ compared with DD–.

†For $P < 0.05$ compared with DD±.

Figure 3 Diagnostic performance of measurements of the left atrium and walking distance to identify diastolic dysfunction. (A) Receiver operating characteristic curves of left atrial (LA) end-diastolic volume (EDV), area of three-chamber view, and triplane mean area indexed to height (H). (B) Receiver operating characteristic curve of walking distance assessed by 6 min walk test.

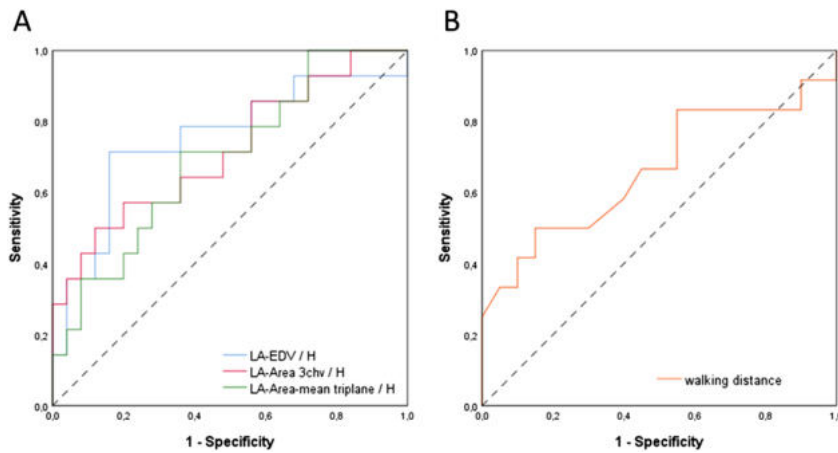


Table 2 Findings of LV and LA analysis of DD– and DD+

	DD–	DD+	P-value
Left ventricle			
LVEDV (mL)	122.6 ± 34.3	130.5 ± 32.4	0.429
LVEDV/BSA (mL/m ²)	63.7 ± 14.0	66.3 ± 14.9	0.639
LV-SV (mL)	83.3 ± 21.3	86.0 ± 22.2	0.548
LVEF (%)	69.0 ± 7.6	66.0 ± 7.4	0.334
LVM (g)	96.5 ± 29.9	110.2 ± 30.6	0.092
LVM/H (g/cm)	0.6 ± 0.1	0.7 ± 0.2	0.050
LVM/BSA (g/m ²)	49.9 ± 11.3	55.6 ± 12.3	0.079
LVRI (g/mL)	0.8 ± 0.1	0.9 ± 0.2	0.412
Left atrium—quantification based on full coverage (volume)			
LA-EDV (mL)	74.4 ± 17.2	93.3 ± 26.2	0.014*
LA-EDV/H (mL/cm)	0.4 ± 0.1	0.6 ± 0.1	0.010*
LA-EDV/BSA (mL/m ²)	39.2 ± 8.9	46.6 ± 12.0	0.069
LA-SV (mL)	38.7 ± 8.4	41.2 ± 13.0	0.578
LAEF (%)	52.7 ± 7.4	45.7 ± 13.1	0.151
Left atrium—quantification based on area			
LA area 4CV (mm ²)	20.1 ± 6.2	22.1 ± 5.4	0.169
LA area 4CV/H (mm ² /cm)	0.12 ± 0.03	0.13 ± 0.03	0.188*
LA area 3CV (mm ²)	18.6 ± 3.8	22.3 ± 5.9	0.033*
LA area 3CV/H (mm ² /cm)	0.11 ± 0.02	0.13 ± 0.03	0.026*
LA area 2CV (mm ²)	20.4 ± 5.5	24.8 ± 5.6	0.035*
LA area 2CV/H (mm ² /cm)	0.12 ± 0.03	0.15 ± 0.03	0.061
LA area mean biplane (mm ²)	20.2 ± 5.5	23.5 ± 4.8	0.084
LA area mean biplane/H (m ² /cm)	0.12 ± 0.03	0.14 ± 0.03	0.079
LA area mean triplane (mm ²)	19.7 ± 4.6	23.1 ± 5.1	0.084*
LA area mean triplane/H (m ² /cm)	0.12 ± 0.03	0.13 ± 0.03	0.046*

2/3/4CV, two-chamber/three-chamber/four-chamber view; BSA, body surface area; DD–, patients without diastolic dysfunction; DD+, patients with diastolic dysfunction; EDV, end-diastolic volume; H, body height; LA, left atrial; LAEF, left atrial ejection fraction; LV, left ventricular; LVEF, left ventricular ejection fraction; LVM, left ventricular mass; LVRI, left ventricular remodelling index; SV, stroke volume. Data are shown as mean ± standard deviation.

*For $P < 0.05$.

Phase contrast—transmitral flow

For assessment of transmitral flow, two cases had to be excluded. Neither E (DD–: 0.5 ± 0.1 cm/s vs. DD+: 0.5 ± 0.1 cm/s, $P = 0.689$) nor A (DD–: 0.6 ± 0.2 cm/s vs. DD+: 0.6 ± 0.2 cm/s, $P = 0.753$) or E/A (DD–: 0.8 ± 0.3 vs. DD+: 1.1 ± 0.9 , $P = 0.441$) differed significantly between DD– and DD+.

Discussion

CMR provides various techniques to assess cardiac structure and function.²⁵ In this study, we are providing for the first time a comparison of CMR parameters of diastolic function with a published gold standard including invasive measurements. Based on the quantification of LA size, a cut-off can be derived to identify

Figure 4 Regional myocardial differences between patients with and without diastolic dysfunction. Significant differences are highlighted in red. (A) Tissue tracking: early (E) and atrial (A) diastolic peaks of circumferential and radial strain rate \pm standard deviation. P-values of segments showing significant differences are Ecc A peak: basal inferolateral ($P = 0.007$) and apical anterior ($P = 0.014$); Err E peak: basal inferolateral ($P = 0.030$); and Err A peak: basal inferolateral ($P = 0.033$) and apical anterior ($P = 0.019$). (B) Tissue phase mapping (TPM) radial and longitudinal peak diastolic velocities \pm standard deviation. P-values of segments showing significant differences are Vr basal inferolateral ($P = 0.018$), Vz basal anterolateral ($P = 0.007$), and Vz medial anterior ($P = 0.044$). (C) Tagging [spatial modulation of magnetization (SPAMM) and complementary spatial modulation of magnetization (CSPAMM)]: diastolic peak of circumferential strain rate \pm standard deviation.

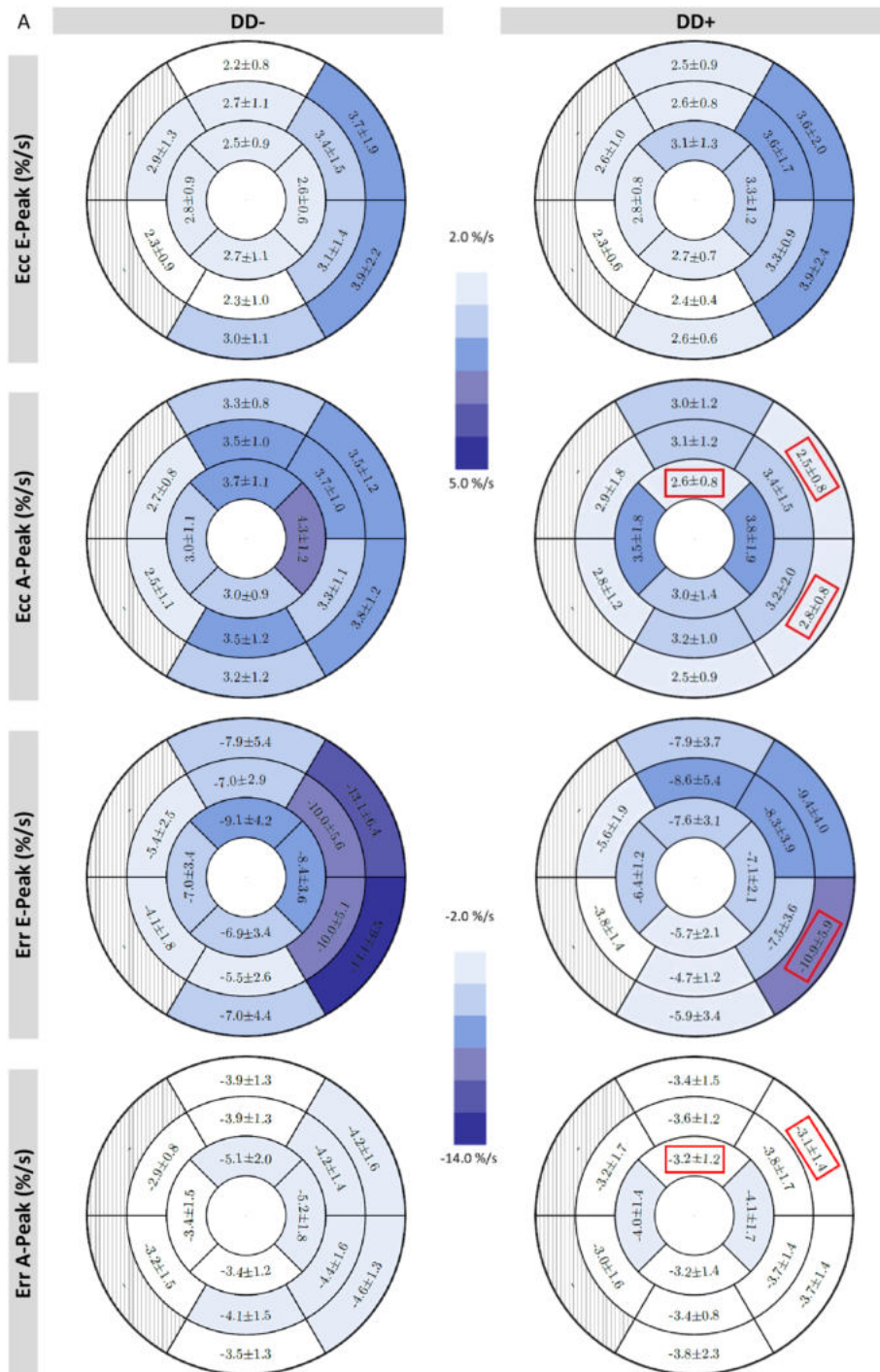
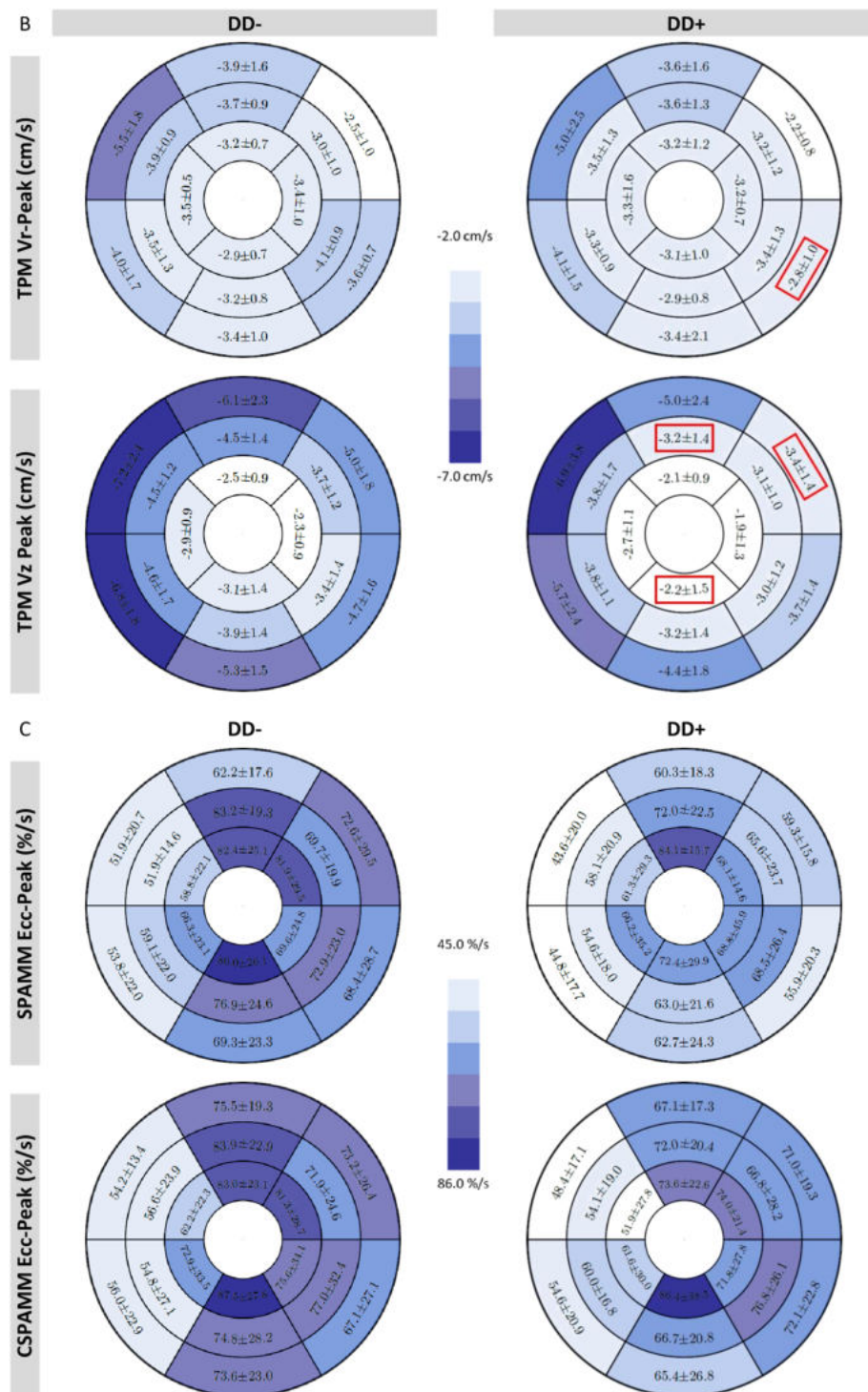


Figure 4 Continued



DD. Furthermore, quantification of diastolic LV deformation has been found to be predictive to identify patients with DD.

Specifically, our main findings are as follows:

- i Enlarged LA dimensions of $LA-EDV/H \geq 0.52 \text{ mL/cm}$ have a diagnostic accuracy of 0.75 (AUC = 0.75) on our data to identify DD.
- ii Tissue tracking and TPM reveal impaired diastolic deformation of the basal lateral wall in DD+ as a direct sign of DD.

LA enlargement is well known in LVDD, caused by a chronic increase of LV filling pressure due to impaired relaxation and reduced compliance.²⁶ LA dilatation already is part of the diagnostic algorithm of DD in both the consensus statement of the Heart Failure and Echocardiography Association of the European Society of Cardiology published in 2007² and the current recommendations of the American Society of Echocardiography and the European Association of Cardiovascular Imaging published in 2016.³ They recommended cut-off values of 40 and 34 mL/m², respectively, for echocardiographic LA maximal volume indexed to BSA. LA-EDV/BSA did not show significant differences between DD+ and DD- in our study. Compared with the echocardiographic cut-offs, both groups reached borderline or higher mean values (DD-: $39.2 \pm 8.9 \text{ mL/m}^2$ vs. DD+: $46.6 \pm 12.0 \text{ mL/m}^2$), but echocardiography is known to show systematically smaller LA volumes as compared with CMR.²⁷ Furthermore, our DD+ group had a significantly higher body mass index than DD-. Patel *et al.*²⁸ showed that LA-EDV/BSA underestimates the prevalence of LA enlargement in obese populations, whereas the level of obesity did not affect indices to height. As increased LA volume is associated with prognosis and cardiovascular events,²⁶ investigation of LA size is of general importance. But enlarged LA size is correlated with both HFpEF and HF with reduced EF.²⁹

In our study, LA volume quantification was based on the evaluation of a stack of SAX as reported by Maceira *et al.*¹⁹ In principle, it could also be assessed by reliance on transverse slices, which is mainly used in congenital heart disease and has also recently been applied in the detection of subclinical atrial fibrillation.^{30,31} As a consequence, more subtle differences that might be captured by transverse slices may have been missed. Currently, there are no head-to-head comparisons published regarding superiority, for example, to predict outcome. Unfortunately, constraints in scan time did not allow to collect scans in the transverse orientation. If scan time is limited, it is also acceptable to assess LA volume by two-dimensional area-length method.²³

A 6 min walk test is one of the most popular clinical exercise tests.³² It is often used to objectify and compare functional exercise capacity between different groups or before and after medical interventions. In our study, walking distance did not differ significantly between DD+ and DD-. Furthermore, ROC curve analyses showed numerically better

diagnostic ability for LA-EDV/H than walking distance without reaching statistical significance.

Echocardiographic E and A peaks of transmural flow are part of the clinical standard for estimating LV filling pressure and grading DD.³ PC imaging is able to assess blood flow velocities.⁷ Our study was not designed to compare equivalent echocardiographic and CMR parameters. But previous studies showed good correlation between echocardiographic and CMR-derived parameters and a general underestimation of transmural flow parameters by CMR.³³⁻³⁵ In our study, E and A peaks as well as E/A ratio did not differ significantly between DD+ and DD-. Graca *et al.* studied 48 healthy volunteers using CMR and detected a higher prevalence of DD in men than in women. They defined and graded DD by PC CMR-derived transmural E/A ratio, mitral deceleration time, and LA size.³⁶

Changes in LA morphology and transmural flow patterns merely represent a consequence of DD. One would expect that the evaluation of intrinsic myocardial characteristics offers new insights into DD. In echocardiography, global longitudinal SR is a frequently applied parameter to evaluate diastolic function and also known for the assessment of systolic function. It is known to have a significant association with the time constant of LV relaxation and has been used to predict outcomes in several disease stages.³ In our study, we found significantly reduced EII SR assessed by tagging SPAMM in DD+. Because of technical limitations, tissue tracking-derived EII SR was not reliable in our setting. Future technical improvements may overcome these limitations.

On the other hand, CMR offers a wide spectrum of additional parameters to assess diastolic myocardial deformation applying tagging, tissue tracking, and TPM. Several studies examined applicability of CMR tagging to evaluate diastolic function using different diastolic parameters. We focused on peak early diastolic SR. Diastolic Ecc did not show significant differences between DD+ and DD-. In contrast, both Ennis *et al.*¹⁷ and Edvardsen *et al.*¹⁶ detected significantly decreased early diastolic Ecc SR in patients suffering from familial hypertrophic cardiomyopathy or LV hypertrophy, respectively. Among other reasons, these divergent findings may be due to different study populations, variable degrees of cardiac remodelling, and technical issues including the use of different approaches.

Tissue tracking is a recently introduced post-processing technique to evaluate myocardial strain and SR based on SSFP cine images.¹⁰ Segmental analysis of E and A peak Ecc and Err diastolic SR showed significant reduction in DD+ in the basal lateral wall. Kuetting *et al.*¹² evaluated global midventricular early and peak diastolic Ecc SR in patients with echocardiographically diagnosed DD and controls. Both parameters appeared significantly reduced in patients with DD. We did not find similar differences on the midventricular level of global Ecc. However, healthy controls in the study by Kuetting *et al.* were younger and Ecc early diastolic SR has

been shown to decrease with age.¹¹ For this method, comparison across studies may be misleading as most studies are focusing on systolic strain and SR as well as due to technical reasons and different approaches.^{11,12,37} Similar challenges are known from other imaging techniques.^{38,39} A comparison with healthy volunteers could help to interpret the published literature, but currently published normal values for segmental diastolic SR analysis based on tissue tracking or tagging are lacking.

The findings in the basal lateral wall using tissue tracking are supported by the TPM results of our study. TPM has been shown to be a reliable technique to evaluate and discriminate myocardial velocities of healthy volunteers and patients.⁸ The present study demonstrated impaired Vz in the apical slice. These findings could only partially be reproduced in a segmental analysis. In contrast, we found significantly reduced regional diastolic peak velocities again in the basal lateral wall of DD+. Von Knobelsdorff-Brenkenhoff *et al.*¹⁵ and Foell *et al.*¹³ analysed TPM-derived myocardial velocities in healthy volunteers and patients with hypertensive heart disease and preserved EF. Both studies found significantly reduced diastolic Vr and Vz peak velocities in patients. We did not include healthy volunteers, but patients without signs for DD that may explain the differing results. The reduced peak velocities might be caused by the predominant presence of arterial hypertension and higher age. Diastolic Vz and Vr are known to decrease in the elderly.⁸ However, the differentiation of age-dependent reduced relaxation and pathological DD is essential and needs further attention in an ageing society. Potentially, reduced diastolic peak velocities in the basal lateral wall play a particular role in this differentiation.

In our cohort, reduced myocardial deformation was mainly detected in the basal lateral segments. Several types of cardiomyopathy like viral myocarditis^{40,41} and myocardial dystrophies such as myotonic dystrophy type 2,⁴² facioscapulohumeral muscular dystrophy 1,⁴³ and Becker muscular dystrophy^{44,45} show focal and subclinical diffuse fibrosis predominantly in the inferolateral wall. Both focal and diffuse fibrosis have also been seen in HF with preserved ejection fraction or hypertensive heart disease.^{21,46} Furthermore, the myocardial deformation response to isometric exercise in subjects with hypertensive heart disease was predominantly abnormal in the lateral segments.¹⁵ Taken together, there is evidence that the inferolateral wall may be a region of early or increased vulnerability for pathological structural and functional changes even though up to now a mechanistic explanation for this observation is lacking.

To underpin our findings of LA enlargement and impairment of diastolic function in the basal lateral wall, a reclassification would have been desirable. But DD± was limited by a small sample size due to missing data regarding group defining measurements ($n = 4$) and exclusions due to technical reasons (see Supporting Information, *Table S3*). Therefore, the group of DD± would not have been sufficient to perform a reclassification.

Beyond the detection of DD itself, graduation of DD could offer more insights in disease staging and pathophysiology. Our approach did not focus on grading DD and therefore patients with Grade I DD were probably missed or went undetected. The identification of borderline cases and parameters for reclassification should be addressed in future studies.

Irrespective of a potential future implementation of our parameters to clinical practice, transthoracic echocardiography will remain the first-line method to evaluate diastolic function. But in cases of primarily performed CMR, for example, in patients with suspected cardiomyopathy, it may be useful to being able to reliably assess diastolic function as an additional parameter. CMR scans have to be time efficient in clinical routine, which enhances the potential role of a fast biplane LA-EDV/H assessment and tissue tracking analyses with no need for additional image acquisitions.

The present study shows some limitations. First, study results are based on a small sample size even though demographic confounders could be excluded. Second, the definition of study groups was based on the consensus statement by Paulus *et al.*,² which shows some minor deviation to the updated recommendations for evaluation of LV diastolic function by echocardiography,³ which were published after realization of the study. Third, we had not the possibility to run invasive measurements in healthy volunteers; only patients with clinical indication for left heart catheterization were screened. As a consequence, by study design, a group of healthy volunteers with definitive normal diastolic function is lacking in the current study.

In conclusion, CMR is able to identify patients with DD. Enlarged LA is most predictive for DD among evaluated comprehensive CMR parameters. TPM and tissue tracking reflect intrinsic aberration by revealing impaired deformation patterns in the basal lateral segments in comparison with patients with normal diastolic function.

Acknowledgements

We sincerely thank Joost P. A. Kuijper for providing his CMR tagging sequences, Carsten Schwenke for supporting in the statistical analysis, Thomas Grandy for his helpful comments and careful reading, the technicians Kerstin Kretschel, Evelyn Polzin, and Denise Kleindienst for acquiring the CMR data, and the study nurse Annette Köhler-Rhode for assisting in the organization of the CMR scans.

Conflict of interest

A.G. reports personal fees from Siemens Healthcare GmbH, outside the submitted work. P.B. is an employee of Circle

Cardiovascular Imaging Inc. The other authors declare no conflicts of interest.

Funding

J.S.-M. is holding institutional grants of the Charité—Universitätsmedizin Berlin.

References

- Owan TE, Hodge DO, Herges RM, Jacobsen SJ, Roger VL, Redfield MM. Trends in prevalence and outcome of heart failure with preserved ejection fraction. *N Engl J Med* 2006; **355**: 251–259.
- Paulus WJ, Tschöpe C, Sanderson JE, Rusconi C, Flachskampf FA, Rademakers FE, Marino P, Smiseth OA, De Keulenaer G, Leite-Moreira AF, Borbély A. How to diagnose diastolic heart failure: a consensus statement on the diagnosis of heart failure with normal left ventricular ejection fraction by the Heart Failure and Echocardiography Associations of the European Society of Cardiology. *Eur Heart J* 2007; **28**: 2539–2550.
- Nagueh SF, Smiseth OA, Appleton CP, Byrd BF, Dokainish H, Edvardsen T, Flachskampf FA, Gillebert TC, Klein AL, Lancellotti P, Marino P. Recommendations for the evaluation of left ventricular diastolic function by echocardiography: an update from the American Society of Echocardiography and the European Association of Cardiovascular Imaging. *J Am Soc Echocardiography* 2016; **29**: 277–314.
- Ponikowski P, Voors AA, Anker SD, Bueno H, Cleland JG, Coats AJ, Falk V, González-Juanatey JR, Harjola VP, Jankowska EA, Jessup M, Linde C, Nihoyannopoulos P, Parissis JT, Pieske B, Riley JP, Rosano GM, Ruilope LM, Ruschitzka F, Rutten FH, van der Meer P. 2016 ESC guidelines for the diagnosis and treatment of acute and chronic heart failure. *Kardiol Pol* 2016; **74**: 1037–1147.
- Paelinck BP, de Roos A, Bax JJ, Bosmans JM, van Der Geest RJ, Dhondt D, Parizel PM, Vrints CJ, Lamb HJ. Feasibility of tissue magnetic resonance imaging: a pilot study in comparison with tissue Doppler imaging and invasive measurement. *J Am Coll Cardiol* 2005; **45**: 1109–1116.
- Jung B, Schneider B, Markl M, Saurbier B, Geibel A, Hennig J. Measurement of left ventricular velocities: phase contrast MRI velocity mapping versus tissue-Doppler-ultrasound in healthy volunteers. *J Cardiovasc Magn Reson* 2004; **6**: 777–783.
- Duarte R, Fernandez G. Assessment of left ventricular diastolic function by MR: why, how and when. *Insights Imaging* 2010; **1**: 183–192.
- Foll D, Jung B, Schilli E, Staehle F, Geibel A, Hennig J, Bode C, Markl M. Magnetic resonance tissue phase mapping of myocardial motion: new insight in age and gender. *Circ Cardiovasc Imaging* 2010; **3**: 54–64.
- Ibrahim el SH. Myocardial tagging by cardiovascular magnetic resonance: evolution of techniques—pulse sequences, analysis algorithms, and applications. *J Cardiovasc Magn Reson* 2011; **13**: 36.
- Ortega M, Triedman JK, Geva T, Harrild DM. Relation of left ventricular dyssynchrony measured by cardiac magnetic resonance tissue tracking in repaired tetralogy of fallot to ventricular tachycardia and death. *Am J Cardiol* 2011; **107**: 1535–1540.
- Andre F, Steen H, Mattheis P, Westkott M, Breuninger K, Sander Y, Kammerer R, Galuschky C, Giannitsis E, Korosoglou G, Katus HA, Buss SJ. Age- and gender-related normal left ventricular deformation assessed by cardiovascular magnetic resonance feature tracking. *J Cardiovasc Magn Reson* 2015; **17**: 25.
- Kuetting D, Sprinkart AM, Doerner J, Schild H, Thomas D. Comparison of magnetic resonance feature tracking with harmonic phase imaging analysis (CSPAMM) for assessment of global and regional diastolic function. *Eur J Radiol* 2015; **84**: 100–107.
- Foell D, Jung B, Germann E, Staehle F, Bode C, Markl M. Hypertensive heart disease: MR tissue phase mapping reveals altered left ventricular rotation and regional myocardial long-axis velocities. *Eur Radiol* 2013; **23**: 339–347.
- Jung B, Foll D, Bottler P, Petersen S, Hennig J, Markl M. Detailed analysis of myocardial motion in volunteers and patients using high-temporal-resolution MR tissue phase mapping. *JMRI* 2006; **24**: 1033–1039.
- von Knobelsdorff-Brenkenhoff F, Hennig P, Menza M, Dieringer MA, Foell D, Jung B, Schulz-Menger J. *Myocardial dysfunction in patients with aortic stenosis and hypertensive heart disease assessed by MR tissue phase mapping*. *JMRI: Journal of magnetic resonance imaging*; 2015.
- Edvardsen T, Rosen BD, Pan L, Jerosch-Herold M, Lai S, Hundley WG, Sinha S, Kronmal RA, Bluemke DA, Lima JAC. Regional diastolic dysfunction in individuals with left ventricular hypertrophy measured by tagged magnetic resonance imaging—the Multi-Ethnic Study of Atherosclerosis (MESA). *Am Heart J* 2006; **151**: 109–114.
- Ennis DB, Epstein FH, Kellman P, Fananapazir L, McVeigh ER, Arai AE. Assessment of regional systolic and diastolic dysfunction in familial hypertrophic cardiomyopathy using MR tagging. *Magn Reson Med* 2003; **50**: 638–642.
- Moody WE, Taylor RJ, Edwards NC, Chue CD, Umar F, Taylor TJ, Ferro CJ, Young AA, Townend JN, Leyva F, Steeds RP. Comparison of magnetic resonance feature tracking for systolic and diastolic strain and strain rate calculation with spatial modulation of magnetization imaging analysis. *JMRI* 2015; **41**: 1000–1012.
- Maceira AM, Cosin-Sales J, Roughton M, Prasad SK, Pennell DJ. Reference left atrial dimensions and volumes by steady state free precession cardiovascular magnetic resonance. *J Cardiovasc Magn Reson* 2010; **12**: 65.
- Zwanenburg JJ, Kuijer JP, Marcus JT, Heethaar RM. Steady-state free precession with myocardial tagging: CSPAMM in a single breathhold. *Magn Reson Med* 2003; **49**: 722–730.
- Schulz-Menger J, Abdel-Aty H, Rudolph A, Elgeti T, Messroghli D, Utz W, Boyé P, Bohl S, Busjahn A, Hamm B, Dietz R. Gender-specific differences in left ventricular remodelling and fibrosis in hypertrophic cardiomyopathy: insights

Supporting information

Additional supporting information may be found online in the Supporting Information section at the end of the article.

Table S1. Strain rate, myocardial velocity, LV-, LA- and transmural flow- analysis per slice

Table S2. Findings of regional strain rate and myocardial velocity analysis of DD+ and DD-.

Table S3. Causes for exclusion of cases.

- from cardiovascular magnetic resonance. *Eur J Heart Fail* 2008; **10**: 850–854.
22. Schulz-Menger J, Bluemke DA, Bremerich J, Flamm SD, Fogel MA, Friedrich MG, Kim RJ, von Knobelsdorff-Brenkenhoff F, Kramer CM, Pennell DJ, Plein S, Nagel E. Standardized image interpretation and post processing in cardiovascular magnetic resonance: Society for Cardiovascular Magnetic Resonance (SCMR) Board of Trustees Task Force on Standardized Post Processing. *J Cardiovasc Magn Reson* 2013; **15**: 35.
 23. Funk S, Kerner J, Doganguezel S, Schwenke C, von Knobelsdorff-Brenkenhoff F, Schulz-Menger J. Quantification of the left atrium applying cardiovascular magnetic resonance in clinical routine. *SCJ* 2018; 1–8.
 24. Cerqueira MD, Weissman NJ, Dilsizian V, Jacobs AK, Kaul S, Laskey WK, Pennell DJ, Rumberger JA, Ryan T, Verani MS, Myoca AHAWG. Standardized myocardial segmentation and nomenclature for tomographic imaging of the heart. A statement for healthcare professionals from the Cardiac Imaging Committee of the Council on Clinical Cardiology of the American Heart Association. *Circulation* 2002; **105**: 539–542.
 25. Buckberg G, Hoffman JI, Mahajan A, Saleh S, Coghlan C. Cardiac mechanics revisited: the relationship of cardiac architecture to ventricular function. *Circulation* 2008; **118**: 2571–2587.
 26. Tsang TS, Barnes ME, Gersh BJ, Bailey KR, Seward JB. Left atrial volume as a morphophysiological expression of left ventricular diastolic dysfunction and relation to cardiovascular risk burden. *Am J Cardiol* 2002; **90**: 1284–1289.
 27. Madueme PC, Mazur W, Hor KN, Germann JT, Jefferies JL, Taylor MD. Comparison of area-length method by echocardiography versus full-volume quantification by cardiac magnetic resonance imaging for the assessment of left atrial volumes in children, adolescents, and young adults. *Pediatr Cardiol* 2014; **35**: 645–651.
 28. Patel DA, Lavie CJ, Gilliland Y, Shah S, Ventura H, Milani R. Abstract 712: Left atrial volume and mortality prediction: does the method of indexing matter? *Circulation* 2009; **120**: S382-S.
 29. Upadhyia B, Taffet GE, Cheng CP, Kitzman DW. Heart failure with preserved ejection fraction in the elderly: scope of the problem. *J Mol Cell Cardiol* 2015; **83**: 73–87.
 30. Bertelsen L, Diederichsen SZ, Haugan KJ, Brandes A, Graff C, Krieger D, Kronborg C, Køber L, Højberg S, Vejlstrup N, Svendsen JH. Left atrial volume and function assessed by cardiac magnetic resonance imaging are markers of subclinical atrial fibrillation as detected by continuous monitoring. *Europace* 2020.
 31. Wandelt LK, Kowallick JT, Schuster A, Wachter R, Stümpfig T, Unterberg-Buchwald C, Steinmetz M, Ritter CO, Lotz J, Staab W. Quantification of left atrial volume and phasic function using cardiovascular magnetic resonance imaging—comparison of biplane area-length method and Simpson's method. *Int J Cardiovasc Imaging* 2017; **33**: 1761–1769.
 32. ATS statement: guidelines for the six-minute walk test. *Am J Respir Crit Care Med* 2002; **166**: 111–117.
 33. Rathi VK, Doyle M, Yamrozik J, Williams RB, Caruppannan K, Truman C, Vido D, Biederman RW. Routine evaluation of left ventricular diastolic function by cardiovascular magnetic resonance: a practical approach. *J Cardiovasc Magn Reson* 2008; **10**: 36.
 34. Bollache E, Redheuil A, Clément-Guinaudeau S, Defrance C, Perdriz L, Ladouceur M, Lefort M, de Cesare A, Herment A, Diebold B, Mousseaux E. Automated left ventricular diastolic function evaluation from phase-contrast cardiovascular magnetic resonance and comparison with Doppler echocardiography. *J Cardiovasc Magn Reson* 2010; **12**: 63.
 35. Rubinstein R, Glockner JF, Feng D, Araoz PA, Kirsch J, Syed IS, Oh JK. Comparison of magnetic resonance imaging versus Doppler echocardiography for the evaluation of left ventricular diastolic function in patients with cardiac amyloidosis. *Am J Cardiol* 2009; **103**: 718–723.
 36. Graca B, Ferreira MJ, Donato P, Castelo-Branco M, Caseiro-Alves F. Cardiovascular magnetic resonance imaging assessment of diastolic dysfunction in a population without heart disease: a gender-based study. *Eur Radiol* 2014; **24**: 52–59.
 37. Taylor RJ, Moody WE, Umar F, Edwards NC, Taylor TJ, Stegemann B, Townsend JN, Hor KN, Steeds RP, Mazur W, Leyva F. Myocardial strain measurement with feature-tracking cardiovascular magnetic resonance: normal values. *Eur Heart J Cardiovasc Imaging* 2015; **16**: 871–881.
 38. Farsalinos KE, Daraban AM, Unlu S, Thomas JD, Badano LP, Voigt JU. Head-to-head comparison of global longitudinal strain measurements among nine different vendors: the EACVI/ASE Inter-Vendor Comparison Study. *J Am Soc Echocardiogr* 2015; **28**: 1171–1181 e2.
 39. Messroghli DR, Moon JC, Ferreira VM, Grosse-Wortmann L, He T, Kellman P, Mascherbauer J, Nezafat R, Salerno M, Schelbert EB, Taylor AJ, Thompson R, Ugander M, van Heeswijk R, Friedrich MG. Clinical recommendations for cardiovascular magnetic resonance mapping of T1, T2, T2* and extracellular volume: a consensus statement by the Society for Cardiovascular Magnetic Resonance (SCMR) endorsed by the European Association for Cardiovascular Imaging (EACVI). *J Cardiovasc Magn Reson* 2017; **19**: 75.
 40. Aquaro GD, Perfetti M, Camastra G, Monti L, Dellegrottaglie S, Moro C, Pepe A, Todiere G, Lanzillo C, Scattiea A, di Roma M, Pontone G, Perazzolo Marra M, Barison A, di Bella G, Cardiac Magnetic Resonance Working Group of the Italian Society of Cardiology. Cardiac MR with late gadolinium enhancement in acute myocarditis with preserved systolic function: ITAMY study. *J Am Coll Cardiol* 2017; **70**: 1977–1987.
 41. Mahrholdt H, Wagner A, Deluigi CC, Kispert E, Hager S, Meinhardt G, Vogelsberg H, Fritz P, Dippol J, Bock CT, Klingel K, Kandolf R, Sechtem U. Presentation, patterns of myocardial damage, and clinical course of viral myocarditis. *Circulation* 2006; **114**: 1581–1590.
 42. Schmacht L, Traber J, Grieben U, Utz W, Dieringer MA, Kellman P, Blaszczyk E, von Knobelsdorff-Brenkenhoff F, Spuler S, Schulz-Menger J. Cardiac involvement in myotonic dystrophy type 2 patients with preserved ejection fraction: detection by cardiovascular magnetic resonance. *Circ Cardiovasc Imaging* 2016; **9**.
 43. Blaszczyk E, Grieben U, von Knobelsdorff-Brenkenhoff F, Kellman P, Schmacht L, Funk S, Spuler S, Schulz-Menger J. Subclinical myocardial injury in patients with Facioscapulohumeral muscular dystrophy 1 and preserved ejection fraction—assessment by cardiovascular magnetic resonance. *J Cardiovasc Magn Reson* 2019; **21**: 25.
 44. Mavrogeni S, Papavasiliou A, Skouteli E, Magoutas A, Dangas G. Cardiovascular magnetic resonance imaging evaluation of two families with Becker muscular dystrophy. *NMD* 2010; **20**: 717–719.
 45. Yilmaz A, Gdynia HJ, Baccouche H, Mahrholdt H, Meinhardt G, Basso C, Thiene G, Sperfeld AD, Ludolph AC, Sechtem U. Cardiac involvement in patients with Becker muscular dystrophy: new diagnostic and pathophysiological insights by a CMR approach. *J Cardiovasc Magn Reson* 2008; **10**: 50.
 46. Kanagalap P, Cheng ASH, Singh A, Khan JN, Gulsin GS, Patel P, Gupta P, Arnold JR, Squire IB, Ng LL, McCann GP. Relationship between focal and diffuse fibrosis assessed by CMR and clinical outcomes in heart failure with preserved ejection fraction. *J Am Coll Cardiol Img* 2019; **12**: 2291–2301.



Quantification of the left atrium applying cardiovascular magnetic resonance in clinical routine

Stephanie Funk, Josephine Kermer, Serkan Doganguezel, Carsten Schwenke, Florian von Knobelsdorff-Brenkenhoff & Jeanette Schulz-Menger

To cite this article: Stephanie Funk, Josephine Kermer, Serkan Doganguezel, Carsten Schwenke, Florian von Knobelsdorff-Brenkenhoff & Jeanette Schulz-Menger (2018) Quantification of the left atrium applying cardiovascular magnetic resonance in clinical routine, Scandinavian Cardiovascular Journal, 52:2, 85-92, DOI: [10.1080/14017431.2017.1423107](https://doi.org/10.1080/14017431.2017.1423107)

To link to this article: <https://doi.org/10.1080/14017431.2017.1423107>



[View supplementary material](#)



Published online: 05 Jan 2018.



[Submit your article to this journal](#)



Article views: 116



[View related articles](#)



[View Crossmark data](#)

ORIGINAL ARTICLE



Quantification of the left atrium applying cardiovascular magnetic resonance in clinical routine

Stephanie Funk^{a,b}, Josephine Kermer^a, Serkan Doganguezel^a, Carsten Schwenke^c, Florian von Knobelsdorff-Brenkenhoff^{a,d} and Jeanette Schulz-Menger^{a,b}

^aWorking Group on Cardiovascular Magnetic Resonance, Experimental and Clinical Research Center, a joint cooperation between the Charité – Universitätsmedizin Berlin, Department of Internal Medicine and Cardiology and the Max-Delbrueck Center for Molecular Medicine, and HELIOS Klinikum Berlin Buch, Department of Cardiology and Nephrology, Berlin, Germany; ^bDZHK (German Center for Cardiovascular Research), partner Site Berlin, Germany; ^cScossis, Berlin, Germany; ^dDepartment of Cardiology, Clinic Agatharied, Ludwig-Maximilians-University Munich, Hausham, Germany

ABSTRACT

Objectives. In recent years the impact of the left atrium (LA) has become more evident in different cardiovascular pathologies. We aim to provide LA parameters in healthy volunteers for cardiovascular magnetic resonance (CMR) using a fast approach. **Design.** We analyzed 203 healthy volunteers (mean age 44.6 years (y), range 19y–76y) at 1.5 and 3.0 Tesla (T) using steady-state free precession (SSFP) cine in routine long axis view. Left atrial enddiastolic volume (LA-EDV), endsystolic volume (LA-ESV), stroke volume (LA-SV) and ejection fraction (LA-EF) were quantified and indexed to body-surface-area (BSA). Dependency on age and sex was analyzed. **Results.** 21 subjects had to be excluded. In the remaining, there was no significant difference between 1.5 T and 3.0 T. Absolut LA-EDV and LA-ESV were larger in men than in women (LA-EDV: male 70 ± 19 ml vs. female 61 ± 16 ml ($p = .001$); LA-ESV: male 24 ± 9 ml vs. female 21 ± 8 ml ($p = .01$)). These differences disappeared after indexing to BSA (LA-EDV/BSA: male 34 ± 10 ml/m² vs. female 33 ± 9 ml/m² ($p = .65$) and LA-ESV/BSA: male 12 ± 4 ml/m² vs. female 11 ± 4 ml/m² ($p = .71$)). LA-EDV/BSA decreased with older age. **Conclusions.** Reference values for LA size and function based on a fast approach are provided. LA size decreases with older age. Normalization to body size overcomes sex-dependency. Reports should be related to body size.

ARTICLE HISTORY

Received 27 April 2017
Revised 18 December 2017
Accepted 19 December 2017

KEYWORDS

Cardiac magnetic resonance; left atrial volumes; normal values; age; sex

Introduction

Within the last several years, the impact of the left atrium (LA) has become more evident as several studies have shown clinical association and prognostic value of left atrial volumes [1–6].

There is a correlation between left atrial function and heart failure development. Several studies found a decreased left atrial ejection fraction (LA-EF) in systolic and diastolic heart failure [2] as well as in heart failure with preserved left ventricular ejection fraction (LVEF) independently of a history of atrial fibrillation [5]. The MESA (Multi-Ethnic Study of Atherosclerosis) Study identified maximal and minimal left atrial volume indexes as independent predictors of heart failure [3].

Left atrial enlargement in arterial hypertension is a known risk factor of cardiac death [7].

In patients with cardiomyopathies, left atrial parameters can be a predictor of clinical outcome. Higher left atrial volumes are directly associated with a higher mortality and worse clinical outcome [6] in patients with dilated cardiomyopathy. In patients with hypertrophic

cardiomyopathy, the risk of developing atrial fibrillation is higher in patients with higher left atrial enddiastolic volume (LA-EDV) and lower LA-EF [4]. The European Society of Cardiology recommends the quantification of left atrial size as a part of the risk assessment of sudden cardiac death [8].

Independent of underlying causes left atrial volumes predict the risk of cardiovascular events in patients with atrial fibrillation [9]. Left atrial volumes are not only a risk factor for the development of atrial fibrillation [2,10], but also a predictor of success of pulmonary vein isolation [11].

Cardiovascular magnetic resonance (CMR) is known to be the gold standard for quantification of ventricular volumes and function [12,13]. Its accuracy helps to reduce the sample size in research trials [14]. On the other hand CMR is often regarded as time consuming in terms of acquisition as well as for quantification and it is therefore far less used. Different studies are already providing reference values for the assessment of left atrial morphology applying CMR [15–19], but they are based on multi-slice full-coverage of the LA. We aim to add systematic values for volume and function related to sex and age at 1.5 and 3.0 Tesla (T) using a time-efficient approach as a part of a routine protocol.

Material and Methods

We included 207 volunteers after initial screening. They were prospectively included in other studies and other parameters except LA have already been published [20,21]. 111 volunteers were not published until now.

Only healthy volunteers without any known risk factors or history of cardiac diseases or arterial hypertension as well as a normal ECG and LVEF were included.

Those with any kind of illness at the time of investigation ($n=1$) as well as those with any incidental findings at CMR were excluded ($n=2$). Volunteers with arrhythmias or insufficient gating were excluded as well ($n=1$).

203 healthy volunteers remained for analysis.

We excluded scans with insufficient delineation of the LA. Inclusion criteria were full visualization of all four cardiac chambers including valvular level. We excluded images with incomplete depiction of the LA during the cardiac cycle and those with impaired delineation of the atrial wall due to artifacts or overlap with vessels (Figure 1).

We analyzed the relation to age and sex. Age analysis is provided as a continuous variable as well as in three age groups as published recently [20]. The groups were as

follows: group 1 from 20 to 39 years, group 2 from 40 to 59 years and group 3 60 years and older.

The ethical committee approved all of the studies. All participants were enrolled after informed consent was obtained.

CMR protocol

111 CMR exams were performed at 1.5 T and 92 at 3.0 T.

At 3.0 T (Magnetom Verio, Siemens Healthcare, Erlangen, Germany), a 32-channel radio frequency coil and at 1.5 T (Magnetom Avanto, Siemens Healthcare, Erlangen, Germany) a 12-channel radio frequency coil were used.

Steady-state free precession (SSFP) cine was acquired during repeated breathholds in two long axes (2-chamber and 4-chamber view). Sequence details were as follows:

At 1.5 T: repetition time 2.8 ms, slice thickness 6 mm, flip angle 80 degrees, echo time 1.2 ms, field of view $276 \times 340 \text{ mm}^2$, matrix 156×192 , reconstructed to $1.77 \text{ mm} \times 1.77 \text{ mm}$, 30 cardiac phases [21].

At 3.0 T: repetition time 3.1 ms, slice thickness 6 mm, flip angle 45 degrees, echo time 1.3 ms, field of view

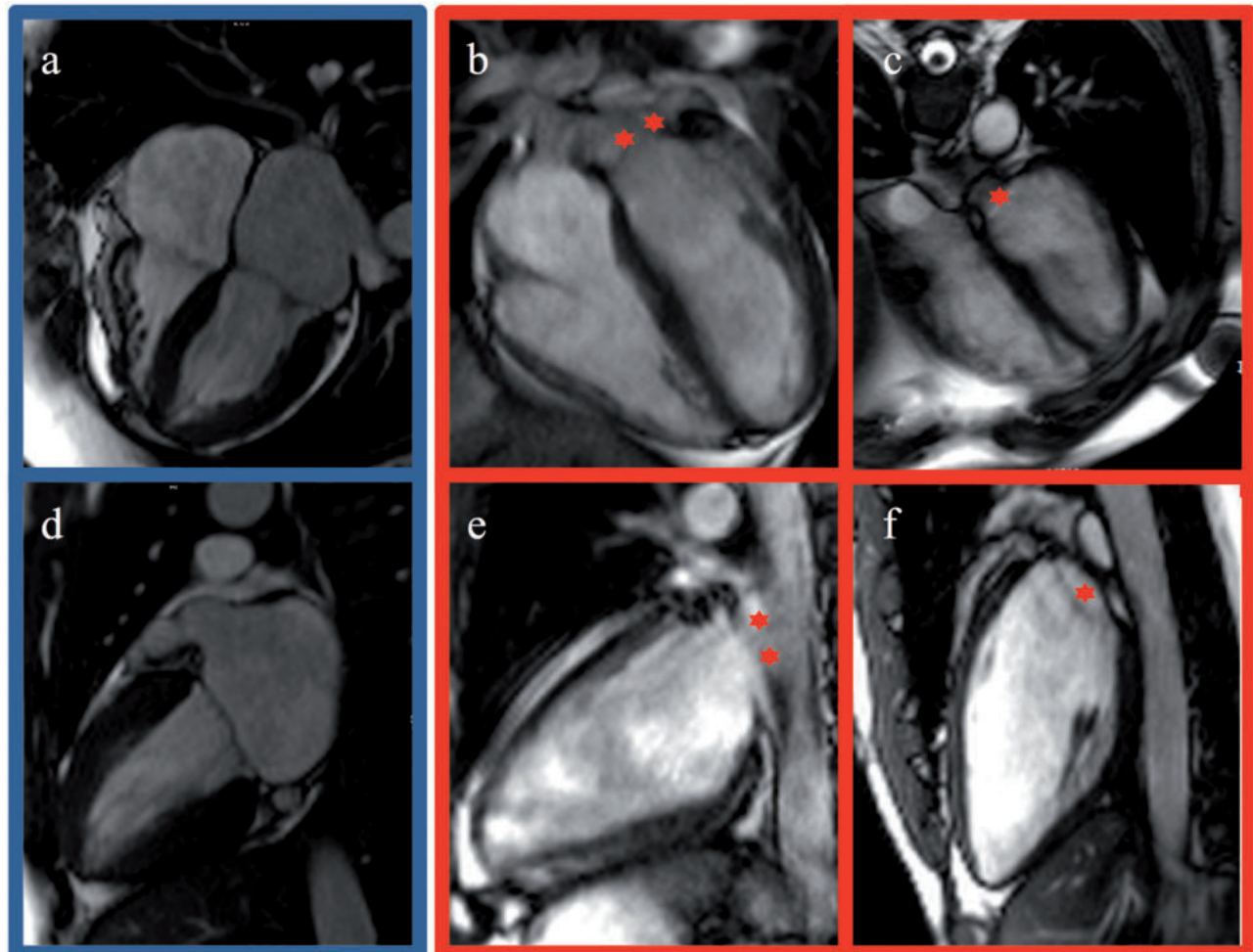


Figure 1. Delineation of atria, upper row 4-chamber views, lower row 2-chamber views. (a) and (d) (left): Optimal presentation of LA in LA-enddiastole. (b)-(f) (right): Suboptimal presentation of LA - Examples of excluded LA (incorrect region marked with red stars). (b): Suboptimal presentation due to artifacts. (c): Incomplete presentation in systole in 4-chamber view. (e): Suboptimal presentation due to overlap with vessels. (f): Incomplete presentation in systole in 2-chamber view.

$276 \times 340 \text{ mm}^2$, matrix 156×192 , reconstructed to $1.77 \text{ mm} \times 1.77 \text{ mm}$, 30 cardiac phases [20].

Image analysis

We quantified the LA based on the biplanar approach using 2- and 4-chamber views. Pulmonary veins and the left atrium appendage were excluded (see also Figure 2). Images were analyzed in LA systole and diastole.

In clinical routine, LA endsystole and enddiastole are often quantified at the same time point of the cardiac cycle as LV enddiastole and endsystole. However, the LV enddiastole is often not exactly at the same time point as the LA endsystole, but milliseconds later as known from basic research. We compared both approaches in 20 scans. Time point 1 - "LA systole 1" - is defined as LA systole at the same time point as the LV diastole. Time point 2 reflects the true systole and is named "LA systole 2".

We also compared volumes at the LA diastole at the time point of LV endsystole ("LA diastole 1") to the time point of the true LA enddiastole ("LA diastole 2").

A subgroup of 20 volunteers was analyzed by a second independent observer to assess interobserver variability.

All analyses were performed using cvi42® Version 5.1 (circle, cvi, Canada, Calgary).

Statistics

All statistics was calculated using IBM® SPSS® Statistics version 23.

We calculated mean values and standard deviation for left atrial enddiastolic volume (LA-EDV), endsystolic volume (LA-ESV), stroke volume (LA-SV) and ejection fraction (LA-EF). All volumes were correlated to body surface area (BSA) and height (H).

Normality of data was assessed graphically and by Kolmogorov-Smirnov-test. We used t-test, univariate and multivariate analyses to compare field strengths, age, age groups and sex. Time points of "LA-Systole 1" respectively "LA-Diastole 1" to "LA-Systole 2" respectively "LA-Diastole 2" were analyzed using Pearson's correlation coefficient, volumes at both time points were compared by using t-test.

Interobserver variability was evaluated by intraclass correlation coefficient and Bland-Altman plots.

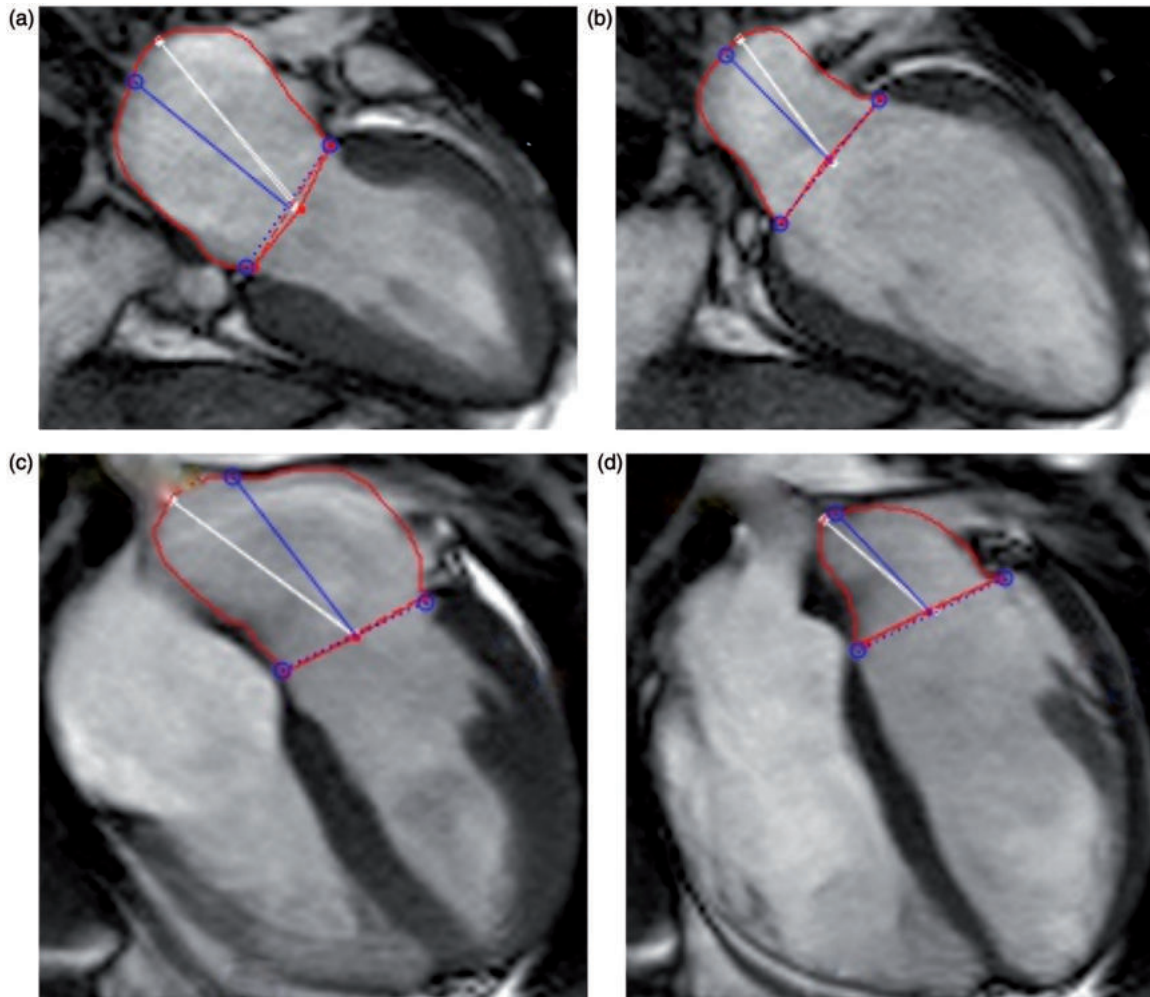


Figure 2. Measurement of the LA volumes in enddiastolic phase in 2-chamber view (a) and 4-chamber view (c) as well as in endsystolic phase in 2-chamber view (b) and 4-chamber view (d).

Table 1. Baseline characteristics of the healthy volunteers at 1.5 and 3.0 Tesla.

	1.5 Tesla (mean \pm SD (minimum/ maximum))	3.0 Tesla (mean \pm SD (minimum/ maximum))
N (total)	93	87
Age (yrs)	38 \pm 14 (19/70)	52 \pm 15 (21/76)
Height (cm)	175 \pm 9 (153/197)	171 \pm 11 (118/193)
Weight (kg)	72 \pm 12 (48/105)	77 \pm 15 (53/116)
BMI (kg/m ²)	23 \pm 3 (18/30)	26 \pm 7 (17/35)
BSA (m ²)	1.9 \pm 0.2 (1.5/2.4)	1.5 \pm 0.6 (0.6/2.4)
Heart rate (bpm)	71 \pm 13 (37/118)	70 \pm 11 (46/102)
Systolic blood pressure (mmHg)	126 \pm 15 (105/185)	133 \pm 13 (107/186)
Diastolic blood pressure (mmHg)	75 \pm 8 (63/94)	76 \pm 12 (47/109)
LVEF (%)	63 \pm 4 (55/75)	63 \pm 5 (51/77)

Results

We had to exclude 21 volunteers (10%) due to insufficient presentation of the LA in the standard 2- and 4-chamber views.

The most common cause for exclusion was the incomplete delineation of the LA during the whole cardiac cycle ($n = 14$, 7%) followed by overlap with vessels ($n = 6$, 3%) and other artifacts ($n = 1$, 0.5%).

182 volunteers remained for analysis. 89 were examined at 3.0 T and 93 at 1.5 T. Detailed demographics are given in Table 1.

There was no significant difference in the absolute volumes between field strengths (LA-EDV: 1.5 T: 68 ± 19 ml vs. 3.0 T 64 ± 18 ml ($p = .19$); LA-ESV: 1.5 T 23 ± 9 ml vs. 3.0 T 23 ± 9 ml ($p = .6$); LA-EF: 1.5 T $66 \pm 7\%$ vs. 3.0 T $66 \pm 7\%$ ($p = .6$)).

Analysis of sex-differences

Assessing sex-related differences, we found a significant difference in LA-EDV and LA-ESV ($p < .01$) with men having higher LA-EDV than women. When adjusted to BSA or height both parameters did not show any significant differences anymore (see also Figure 3). Details are given in Table 2.

Analysis of age

The continuous analysis of age showed a significant association between age and LA-EDV/BSA. A decrease of LA size related to age could be depicted (see Figure 4). Standardizing to height showed the same result. The decrease of LA size was independent of sex.

The comparison of the three age groups showed the same result (see Figure 5). The values are displayed in Table 3.

Detailed parameters for all age groups are given in appendix Tables 1–4.

Comparison of LA size at different time points

Volumes at time point of LA-systole 1 differed significantly from those measured at LA-systole 2 (LA-ESV: 38 ± 11 ml in group 1, 28 ± 8 ml in group 2 ($p < .001$)) as well as those at LA-diastole 1 from those at LA-diastole 2 (LA-EDV: 92 ± 21 ml in group 1, 74 ± 18 ml in group 2 ($p < .001$)). As a result, also the LA-EF differed significantly (LA-EF: $59 \pm 6\%$ in group 1, $63 \pm 7\%$ in group 2 ($p < .001$)).

Interobserver variability

The interobserver variability was small. There was no significant difference between the measurements of the two observers (see also Figure 6).

Discussion

In this study we provide LA reference values acquired with CMR at 1.5 T and 3.0 T based on a fast approach.

The values are based on a biplanar approach using calculated volumes. This approach could avoid the acquisition of additional slices and offers an easily usable instrument in daily routine.

Our main findings are: i) LA-size decreases with age in healthy volunteers, ii) LA size is independent from sex when indexed to BSA and height and iii) reference values are equal for 1.5 T and 3.0 T.

Notably, there is a decrease in LA-EDV in the older volunteers. This matches the result of Maceira et al. [15]. They found a decrease of LA diameter with age. In contrast, Thomas et al. did not find any significant age-dependent changes in LA volumes in 92 healthy subjects in echocardiography and Sievers et al. did not find a significant age-dependent difference in LA volumes in CMR [17,22]. Both, however, compared those over 50 years of age to those under 50 years. As we have shown, the change in morphology starts earlier.

Maceira et al. recently published reference values for normal reservoir and conduit volumes as well as booster pump function of the LA [23]. In these volumes, they found the same effect of decrease in older age. The effect remained even after adjusting to BSA.

Sex differences are not evident anymore when LA size is related to BSA. This is supported by Maceira et al. [15], who also found a significant influence of BSA on LA diameter and area. Hudsmith et al. [16] also showed a significant difference in LA-EDV and LA-ESV in men and women, but did not adjust the parameters to BSA or height. This underlines the importance of adjusted normal values.

Our findings support that all cardiac parameters should be standardized based on normalization to body surface area and/or height. Otherwise, the results may lead to misjudgment of morphology depending on sex and age.

Results did not differ between field strengths. This is not unexpected, as the application of SSFP cine imaging at different field strengths did not show significant differences in the evaluation of left ventricular volumes and function [24].

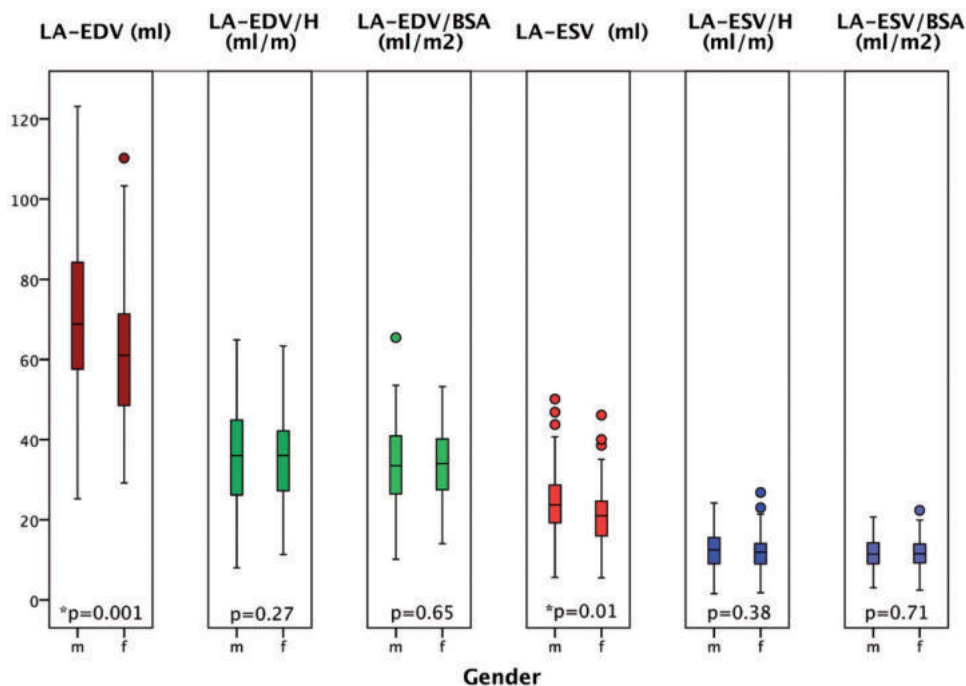


Figure 3. Comparison of LA-EDV and LA-ESV between males (m) and females (f). Consideration of body size reveals similar size of LA.

Table 2. Left atrial reference values for male and female by cardiovascular magnetic resonance.

	male (n = 105) (mean ± SD (minimum/maximum))	female (n = 77) (mean ± SD (minimum/maximum))
LA-EDV (ml)	70 ± 19 (25/123)	61 ± 16 (29/110)
LA-ESV (ml)	24 ± 9 (6/50)	21 ± 8 (4/46)
LA-SV (ml)	46 ± 13 (17/84)	46 ± 9 (24/70)
LA-EF (%)	66 ± 7 (50/85)	66 ± 8 (48/91)
LA-EDV/H (ml/m)	36 ± 12 (8/65)	34 ± 12 (11/63)
LA-ESV/H (ml/m)	12 ± 5 (2/24)	12 ± 5 (2/27)
LA-EDV/BSA (ml/m ²)	34 ± 10 (10/65)	33 ± 9 (13/53)
LA-ESV/BSA (ml/m ²)	12 ± 4 (3/21)	11 ± 4 (2/22)

However, in other measurements results are influenced by field strength [25].

LA volumetry can be performed using a straightforward biplanar approach or a 3D-assessment. It has previously been proven that both long and short axis techniques are highly accurate [26].

Currently, area- as well as volume-based approaches exist [15,17–19]. The volume-based approach is a superior marker of cardiovascular events compared to the area-based approach [27]. We have chosen the long axis views as more time-efficient approach to support the implementation into clinical routine.

In our study, the LA was not reliably depicted in 10% of the scans. In clinical routine, this number could be higher as patients are sicker. That was reflected in an ad-hoc analysis

of all routine scans performed within one week at our site (n = 57). In 70% (n = 40) of the scans the LA could be evaluated with this time-efficient approach without any problems. In 30% of the scans positioning had to be optimized using additional slices. That challenge can impact the fast approach. But faster acquisition as well as automatic evaluation could enter the clinical arena soon.

Faster sequences such as compressed sensing techniques will help to shorten the scan-time [28,29]. That would allow a full coverage of the LA in an acceptable scan-time. Automatic contour detection probably based on machine learning approaches will help to get the results of a three-dimensional LA coverage immediately.

Interestingly, in the recently published recommendation for cardiac chamber quantification in echocardiography [30] the maximum LA volumes are slightly lower than ours. However, it has previously been shown that volumes tend to be higher in CMR than in 2D echocardiography [31]. This may be related to the better delineation of structures. This assumption is supported by the fact that the new maximum Echo-LA volumes had to be adjusted as well. Previously they were even lower with 28 ml/m², adjusted now to 34 ml/m².

Currently, although most of the postprocessing tools allow a quantification of area and volumes, the quantification of LA-EF is not included on a routine base. However, the awareness of LA-EF as an outcome predictor increases. A decreased LA-EF is found in systolic and diastolic heart failure [2] as well as in heart failure with preserved LVEF [5].

In the ageing society, atrial fibrillation has an increasing impact. Accurate assessment of morphology is meaningful as therapeutic strategies exist. Patients with atrial fibrillation have a lower atrial output due to dissonant movement of

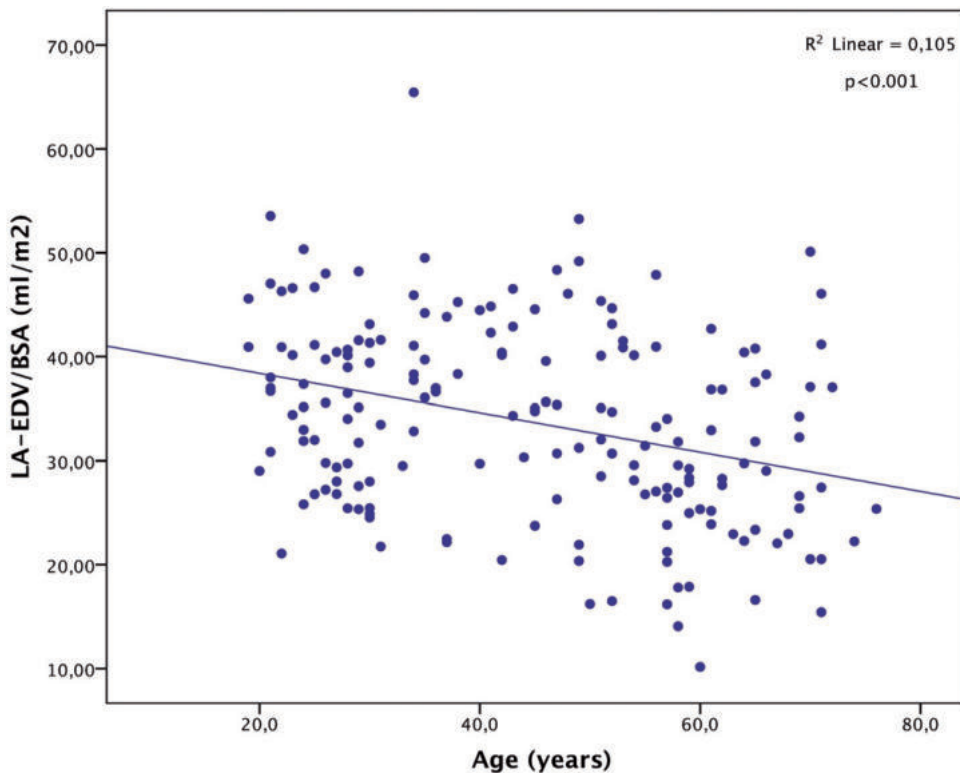


Figure 4. Association of LA-EDV/BSA with age.

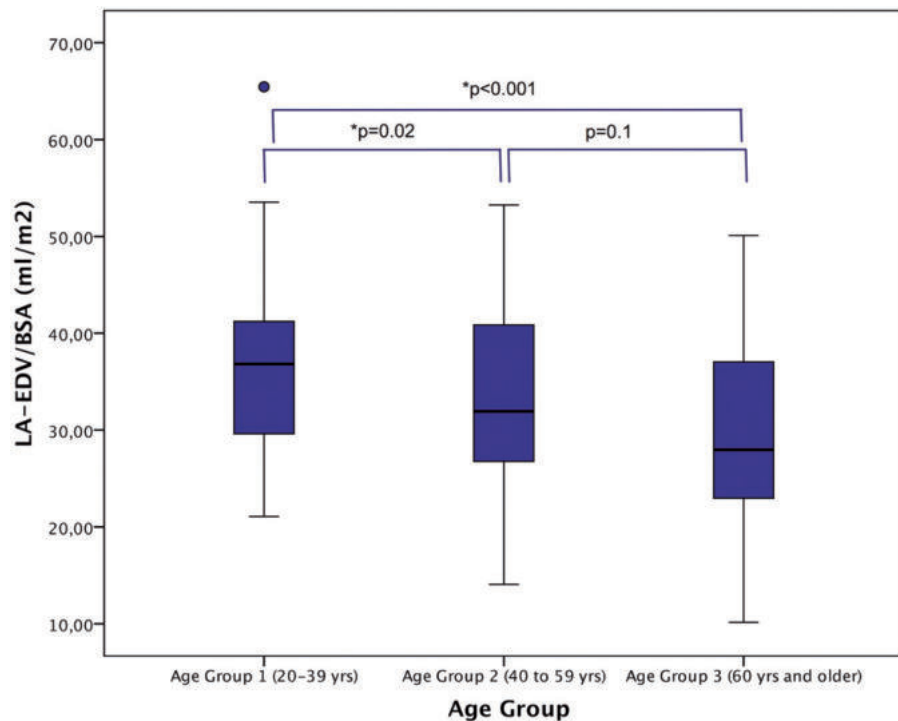


Figure 5. Relation of LA-size to age groups. LA size is decreasing with older age.

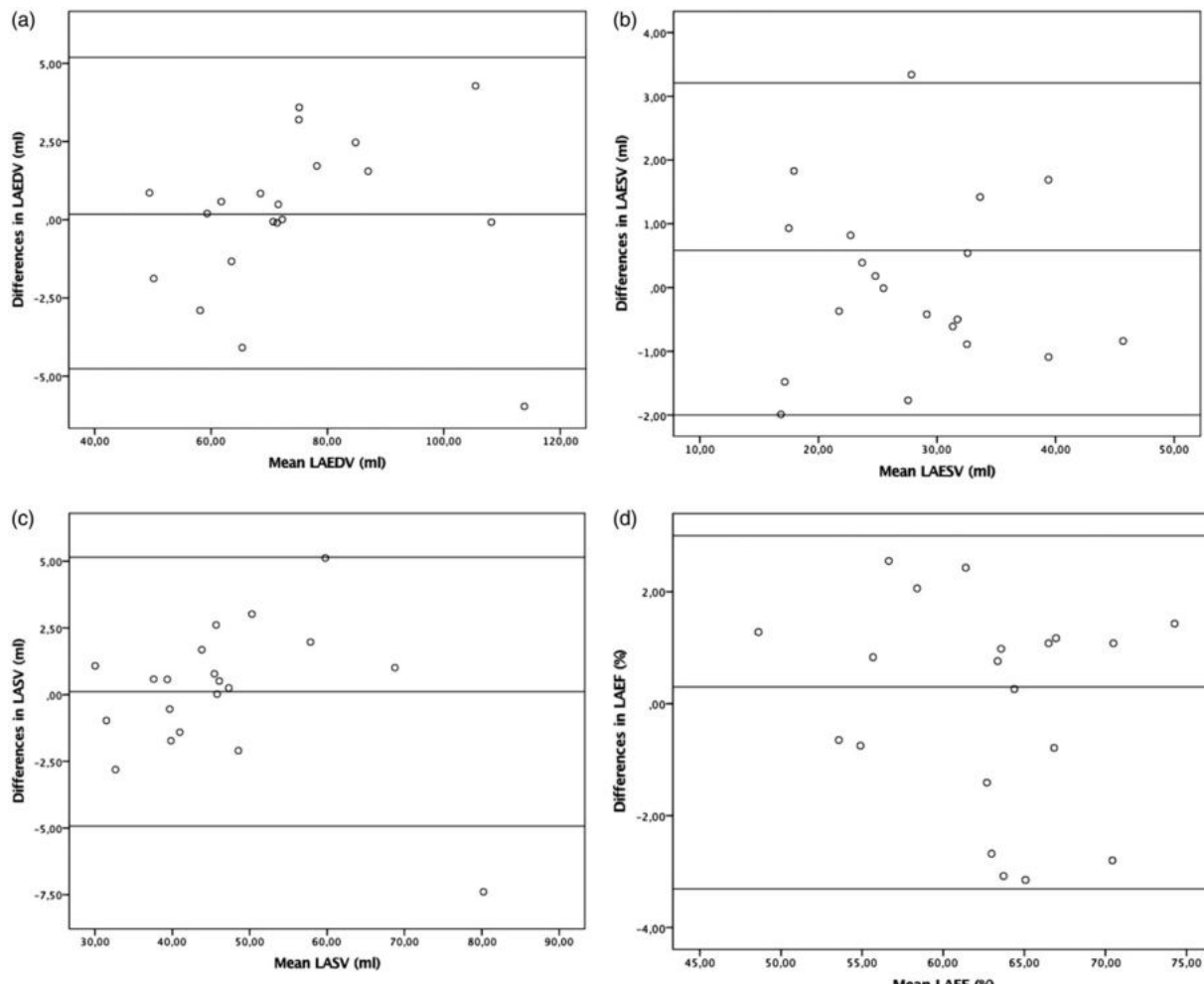
ventricle and atrium leading to symptoms of heart failure. This supports the importance of the atrial contraction. LA-morphology and function have a prognostic impact, are easily assessable and should therefore be a part of the cardiac evaluation.

Limitations

This study did not compare the same volunteer at 1.5 T and 3.0 T. With a total of 182 volunteers and strict inclusion criteria, the study aimed for an equal distribution of volunteer characteristics at both field strengths.

Table 3. LA-EDV/H and LA-EDV/BSA in different age groups.

	Age group 1	Age group 2	Age group 3	P value (Group 1 and 2)	P value (Group 1 and 3)
LA-EDV/H (ml/m)	38 ± 10 (8/65)	34 ± 11 (12/63)	31 ± 12 (8/60)	p < .05	p < .01
LA-EDV/BSA (ml/m ²)	36 ± 8 (21/65)	33 ± 10 (13/53)	29 ± 9 (10/50)	p = .01	p < .01

**Figure 6.** Interobserver variability LA-EDV (a), LA-ESV (b), LA-SV (c) and LA-EF (d).

This evaluation was carried out retrospectively in prospectively enrolled volunteers. A prospectively designed study might have less scans excluded due to suboptimal LA assessment. Our setting represents a routine clinical work environment.

In this study, only standard long axis views were applied and evaluated. To ensure a sufficient LA quality, 10% of the scans had to be excluded due to insufficient presentation and/or artifacts. In clinical routine, that number is expected to be higher. In an ad-hoc analysis at our site we found an exclusion rate of 30%, in which case an optimization of the position by adding two more slices would be necessary.

Conclusion

In this study we provide reference values in healthy volunteers for the left atrium for men and women. Age as well as

sex aspects should be recognized when quantifying the LA. Assessment of LA volume and function can be simplified by obtaining two long axis views of the LA during cine imaging.

Acknowledgements

We would like to thank Simone Fritschi for helping with editing the manuscript and the technicians Kerstin Kretschel, Evelyn Polzin and Denise Kleindienst for assisting in acquiring the CMR data, the study nurses Elke Nickel-Szczech and Annette Köhler-Rohde for assisting in the organization of the CMR scans.

Disclosure statement

All authors declare that they do not have any actual or potential conflict of interest including any financial, personal or other relationships with other people or organizations that could inappropriately influence their work.

Funding

This research did not receive any specific grant from funding agencies in the public, commercial, or not-for-profit sectors.

References

- [1] Kuchynka P, Podzimkova J, Masek M, et al. The Role of Magnetic Resonance Imaging and Cardiac Computed Tomography in the Assessment of Left Atrial Anatomy, Size, and Function. *BioMed Res Int.* 2015;2015:247865.
- [2] Pellicori P, Zhang J, Lukaschuk E, et al. Left atrial function measured by cardiac magnetic resonance imaging in patients with heart failure: clinical associations and prognostic value. *Eur Heart J.* 2015;36:733–742.
- [3] Habibi M, Chahal H, Opdahl A, et al. Association of CMR-measured LA function with heart failure development: results from the MESA study. *JACC Cardiovascular Imaging.* 2014;7:570–579.
- [4] Maron BJ, Haas TS, Maron MS, et al. Left atrial remodeling in hypertrophic cardiomyopathy and susceptibility markers for atrial fibrillation identified by cardiovascular magnetic resonance. *Am J Cardiol.* 2014;113:1394–1400.
- [5] Santos AB, Kraigher-Krainer E, Gupta DK, et al. Impaired left atrial function in heart failure with preserved ejection fraction. *Eur J Heart Fail.* 2014;16:1096–1103.
- [6] Gulati A, Ismail TF, Jabbour A, et al. Clinical utility and prognostic value of left atrial volume assessment by cardiovascular magnetic resonance in non-ischaemic dilated cardiomyopathy. *Eur J Heart Fail.* 2013;15:660–670.
- [7] Ciolfi G, Mureddu GF, Stefenelli C, et al. Relationship between left ventricular geometry and left atrial size and function in patients with systemic hypertension. *J Hypertension.* 2004;22:1589–1596.
- [8] Authors/Task Force m, Elliott PM, Anastasakis A, et al. 2014 ESC Guidelines on diagnosis and management of hypertrophic cardiomyopathy: the Task Force for the Diagnosis and Management of Hypertrophic Cardiomyopathy of the European Society of Cardiology (ESC). *Eur Heart J.* 2014;35:2733–2779.
- [9] Benjamin EJ, D'Agostino RB, Belanger AJ, et al. Left atrial size and the risk of stroke and death. The Framingham Heart Study. *Circulation.* 1995;92:835–841.
- [10] Tsang TS, Barnes ME, Bailey KR, et al. Left atrial volume: important risk marker of incident atrial fibrillation in 1655 older men and women. *Mayo Clin Proc.* 2001;76:467–475.
- [11] Jahnke C, Fischer J, Mirelis JG, et al. Cardiovascular magnetic resonance imaging for accurate sizing of the left atrium: predictability of pulmonary vein isolation success in patients with atrial fibrillation. *J Magn Reson Imaging.* 2011;33:455–463.
- [12] Ahmed S, Shellock FG. Magnetic resonance imaging safety: implications for cardiovascular patients. *J Cardiovasc Magn Reson.* 2001;3:171–182.
- [13] Pennell DJ. Cardiovascular magnetic resonance: twenty-first century solutions in cardiology. *Clin Med.* 2003;3:273–278.
- [14] Bellenger NG, Davies LC, Francis JM, et al. Reduction in sample size for studies of remodeling in heart failure by the use of cardiovascular magnetic resonance. *J of Cardiovascular Magnetic Resonance.* 2000;2:271–278.
- [15] Maceira AM, Cosin-Sales J, Roughton M, et al. Reference left atrial dimensions and volumes by steady state free precession cardiovascular magnetic resonance. *J Cardiovasc Magn Reson.* 2010;12:65.
- [16] Hudsmith LE, Petersen SE, Francis JM, et al. Normal human left and right ventricular and left atrial dimensions using steady state free precession magnetic resonance imaging. *J Cardiovasc Magn Reson.* 2005;7:775–782.
- [17] Sievers B, Kirchberg S, Franken U, et al. Determination of normal gender-specific left atrial dimensions by cardiovascular magnetic resonance imaging. *J Cardiovasc Magn Reson.* 2005;7:677–683.
- [18] Anderson JL, Horne BD, Pennell DJ. Atrial dimensions in health and left ventricular disease using cardiovascular magnetic resonance. *J Cardiovasc Magn Reson.* 2005;7:671–675.
- [19] Kawel-Boehm N, Maceira A, Valsangiocomo-Buechel ER, et al. Normal values for cardiovascular magnetic resonance in adults and children. *J Cardiovasc Magn Reson.* 2015;17:29.
- [20] von Knobelsdorff-Brenkenhoff F, Prothmann M, Dieringer MA, et al. Myocardial T1 and T2 mapping at 3 T: reference values, influencing factors and implications. *J Cardiovasc Magn Reson.* 2013;15:53.
- [21] Wassmuth R, Prothmann M, Utz W, et al. Variability and homogeneity of cardiovascular magnetic resonance myocardial T2-mapping in volunteers compared to patients with edema. *J Cardiovasc Magn Reson.* 2013;15:27.
- [22] Thomas L, Levett K, Boyd A, et al. Compensatory changes in atrial volumes with normal aging: is atrial enlargement inevitable? *J Am Coll Cardiol.* 2002;40:1630–1635.
- [23] Maceira AM, Cosin-Sales J, Prasad SK, et al. Characterization of left and right atrial function in healthy volunteers by cardiovascular magnetic resonance. *J Cardiovasc Magn Reson.* 2016;18:64.
- [24] Hudsmith LE, Petersen SE, Tyler DJ, et al. Determination of cardiac volumes and mass with FLASH and SSFP cine sequences at 1.5 vs. 3 Tesla: a validation study. *Journal of magnetic resonance imaging.* JMRI. 2006;24:312–318.
- [25] Kawel N, Nacif M, Zavodni A, et al. T1 mapping of the myocardium: intra-individual assessment of the effect of field strength, cardiac cycle and variation by myocardial region. *J Cardiovasc Magn Reson.* 2012;14:27.
- [26] Childs H, Ma L, Ma M, et al. Comparison of long and short axis quantification of left ventricular volume parameters by cardiovascular magnetic resonance, with ex-vivo validation. *J Cardiovasc Magn Reson.* 2011;13:40.
- [27] Tsang TS, Abhayaratna WP, Barnes ME, et al. Prediction of cardiovascular outcomes with left atrial size: is volume superior to area or diameter? *J Am Coll Cardiol.* 2006;47:1018–1023.
- [28] Sudarski S, Henzler T, Haubenreisser H, et al. Free-breathing Sparse Sampling Cine MR Imaging with Iterative Reconstruction for the Assessment of Left Ventricular Function and Mass at 3.0 T. *Radiology.* 2017;282:74–83. Epub 2016/07/12.
- [29] Vincenti G, Monney P, Chaptinel J, et al. Compressed sensing single-breath-hold CMR for fast quantification of LV function, volumes, and mass. *JACC Cardiovascular Imaging.* 2014;7:882–892.
- [30] Lang RM, Badano LP, Mor-Avi V, et al. Recommendations for cardiac chamber quantification by echocardiography in adults: an update from the American Society of Echocardiography and the European Association of Cardiovascular Imaging. European. *Eur Heart J Cardiovasc Imaging.* 2015;16:233–270.
- [31] Boyd AC, Thomas L. Left atrial volumes: two-dimensional, three-dimensional, cardiac magnetic resonance and computed tomography measurements. *Curr Opinion Cardiol.* 2014;29:408–416.

RESEARCH

Open Access



CrossMark

Comparison of fast multi-slice and standard segmented techniques for detection of late gadolinium enhancement in ischemic and non-ischemic cardiomyopathy – a prospective clinical cardiovascular magnetic resonance trial

Fabian Muehlberg^{1*} , Kristin Arnhold¹, Simone Fritschi¹, Stephanie Funk¹, Marcel Prothmann¹, Josephine Kermer¹, Leonora Zange¹, Florian von Knobelsdorff-Brenkenhoff² and Jeanette Schulz-Menger¹

Abstract

Background: Segmented phase-sensitive inversion recovery (PSIR) cardiovascular magnetic resonance (CMR) sequences are reference standard for non-invasive evaluation of myocardial fibrosis using late gadolinium enhancement (LGE). Several multi-slice LGE sequences have been introduced for faster acquisition in patients with arrhythmia and insufficient breathhold capability.

The aim of this study was to assess the accuracy of several multi-slice LGE sequences to detect and quantify myocardial fibrosis in patients with ischemic and non-ischemic myocardial disease.

Methods: Patients with known or suspected LGE due to chronic infarction, inflammatory myocardial disease and hypertrophic cardiomyopathy (HCM) were prospectively recruited. LGE images were acquired 10–20 min after administration of 0.2 mmol/kg gadolinium-based contrast agent. Three different LGE sequences were acquired: a segmented, single-slice/single-breath-hold fast low angle shot PSIR sequence (FLASH-PSIR), a multi-slice balanced steady-state free precession inversion recovery sequence (bSSFP-IR) and a multi-slice bSSFP-PSIR sequence during breathhold and free breathing. Image quality was evaluated with a 4-point scoring system. Contrast-to-noise ratios (CNR) and acquisition time were evaluated. LGE was quantitatively assessed using a semi-automated threshold method. Differences in size of fibrosis were analyzed using Bland-Altman analysis.

(Continued on next page)

* Correspondence: fabian.muehlberg@gmail.com

¹Working Group on Cardiovascular Magnetic Resonance, Experimental and Clinical Research Center - a joint cooperation between the Charité Medical Faculty and the Max-Delbrück Center for Molecular Medicine and HELIOS Hospital Berlin-Buch, Department of Cardiology and Nephrology, Lindenberger Weg 80, 13125 Berlin, Germany

Full list of author information is available at the end of the article

(Continued from previous page)

Results: Three hundred twelve patients were enrolled ($n = 212$ chronic infarction, $n = 47$ inflammatory myocardial disease, $n = 53$ HCM). Of which 201 patients (67.4%) had detectable LGE ($n = 143$ with chronic infarction, $n = 27$ with inflammatory heart disease and $n = 31$ with HCM). Image quality and CNR were best on multi-slice bSSFP-PSIR. Acquisition times were significantly shorter for all multi-slice sequences (bSSFP-IR: 23.4 ± 7.2 s; bSSFP-PSIR: 21.9 ± 6.4 s) as compared to FLASH-PSIR (361.5 ± 95.33 s). There was no significant difference of mean LGE size for all sequences in all study groups (FLASH-PSIR: 8.96 ± 10.64 g; bSSFP-IR: 8.69 ± 10.75 g; bSSFP-PSIR: 9.05 ± 10.84 g; bSSFP-PSIR free breathing: 8.85 ± 10.71 g, $p > 0.05$).

LGE size was not affected by arrhythmia or absence of breathhold on multi-slice LGE sequences.

Conclusions: Fast multi-slice and standard segmented LGE sequences are equivalent techniques for the assessment of myocardial fibrosis, independent of an ischemic or non-ischemic etiology. Even in patients with arrhythmia and insufficient breathhold capability, multi-slice sequences yield excellent image quality at significantly reduced scan time and may be used as standard LGE approach.

Trial registration: [ISRCTN48802295](#) (retrospectively registered).

Keywords: Cardiac MR, CMR, Late gadolinium enhancement, Single-shot, Hypertrophic cardiomyopathy, Myocardial infarction, Inflammatory heart disease, Myocarditis

Background

Late gadolinium enhancement (LGE) cardiovascular magnetic resonance (CMR) is a well-established method for assessment of focal myocardial fibrosis and scarring in ischemic and non-ischemic cardiomyopathies [1–4]. The presence and extent of LGE has been shown to be associated with worse patient outcome in a variety of diseases, i.e. myocardial infarction, hypertrophic cardiomyopathy (HCM) and acute or chronic inflammatory heart disease [5–7]. Hence, the assessment of LGE is integrated into many clinical guidelines and is an integral part of most contrast-based CMR protocols [8–10].

The reference standard technique for LGE assessment is typically based on phase-sensitive inversion recovery (PSIR) sequences that are acquired in a single-slice, single-breathhold fashion [11, 12]. These segmented PSIR LGE images generate excellent image quality at a high spatial resolution if the individual patient has sufficient breathhold capabilities and is in sinus rhythm [13].

However, with the more widespread use of CMR in clinical routine increasing numbers of patients referred for CMR present with arrhythmias or an inability for sufficient breathhold for CMR scan. In these patients, conservative segmented PSIR LGE sequences sometimes fail to provide satisfactory image quality for accurate assessment.

Furthermore, standard segmented LGE sequences typically require 5 to 10 min of scan time for complete myocardial coverage. There is a need for faster and more efficient imaging in CMR in order to enable a more wide-spread use of CMR in clinical routine as well as in smaller institutions where access to CMR scanners maybe more restricted [14]. CMR also competes with other non-invasive imaging techniques in terms of scan time optimization leading to efforts for faster standardized CMR scan protocols [15].

In order to address these issues, multi-slice LGE sequences have been developed with acquisition of the entire k-space of an individual image slice within one heart cycle [16]. Different approaches utilize navigator-based, free breathing sequencing which works without breathhold but mostly still requires stable heart rhythm for optimal image quality [17].

Several small clinical studies have shown that multi-slice LGE sequences provide similar image quality to standard segmented LGE sequences [18, 19]. However, the vast majority of these studies investigated only patients with a single disease entity, i.e. myocardial infarction or HCM and/or excluded patients with arrhythmia. Hence, these studies are not reflecting clinical reality where the underlying cause of LGE is often not known prior to the CMR scan and sinus rhythm is often unstable or non-existent.

In this prospective study we intended to determine the comparability of standard segmented PSIR LGE imaging with two different multi-slice LGE sequences with and without breathhold in a large number of patients with ischemic and non-ischemic cardiomyopathy, namely chronic myocardial infarction, HCM and inflammatory heart disease. Furthermore, we explicitly did not exclude patients with arrhythmia. We aimed to assess if multi-slice LGE sequences represent a robust alternative for LGE assessment independent of pathophysiologic origin of LGE, heart rhythm and patient breathhold capabilities.

Methods

Study population

312 consecutive patients with known or suspected LGE were prospectively recruited. All patients were referred for clinical LGE assessment using CMR for both, ischemic and non-ischemic cardiomyopathies, based on the

clinical information provided by the referring cardiologist. A total of 212 patients had chronic myocardial infarction, 53 patients had HCM and 47 patients had inflammatory heart disease.

All patients underwent a single CMR scan with three different LGE sequences. Exclusion criteria were contraindications to CMR and severe chronic renal disease with an estimated glomerular filtration rate $< 30 \text{ ml/min}/1.73\text{m}^2$. All studies were performed in accordance with the local institutional review board and local ethics committee approval.

Image protocol

All CMR studies were performed on a 1.5 Tesla scanner (AvantoFit®, Siemens Healthineers, Erlangen, Germany). Patients were scanned with electrocardiogram (ECG)-triggering in the supine position using 16-channel surface phased array coils.

All imaging protocols included assessment of myocardial function in balanced steady-state free precession (bSSFP) cine sequences and of myocardial morphology by LGE imaging.

bSSFP cine imaging (TE 1.19 ms, TR 33.36 ms, flip angle 55°, retrospective ECG-triggered gating, matrix 192x156mm, FOV 340 mm, slice thickness 6 mm, bandwidth 930 Hz, 30 phases per heart cycle, iPAT GRAPPA acceleration factor 2) was performed in long axis two- and four-chamber view for biplanar assessment of left ventricular (LV) end-diastolic volume (LVEDV), LV mass (LVM) and LV ejection fraction (LVEF). Contours were drawn manually and biplanar anatomical and functional parameters calculated automatically by the post-processing software according to an established in-line biplane ellipsoid model. [20] The standard three-point method was used on short axis localizers to define standardized long axis two-chamber (one point in the LV apex, one point in the anterior and one point in the inferior wall of the LV myocardium in the slice with the maximum LV area) and four-chamber view (one point in the LV apex, one point in the interatrial septum below the aorta and one point into the most lateral corner of the right ventricle (RV) on the short axis localizer with the maximum RV area).

For LGE imaging, a 0.2 mmol/kg intravenous injection of contrast agent was administered into an antecubital vein. In patients with myocardial infarction or HCM assessment gadoteridol (ProHance®, Bracco S.p.A., Milan, Italy) was used. For patient with known or suspected inflammatory heart disease gadopentetate (Magnevist®, Bayer Healthcare, Wayne, New Jersey, USA) was administered due to established normal values for this contrast agent for the early enhancement technique which was clinically assessed in these patients independently from this study [21].

Ten minutes after contrast administration, a segmented IR cine bSSFP inversion time (TI) scouting sequence was performed at a mid-ventricular short axis location to determine optimal TI [22]. TI was adapted to optimally null the signal of the remote myocardium. Two-dimensional LGE images were acquired in short-axis views covering the entire LV myocardium by using three different LGE sequences: i) a segmented, single-slice, single-breathhold 2D FLASH-based phase-sensitive inversion recovery sequence (FLASH-PSIR) which was considered as the reference standard; ii) a multi-slice 2D bSSFP-based inversion recovery sequence (bSSFP-IR); iii) a multi-slice 2D bSSFP-based PSIR sequence (bSSFP-PSIR).

Sequence details are displayed in Table 1.

All LGE sequences were acquired in end-expiratory breathhold while the bSSFP-PSIR sequence was additionally acquired in free breathing. In case of suspected artifacts in the LGE images a second perpendicular slice through the affected region was acquired or read-out of the phase encoding direction was swapped. Segmented and multi-slice LGE images were acquired in random order. Acquisition times and occurrence of arrhythmia during image acquisition were noted for all sequences.

Qualitative and quantitative image analysis

For all post-processing analyses commercially available software was used (CVI42 Release 5.6.2, Circle Cardiovascular Imaging, Calgary, Canada). A blinded reader performed LV function assessment in bSSFP cine long axis slices. For assessment of LVEF endocardial contours were drawn in the end-diastolic and end-systolic phase of two- and four-chamber view. All parameters were automatically calculated after contouring by the post-processing software. Separately, image quality and quantitative LGE assessment were performed in a random and blinded order.

For 30 randomly selected individuals, the same reader and a second experienced reader repeated analyses for assessment of intra- and interobserver variability.

Image quality

Visual assessment of image quality was performed on all LGE sequences for each patient using a previously established 4-point-scale using the following grading: excellent quality, no artifacts (score of 1); good quality, minimal artifacts (score of 2); moderate quality, some artifacts which may impair diagnostic quality (score of 3); poor quality, unacceptable artifacts (score of 4) [19].

Signal intensities were measured in regions of interest (ROIs) that covered areas of contrast-enhanced myocardium, as well as areas of remote non-enhanced myocardium with an additional ROI located outside the patient for calculation of background noise. Signal enhancement was measured as recommended by Simonetti et al. [12].

Table 1 LGE sequence parameters

		FLASH-PSIR	SSFP-IR	SSFP-PSIR
Mode		Segmented	Multi-slice (single shot)	Multi-slice (single shot)
TE	[ms]	5.17	1.06	1.05
Flip Angle		30°	50°	65°
Field of view	[mm]	350–450	350–450	350–450
Matrix	[mm]	192 × 256	154 × 192	144 × 192
Slice thickness	[mm]	7	7	7
Slice gap	[mm]	0	0	0

TE Echo time

In detail, we calculated signal intensities and their standard deviations in ROIs of LGE-positive myocardium, as well as areas of remote myocardium. Contrast was defined as difference between mean signal intensity of both ROIs. Image noise was defined as the standard deviation of the signal intensity in the normal-appearing myocardium ROI. Contrast-to-noise ratios (CNR) were calculated by using these values. Measurement of signal-to-noise ratios (SNR) is limited on PSIR images conventionally because the measurement of background noise is invalid in the reconstructed images [23]. Therefore, we did not perform SNR assessment.

Visual LGE assessment

The distribution area and transmurality of fibrosis was evaluated according to the American Heart Association (AHA) 16-segment model. The distribution area of scar in each segment was scored by the proportion of scar to each segment (0: no LGE, 1: 1–25%, 2: 26–50%, 3: 51–75%, 4: 76–100%).

For each subject, the number of segments with presence or absence of fibrosis and location within the myocardial wall (subendocardial, intramural, subepicardial, transmural) was noted for each LGE sequence as previously described [24].

Quantitative LGE assessment

Quantification of LGE was performed with the established semi-automated signal threshold versus reference mean (STRM) method as published previously by our and other groups [21, 25, 26]. On all LGE images, endocardial and epicardial contours were manually traced and ROIs were defined in hyperenhanced and remote myocardium.

True LGE was defined by myocardial signal intensity plus 6 standard deviations (SD) above that of remote, normal-appearing myocardium within the same slice in patients with myocardial infarction. For subjects with HCM and inflammatory heart disease, plus 3 SDs were defined as true LGE [27].

The automated LGE detection could be manually corrected by the reader for a specific location to exclude obvious artifacts. After segmentation, myocardial and scar tissue mass (in grams) were calculated and compared for each AHA segment in each sequence.

Statistical analysis

All statistical analyses were conducted by using statistical software package SPSS 17.0 (International Business Machines, Armonk, New York, USA). Quantitative data are expressed as means ± SD. Sample size was calculated by using power analysis for two proportions to reach a statistical power of more than 80% to detect differences of 5%, using the assumption of 16 ± 12 g scar tissue for patients with chronic myocardial infarction, and 9 ± 5 g for HCM and inflammatory heart disease which were reported previously by our group [26].

Image quality scores were compared by using the Mann-Whitney U test. Interobserver and intraobserver agreement was assessed by using Cohen k statistics.

Statistical comparison of means of LGE size in each individual multi-slice technique against the segmented reference standard technique was performed by using two-tailed paired t tests and Bland-Altman analysis. Scar tissue percentages per segment, CNR and signal enhancement ratios were assessed using the Wilcoxon signed rank test, as these values did not show normal distribution.

Results

Patient characteristics

In total, 312 patients were recruited. Fourteen of these patients were excluded due to incomplete image acquisition. All remaining 298 patients were successfully scanned using all techniques and were included in subsequent analyses (203 patients with chronic myocardial infarction, 50 patients with HCM and 45 patients with inflammatory heart disease). Patient characteristics are shown in Table 2. Study individuals with inflammatory heart disease were significantly younger than patients in the other groups. HCM patients had an increased LVM index (LVM-I), decreased LVEDV index (LVEDV-I) and a slightly elevated LVEF. Figure 1 shows representative images of LGE short axis slices for each group and each sequence.

Acquisition time

The average scan time was significantly longer for the reference standard sequence (361.5 ± 95.3 s including breaks between slice acquisitions) than for any multi-slice sequence (SSFP-IR: 23.4 ± 7.2 s; SSFP-PSIR: 21.9 ± 6.4 s, $p < 0.01$ of all sequences against reference standard).

Table 2 Patient Characteristics

	Chronic myocardial infarction	HCM	Inflammatory heart disease
Number of patients	203	50	45
Gender [♂ / ♀]	160 / 43 (78% / 22%)	35 / 15 (72% / 28%)	32 / 13 (71% / 29%)
Age [years]	66.2 ± 10.7	62.0 ± 14.5	46.3 ± 15.4 *
BMI [kg/m ²]	27.6 ± 4.2	27.9 ± 4.3	25.8 ± 4.8
HR [min ⁻¹]	68.1 ± 11.5	69.8 ± 16.2	72.2 ± 12.9
LVEF [%]	52.9 ± 10.7	63.0 ± 10.9 *	52.6 ± 13.3
LVEDV-I [ml/m ²]	82.5 ± 24.3	69.6 ± 22.1 *	90.9 ± 26.9
SV-I [ml/m ²]	41.9 ± 8.7	43.3 ± 12.6	44.8 ± 8.9
LVM-I [g/m ²]	59.3 ± 15.8	89.5 ± 28.4 *	61.9 ± 17.2
SR / Arrhythmia	166 / 37 (82% / 18%)	39 / 11 (78% / 22%)	38 / 7 (84% / 16%)
LGE detected [yes / no]	176 / 27 (87% / 13%)	39 / 11 (78% / 22%)	32 / 13 (71% / 29%)

HCM Hypertrophic cardiomyopathy; BMI Body mass index; HR Heart rate; LVEF Left ventricular ejection fraction; LVEDV-I Left ventricular end-diastolic volume index; SV-I Stroke volume index; LVM-I Left ventricular mass index. SR Sinus rhythm. * p < 0.05

Image quality assessment

Image quality scores differed significantly between each multi-slice and the reference standard sequence. However, they were not influenced by disease entity or – regarding bSSFP-PSIR sequence – breathhold versus free breathing acquisition. Overall, bSSFP-PSIR images showed the best image quality scores. (Fig. 2).

Arrhythmia had a negative impact on image quality scores on the segmented FLASH-PSIR sequence, resulting in poor or non-diagnostic image quality in 48,8% of all patients. Image quality score was not influenced by arrhythmia in any multi-slice sequence.

Assessment of infarcted-to-remote area CNR is shown in Table 3. Mean infarcted-to-remote myocardium CNR was significantly higher on bSSFP-PSIR than on reference standard sequences ($p < 0.01$), and on bSSFP-IR lower than reference standard ($p < 0.01$). Free breathing acquisition of bSSFP-PSIR slightly decreased mean infarcted-to-remote area CNR as compared to acquisition under breathhold, however, was still superior to reference standard ($p < 0.01$). LGE due to chronic infarction showed significantly higher CNR values in all sequences than LGE due to HCM or inflammatory heart disease ($p < 0.01$).

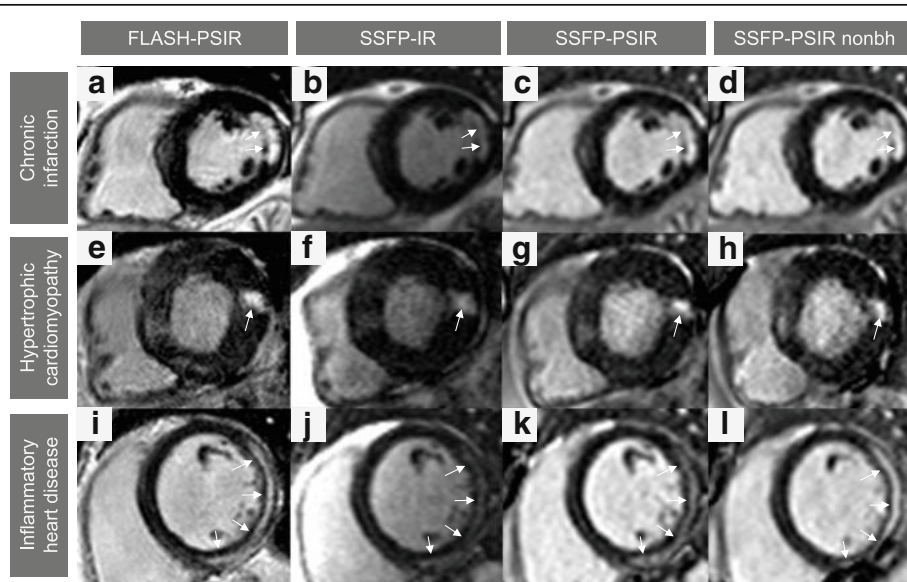


Fig. 1 Representative LGE images. Three selected patients with chronic myocardial infarction (a-d), hypertrophic cardiomyopathy (e-h) and acute myocarditis (i-l) with typical LGE localization: subendocardial for infarction, patchy intramural for HCM and subepicardial for myocarditis. Horizontal rows display corresponding slices of LGE in the same patient, vertical columns show the used techniques: conventional segmented FLASH-PSIR (a,e,i), multi-slice bSSFP-IR (b,f,j), multi-slice bSSFP-PSIR with breathhold (c,g,k) and free-breathing multi-slice bSSFP-IR (d,h,l). nonbh = non-breathhold

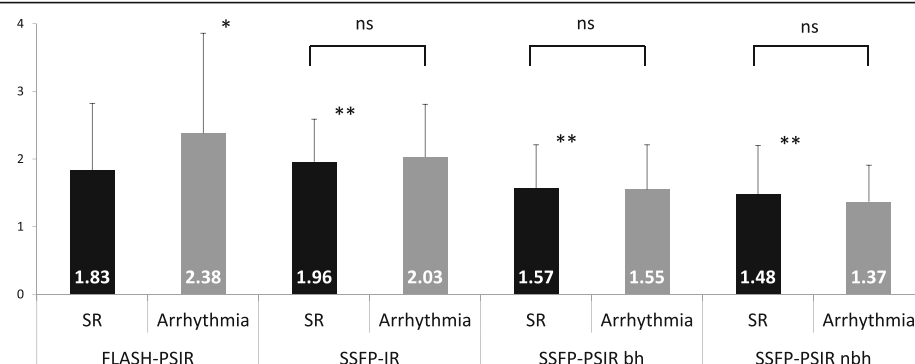


Fig. 2 Image quality scores. Values represent average image quality score for all patients in each group. Score system: 1 = excellent quality, no artifacts; 2 = good quality, minimal artifacts; 3 = moderate quality, some artifacts which may impair diagnostic quality; 4 = poor quality, unacceptable artifacts. * $p < 0.05$ within sequence. ** $p < 0.05$ towards FLASH-PSIR. ns = non-significant, $p > 0.05$. SR = sinus rhythm

Qualitative LGE analysis

Using reference standard sequence, 201 patients (67.4%) had detectable LGE ($n = 143$ with chronic infarction, $n = 31$ with HCM and $n = 27$ with inflammatory heart disease). All 201 LGE-positive patients also had detectable LGE on bSSFP-IR. With both bSSFP-PSIR sequences, two small LGE lesions (< 1 g scar size) were visually not detected in one patient with chronic infarction and one patient with HCM by two blinded readers.

On visual assessment, circumferential extent of scars was similar in all sequences; summation of scores showed excellent matching with reference standard FLASH-PSIR sequence (total score 3875) for bSSFP-PSIR with (total score 3903) and without breathhold (total score 3886) while on bSSFP-IR circumferential scar extent was slightly underestimated (total score 3726). Details are shown in Fig. 3a.

On all multi-slice sequences, the visual allocation of LGE within the myocardial wall (subendocardial, subepicardial, intramural, transmural) showed good matching with FLASH-PSIR for the chronic infarction and inflammatory heart disease group while for inflammatory heart disease there was a higher number of visually transmural LGE areas on bSSFP-PSIR versus FLASH-PSIR (14% versus 10% segments with transmural LGE, see Fig. 3b).

Quantitative LGE analysis

There were no significant differences in mean LGE size between reference standard FLASH-PSIR and multi-slice

sequences independent from LGE origin (Table 4). However, Bland-Altman analysis showed that on bSSFP-PSIR LGE size showed a non-significant trend to be smaller in all study groups compared to reference standard - mean difference in LGE size towards reference standard being 0.58 ± 1.99 g on bSSFP-PSIR with breathhold, 0.96 ± 2.03 g on bSSFP-PSIR with free breathing and 0.26 ± 2.4 g on bSSFP-IR (see Fig. 4 for Bland-Altman plots).

The presence or absence of breathhold during LGE imaging using bSSFP-PSIR had no impact on LGE size for any disease entity (Table 4).

Intraobserver agreement (Pearson coefficient) on LGE size was > 0.95 for all sequences. Interobserver agreement was 0.92 for bSSFP-PSIR under free breathing and 0.88 for all other sequences.

In patients with arrhythmia during image acquisition mean LGE size did not differ in any multi-slice sequence, with bSSFP-IR 7.6 ± 6.1 g and bSSFP-PSIR 7.7 ± 5.6 g under breathhold and 7.4 ± 5.6 g under free breathing. Reference standard FLASH-PSIR sequence was not evaluated in arrhythmic patients due to mostly non-diagnostic image quality.

Discussion

The present study compared for the first time a reference standard segmented (FLASH-PSIR) with two multi-slice LGE sequences (bSSFP-IR and bSSFP-PSIR) in 298 patients with ischemic and non-ischemic cardiomyopathies.

Table 3 Contrast-to-noise ratios

	All groups	Chronic infarction	HCM	Inflammatory heart disease
FLASH-PSIR	65.9 ± 71.9	$67.9 \pm 58.5^*$	80.4 ± 126.8	$37.0 \pm 21.3^*$
SSFP-IR	$40.1 \pm 26.8^\dagger$	$43.2 \pm 28.4^* \dagger$	$38.5 \pm 19.9^\dagger$	$31.5 \pm 22.2^\dagger$
SSFP-PSIR	137.8 ± 103.7	$149.8 \pm 114.9^* \dagger$	$118.4 \pm 66.9^\dagger$	$95.7 \pm 49.2^* \dagger$
SSFP-PSIR nonbh	$125.9 \pm 72.5^\dagger$	$134.5 \pm 72.5^* \dagger$	$101.7 \pm 65.8^\dagger$	$109.0 \pm 73.4^\dagger$

* $p < 0.05$ towards the other disease entities for the individual LGE sequence. $\dagger p < 0.05$ towards FLASH-PSIR gold standard for individual disease entity

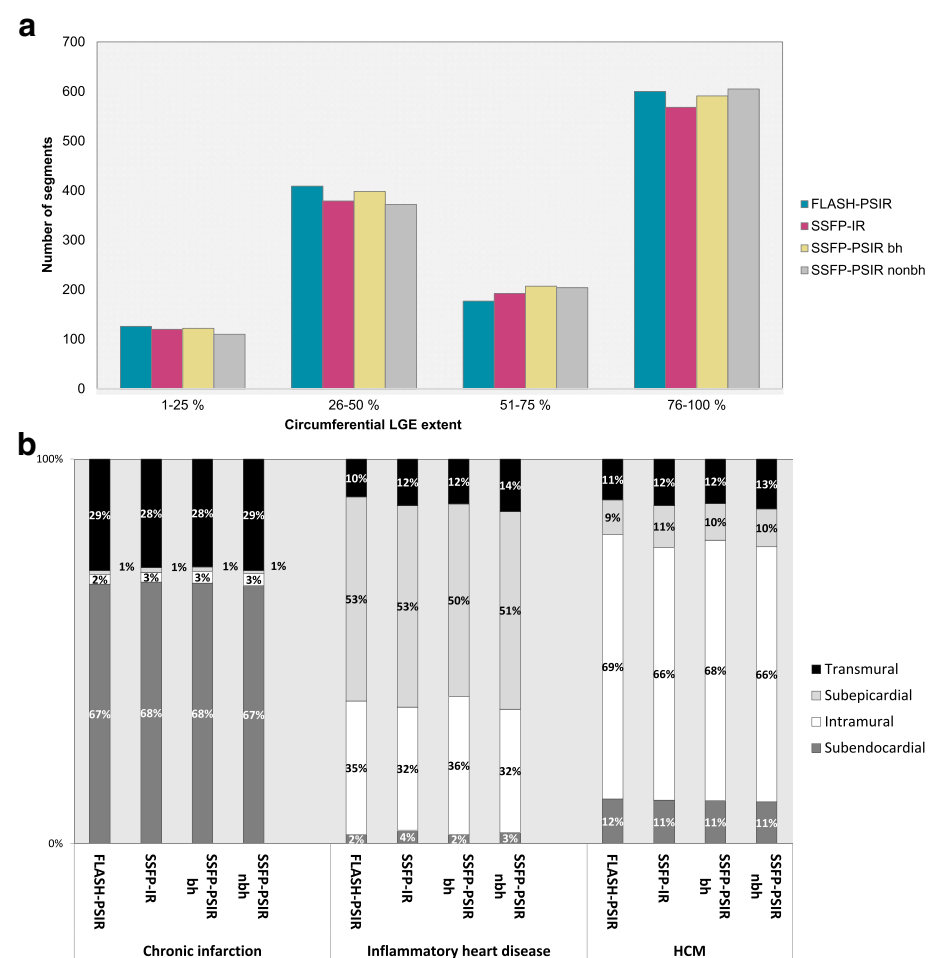


Fig. 3 Visual assessment of LGE. **a:** Visual assessment of circumferential LGE extent. Columns represent number of segments with LGE for different circumferential extents across all study groups (chronic myocardial infarctions, HCM, inflammatory heart disease). **b:** Visual assessment of in-wall LGE location

Our key findings were: Firstly, image quality and CNR were highest on multi-slice bSSFP-PSIR with and without breathhold. Secondly, acquisition time is relevantly shorter on any multi-slice sequence compared to reference standard. Thirdly, visual detection of LGE and visual assessment of LGE extent was consistently very good and equivalent in all sequences. Fourthly, quantification showed no significant difference in LGE size for any multi-slice sequence. Fifthly, in patients with arrhythmia all multi-slice sequences generated good image quality

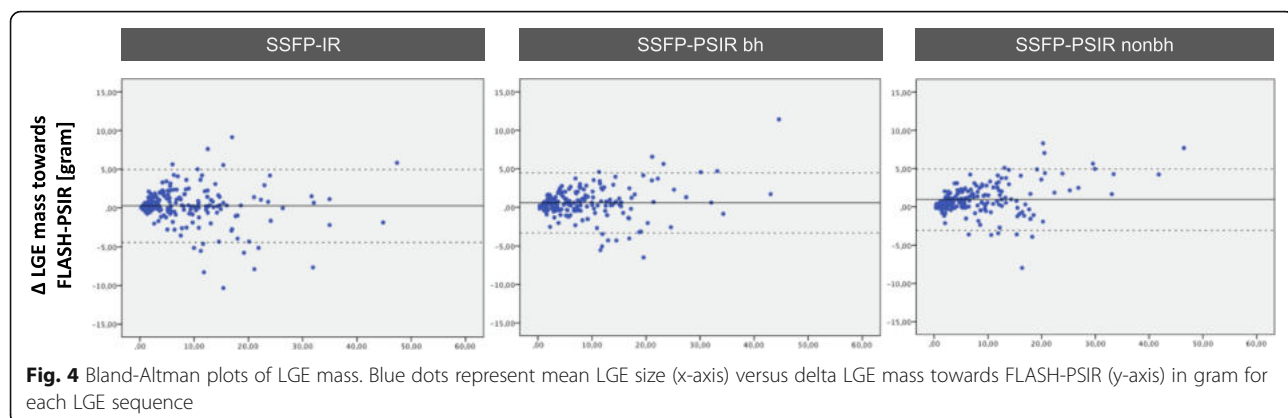
and consistent LGE quantification results, whereas the reference standard provided non-diagnostic image quality in half of all exams. Finally, acquisition of bSSFP-PSIR under free breathing or under breathhold had no impact on LGE detection and quantification. Results were independent of the cause of LGE from ischemic or non-ischemic etiology.

The assessment of myocardial fibrosis has enormous diagnostic and prognostic impact in ischemic and non-ischemic cardiomyopathy [5–7]. Over the last decade

Table 4 Quantitative Assessment - LGE size

	All groups	Chronic infarction	HCM	Inflammatory heart disease
FLASH-PSIR	8.96 ± 10.64 g	7.47 ± 6.65 g	15.42 ± 20.00 g	9.39 ± 10.28 g
SSFP-IR	8.69 ± 10.75 g	7.26 ± 7.03 g	15.31 ± 20.02 g	8.67 ± 9.66 g
SSFP-PSIR	9.05 ± 10.84 g	7.68 ± 7.18 g	15.51 ± 20.31 g	8.89 ± 9.30 g
SSFP-PSIR nonbh	8.85 ± 10.71 g	7.41 ± 6.91 g	15.38 ± 19.96 g	8.97 ± 9.94 g

Values represent mean LGE size in gram. P values for each multi-slice sequence compared to FLASH-PSIR in all study groups



many clinical studies have paved the way for CMR to be integrated into a variety of cardiologic, radiologic and other clinical guidelines [9]. The role of LGE in detection of myocardial fibrosis remains unequivocally important despite the development of new parametric mapping techniques, which play an increasing role especially in detection of diffuse fibrosis [28, 29].

Our study demonstrates that bSSFP-PSIR and bSSFP-IR multi-slice LGE sequences provide excellent alternatives to segmented FLASH-PSIR in routine CMR protocols. We showed that not only for ischemic LGE lesions but also for more diffuse lesions in inflammatory heart disease or HCM multi-slice sequences are sufficient to visualize fibrosis and – when quantified in size – show equivalent results compared to the reference standard. The equivalence of multi-slice LGE sequences to segmented sequences has previously been shown in studies for either HCM, ischemic or inflammatory heart disease [18, 19, 30]. However, these studies each used different sequences, smaller patient groups and mostly looked at single disease entities.

The superiority of multi-slice over segmented PSIR sequences in regard to image quality and CNR is in line with other publications [18, 19]. This is attributable to the reduction of motion artifacts and artifacts due to arrhythmia. CNR also depends on the amount of gadolinium-based contrast media in the myocardium, which is influenced by amount and molarity of contrast agent, distribution volume and hemodynamics. As we strictly dosed gadolinium to body weight and tested sequences in a random order, effects on results should be neglectable.

We have also seen variations in CNR between the different disease entities. Since CNR is dependent on the voxel composition of fibrotic tissue, LGE in chronic infarction with more compact fibrosis is expected to result in higher CNR values than LGE in more diffusely fibrotic tissue such as in HCM and inflammatory heart disease.

On bSSFP-PSIR sequence visual assessment revealed slightly larger scar transmurality as compared to the reference standard. We believe that visual assessment of bSSFP-PSIR images is impacted by its comparably higher CNR values which may lead to subjectively higher transmurality of scars.

In two patients, small LGE lesions detectable with the reference standard sequence, were not detected with multi-slice bSSFP-PSIR but, nevertheless, could be visualized with bSSFP-IR. Note that for these two patients LGE amount was less than one gram, which suggests that partial volume effects or shifted slice position due to heavy respiratory motion may have caused the missed lesion. However, it cannot be safely excluded that very small LGE lesions may be missed with multi-slice bSSFP-PSIR due to its different matrix size as compared to the reference standard.

It has been shown that even a small amount of LGE has prognostic implications in cardiomyopathies [31–34]. In case of inflammatory heart disease missed small subepicardial LGE may even impact diagnosis [35], as Lake Louise criteria define myocarditis as two out of three parameters, LGE being one of them [36].

Our results suggest that in patients with known or suspected myocardial infarction bSSFP-PSIR or bSSFP-IR multi-slice sequences can be primarily utilized for LGE detection. In case of an unknown cardiomyopathy or for assessment of HCM and inflammatory heart disease segmented FLASH-PSIR images should be used in scenarios of stable sinus rhythm and sufficient breathhold capabilities. For patients with arrhythmia and/or insufficient breathhold capabilities at the time of CMR scan we showed that segmented sequences fail to provide sufficient image quality. This is in line with previous studies [37, 38]. In these patients we suggest to primarily use multi-slice sequences such as bSSFP-PSIR and/or bSSFP-IR.

In this study two different contrast media were used; gadoteridol in CAD and HCM patients and

gadopentate for inflammatory heart disease. The reason for use of gadopentate was established normal values for relative enhancement sequences, which were acquired in these patients independently from this study. However, there is good evidence that relaxivity and contrast enhancement are nearly identical for both agents so that impact on results should be neglectable. [39]

In our study we explicitly did not exclude patients with arrhythmia. We demonstrated good to excellent image quality and equivalent amount of LGE quantification with all multi-slice sequences. There is no gold standard for LGE detection and quantification in arrhythmic patients. Hence, we cannot definitely state that results are perfectly correct using multi-slice sequences. Still, due to the consistently high image quality scores and – as compared to patients with sinus rhythm – similar CNR values we feel confident that usage of any multi-slice sequence is superior to attempts of segmented image acquisition and shortens scan protocols significantly in these patients.

Interestingly, presence or absence of breathhold during image acquisition on bSSFP-PSIR did not affect detection or quantification of LGE across all study groups. While there must be minimal slice shifting due to respiratory motion on acquisition of an entire LV short axis package within approximately 20 s of acquisition time we could show in a large number of patients that this has no statistically significant effect on diagnostic value. Lower numbers of breathhold cycles may also positively affect patient comfort and may be considered in all patients when SSFP-PSIR sequence is used.

Alternative methods for LGE assessment include 3D sequences, which have been shown to also accurately visualize fibrosis and scarring [40, 41]. These 3D sequences have the advantage of potentially higher spatial resolution, especially in the vertical axis, and the possibility of free movement through the ventricular myocardium. On the other hand, 3D sequences typically require a relatively long acquisition time. This necessitates a continuous adaptation of the optimal myocardial inversion time, which may impair image quality and CNR. Implementation of 3D LGE sequences with dynamic inversion time adjustments may help to overcome this obstacle [42].

In another recent study dark blood PSIR imaging was published using T2 preparation pulses for improved visualization of fibrosis close to the adjacent LV blood pool in 30 patients with subendocardial infarction [43]. This promising technique also included motion correction for acquisition under free breathing but needs to be validated across myocardial disease entities in larger studies.

Conclusions

LGE sequences are a mandatory part of most CMR protocols in ischemic and non-ischemic cardiomyopathy [8]. The broader spread of CMR in clinical routine has several implications: demand for CMR access increases and there is a continuous need for fast scanning protocols [14]. While segmented LGE sequences may give excellent image quality under stable sinus rhythm and sufficient breathhold the issue of time investment prevails. We demonstrated equivalence of multi-slice LGE sequences (bSSFP-IR and bSSFP-PSIR) and segmented FLASH-PSIR sequence in a large number of patients with ischemic and non-ischemic cardiac disease.

For that reason we suggest further strengthening the role of multi-slice sequences in routine CMR protocols whenever it is reliable to use.

Limitations

In spite of the large patient number in this study, all patients were scanned and analyzed in a single CMR center. Male gender was overrepresented in all study groups. Comparability of LGE sequences maybe impacted by different matrix size and, hence, different in-plane resolution used for each sequence. This may also affect SNR and CNR as well as assessment of LGE-positive areas.

Abbreviations

2D: Two-dimensional; AHA: American Heart Association; BMI: Body mass index; bSSFP: Balanced steady-state free precession; CMR: Cardiovascular magnetic resonance; CNR: Contrast-to-noise ratio; FLASH: Fast low angle shot; HCM: Hypertrophic cardiomyopathy; HR: Heart rate; IR: Inversion recovery; LGE: Late gadolinium enhancement; LV: Left ventricle/left ventricular; LVEDV: Left ventricular end-diastolic volume; LVEDV-I: Left ventricular end-diastolic volume index; LVEF: Left ventricular ejection fraction; LVM: Left ventricular mass; LVM-I: Left ventricular mass index; MR: Magnetic resonance; nbh: Non-breathhold (free breathing); PSIR: Phase-sensitive inversion recovery; ROI: Region-of-interest; RV: Right ventricle/right ventricular; SD: Standard deviation; SNR: Signal-to-noise ratio; SR: Sinus rhythm; STRM: Semi-automated signal threshold versus reference mean; SV-I: Stroke volume index; TE: Echo time; TI: Inversion time

Acknowledgements

We sincerely acknowledge the support of our CMR technicians Denise Kleindienst, Kerstin Kretschel and Evelyn Polzin as well as our study nurses Annette Köhler-Rohde and Elke Nickel-Szczech in conducting all study scans. We sincerely thank Carsten Schwenke PhD for his continuous support in matters of study statistics and power calculation throughout this study. We also acknowledge the help of Johannes Kuttner during internal manuscript review.

Consent for study participation

Study individuals have given their written consent for participating in this study.

Funding

No external funding has been received for the realization of this study.

Availability of data and materials

The datasets analyzed during the current study are available from the corresponding author upon reasonable request. Original imaging data are not publicly available due to lawful data protection in Germany.

Authors' contributions

FM developed study design, applied for ethic board approval, conducted major part of CMR scans, led image analysis and data interpretation and was the major contributor in writing the manuscript. KA conducted major parts of image analysis and statistical data interpretation. SiF was involved in image analysis and manuscript writing. StF was involved in image analysis and manuscript writing. MP conducted CMR scans and was involved in image analysis. JK was involved in image analysis and manuscript writing. LZ was involved in data analysis and manuscript writing. FK was involved in data analysis and manuscript writing. JS supervised overall study design, ensured quality control on image analysis and data interpretation, supervised manuscript writing and provided continuous guidance throughout study realization as head of the working group. All authors have read and approved the final manuscript.

Ethics approval and consent to participate

The study was approved by Charité University Medicine ethics board at Charité Campus Mitte, Berlin, Germany.

Consent for publication

Individuals have given their written consent for anonymous publication.

Competing interests

The authors declare that they have no competing interests.

Publisher's Note

Springer Nature remains neutral with regard to jurisdictional claims in published maps and institutional affiliations.

Author details

¹Working Group on Cardiovascular Magnetic Resonance, Experimental and Clinical Research Center - a joint cooperation between the Charité Medical Faculty and the Max-Delbrück Center for Molecular Medicine and HELIOS Hospital Berlin-Buch, Department of Cardiology and Nephrology, Lindenberger Weg 80, 13125 Berlin, Germany. ²Clinic Agatharied, Department of Cardiology, Ludwig-Maximilians-University Munich, Norbert-Kinkel-Platz, 83734, Hausham, Germany.

Received: 10 July 2017 Accepted: 5 February 2018

Published online: 19 February 2018

References

- Kim RJ, Wu E, Rafael a, Chen EL, Parker MA, Simonetti O, Klocke FJ, Bonow RO, Judd RM. the use of contrast-enhanced magnetic resonance imaging to identify reversible myocardial dysfunction. *N Engl J Med*. 2000;343(20):1445–53.
- Saeed M, Weber O, Lee R, Do L, Martin A, Saloner D, Ursell P, Robert P, Corot C, Higgins CB. Discrimination of myocardial acute and chronic (scar) infarctions on delayed contrast enhanced magnetic resonance imaging with intravascular magnetic resonance contrast media. *J Am Coll Cardiol*. 2006;48(10):1961–8.
- Bondarenko O, Beek AM, Nijveldt R, McCann GP, van Dockum WG, Hofman MB, Twisk JW, Visser CA, van Rossum AC. Functional outcome after revascularization in patients with chronic ischemic heart disease: a quantitative late gadolinium enhancement CMR study evaluating transmural scar extent, wall thickness and periprocedural necrosis. *Journal of cardiovascular magnetic resonance : official journal of the Society for Cardiovascular Magnetic Resonance*. 2007;9(5):815–21.
- Fluechter S, Kuschyk J, Wolpert C, Doesch C, Veltmann C, Haghj D, Schoenberg SO, Sueselbeck T, Germans T, Streitner F, et al. Extent of late gadolinium enhancement detected by cardiovascular magnetic resonance correlates with the inducibility of ventricular tachyarrhythmia in hypertrophic cardiomyopathy. *Journal of cardiovascular magnetic resonance : official journal of the Society for Cardiovascular Magnetic Resonance*. 2010;12:30.
- Adabag AS, Maron BJ, Appelbaum E, Harrigan CJ, Buros JL, Gibson CM, Lesser JR, Hanna CA, Udelson JE, Manning WJ, et al. Occurrence and frequency of arrhythmias in hypertrophic cardiomyopathy in relation to delayed enhancement on cardiovascular magnetic resonance. *J Am Coll Cardiol*. 2008;51(14):1369–74.
- Ise T, Hasegawa T, Morita Y, Yamada N, Funada A, Takahama H, Amaki M, Kanzaki H, Okamura H, Kamakura S, et al. Extensive late gadolinium enhancement on cardiovascular magnetic resonance predicts adverse outcomes and lack of improvement in LV function after steroid therapy in cardiac sarcoidosis. *Heart*. 2014;100(15):165–72.
- Neilan TG, Shah RV, Abbasi SA, Farhad H, Groarke JD, Dodson JA, Coelho-Filho O, McMullan CJ, Heydari B, Michaud GF, et al. The incidence, pattern, and prognostic value of left ventricular myocardial scar by late gadolinium enhancement in patients with atrial fibrillation. *J Am Coll Cardiol*. 2013; 62(23):2205–14.
- Kramer CM, Barkhausen J, Flamm SD, Kim RJ, Nagel E. Society For cardiovascular magnetic resonance Board of Trustees Task Force on standardized P: standardized cardiovascular magnetic resonance (CMR) protocols 2013 update. *Journal of cardiovascular magnetic resonance : official journal of the Society for Cardiovascular Magnetic Resonance*. 2013;15:91.
- von Knobelsdorff-Brenkenhoff F, Schulz-Menger J. Role of cardiovascular magnetic resonance in the guidelines of the European Society of Cardiology. *Journal of cardiovascular magnetic resonance : official journal of the Society for Cardiovascular Magnetic Resonance*. 2016;18:6.
- Ponikowski P, Voors AA, Anker SD, Bueno H, Cleland JG, Coats AJ, Falk V, Gonzalez-Juanatey JR, Harjola VP, Jankowska EA, et al. 2016 ESC guidelines for the diagnosis and treatment of acute and chronic heart failure. *Revista espanola de cardiologia*. 2016;69(12):1167.
- Kellman P, Arai AE, McVeigh ER, Aletras AH. Phase-sensitive inversion recovery for detecting myocardial infarction using gadolinium-delayed hyperenhancement. *Magnetic resonance in medicine : official journal of the Society of Magnetic Resonance in Medicine / Society of Magn Reson Med*. 2002;47(2):372–83.
- Simonetti OP, Kim RJ, Fieno DS, Hillenbrand HB, Wu E, Bundy JM, Finn JP, Judd RM. An improved MR imaging technique for the visualization of myocardial infarction. *Radiology*. 2001;218(1):215–23.
- Sievers B, Rehwald WG, Albert TS, Patel MR, Parker MA, Kim RJ, Judd RM. Respiratory motion and cardiac arrhythmia effects on diagnostic accuracy of myocardial delayed-enhanced MR imaging in canines. *Radiology*. 2008; 247(1):106–14.
- Muehlberg F, Neumann D, Von Knobelsdorff-Brenkenhoff F, Traber J, Alwardt N, Schulz-Menger J. A multicenter cardiovascular MR network for tele-training and beyond: setup and initial experiences. *Journal of the American College of Radiology : JACR*. 2015;12(8):876–83.
- Hendel RC, Friedrich MG, Schulz-Menger J, Zemmlrich C, Bengel F, Berman DS, Camici PG, Flamm SD, Le Guludec D, Kim R, et al. CMR first-pass perfusion for suspected inducible myocardial ischemia. *JACC Cardiovascular imaging*. 2016;9(11):1338–48.
- Sievers B, Elliott MD, Hurwitz LM, Albert TS, Klem I, Rehwald WG, Parker MA, Judd RM, Kim RJ. Rapid detection of myocardial infarction by subsecond, free-breathing delayed contrast-enhancement cardiovascular magnetic resonance. *Circulation*. 2007;115(2):236–44.
- Nguyen TD, Spincemaille P, Weinsaft JW, Ho BY, Cham MD, Prince MR, Wang Y. A fast navigator-gated 3D sequence for delayed enhancement MRI of the myocardium: comparison with breathhold 2D imaging. *Journal of magnetic resonance imaging : JMRI*. 2008;27(4):802–8.
- Viallon M, Jacquier A, Rotaru C, Delattre BM, Mewton N, Vincent F, Croisille P. Head-to-head comparison of eight late gadolinium-enhanced cardiac MR (LGE CMR) sequences at 1.5 tesla: from bench to bedside. *Journal of magnetic resonance imaging : JMRI*. 2011;34(6):1374–87.
- Morita K, Utsunomiya D, Oda S, Komi M, Namimoto T, Hirai T, Hashida M, Takashio S, Yamamoto M, Yamashita Y. Comparison of 3D phase-sensitive inversion-recovery and 2D inversion-recovery MRI at 3.0 T for the assessment of late gadolinium enhancement in patients with hypertrophic cardiomyopathy. *Acad Radiol*. 2013;20(6):752–7.
- Thiele H, Paetsch I, Schnackenburg B, Bornstedt A, Grebe O, Wellnhofer E, Schuler G, Fleck E, Nagel E. Improved accuracy of quantitative assessment of left ventricular volume and ejection fraction by geometric models with steady-state free precession. *Journal of cardiovascular magnetic resonance : official journal of the Society for Cardiovascular Magnetic Resonance*. 2002; 4(3):327–39.
- Rudolph A, Messroghli D, Von Knobelsdorff-Brenkenhoff F, Traber J, Schuler J, Wassmuth R, Schulz-Menger J. prospective, randomized comparison of gadopentetate and gadobutrol to assess chronic myocardial infarction applying cardiovascular magnetic resonance. *BMC Med Imaging*. 2015;15(1):55.

22. Gupta A, Lee VS, Chung YC, Babb JS, Simonetti OP. Myocardial infarction: optimization of inversion times at delayed contrast-enhanced MR imaging. *Radiology*. 2004;233(3):921–6.
23. Dietrich O, Raya JG, Reeder SB, Reiser MF, Schoenberg SO. Measurement of signal-to-noise ratios in MR images: influence of multichannel coils, parallel imaging, and reconstruction filters. *Journal of magnetic resonance imaging* : JMRI. 2007;26(2):375–85.
24. Kino A, Zuehlsdorff S, Sheehan JJ, Weale PJ, Carroll TJ, Jerecic R, Carr JC. Three-dimensional phase-sensitive inversion-recovery turbo FLASH sequence for the evaluation of left ventricular myocardial scar. *AJR Am J Roentgenol*. 2009;193(5):W381–8.
25. Bruder O, Wagner A, Jensen CJ, Schneider S, Ong P, Kispert EM, Nassenstein K, Schlosser T, Sabin GV, Sechtem U, et al. Myocardial scar visualized by cardiovascular magnetic resonance imaging predicts major adverse events in patients with hypertrophic cardiomyopathy. *J Am Coll Cardiol*. 2010; 56(11):875–87.
26. Rudolph A, Von Knobelsdorff-Brenkenhoff F, Wassmuth R, Prothmann M, Utz W, Schulz-Menger J. assessment of nonischemic fibrosis in hypertrophic cardiomyopathy: comparison of gadopentetate dimeglumine and gadobenate dimeglumine for enhanced cardiovascular magnetic resonance imaging. *Journal of magnetic resonance imaging* : JMRI. 2014;39(5):1153–60.
27. Mikami Y, Kolman L, Joncas SX, Stirrat J, Scholl D, Rajchl M, Lydell CP, Weeks SG, Howarth AG, White JA. Accuracy and reproducibility of semi-automated late gadolinium enhancement quantification techniques in patients with hypertrophic cardiomyopathy. *Journal of cardiovascular magnetic resonance : official journal of the Society for Cardiovascular Magnetic Resonance*. 2014;16:85.
28. Messroghli DR, Nordmeyer S, Dietrich T, Dirsch O, Kaschina E, Savvatis K, Dohl KC, Berger F, Kuehne T. assessment of diffuse myocardial fibrosis in rats using small-animal look-locker inversion recovery T1 mapping. *Circulation Cardiovascular imaging*. 2011;4(6):636–40.
29. Messroghli DR, Radjenovic A, Kozerke S, Higgins DM, Sivananthan MU, Ridgway JP. Modified look-locker inversion recovery (MOLLI) for high-resolution T1 mapping of the heart. *Magnetic resonance in medicine : official journal of the Society of Magnetic Resonance in Medicine / Society of Magn Reson Med*. 2004;52(1):141–6.
30. Kellman P, Larson AC, Hsu LY, Chung YC, Simonetti OP, McVeigh ER, Arai AE. Motion-corrected free-breathing delayed enhancement imaging of myocardial infarction. *Magn Reson Med*. 2005;53(1):194–200.
31. Mikami Y, Cornhill A, Heydari B, Joncas SX, Almehmadi F, Zahrani M, Bokhari M, Stirrat J, Yee R, Merchant N, et al. Objective criteria for septal fibrosis in non-ischemic dilated cardiomyopathy: validation for the prediction of future cardiovascular events. *Journal of cardiovascular magnetic resonance : official journal of the Society for Cardiovascular Magnetic Resonance*. 2016;18(1):82.
32. Lee SA, Yoon YE, Kim JE, Park JJ, Oh IY, Yoon CH, Suh JW, Kim JS, Chun EJ, Cho YS, et al. Long-term prognostic value of late gadolinium-enhanced magnetic resonance imaging in patients with and without left ventricular dysfunction undergoing coronary artery bypass grafting. *Am J Cardiol*. 2016; 118(11):1647–54.
33. Hulten E, Agarwal V, Cahill M, Cole G, Vita T, Parrish S, Bittencourt MS, Murthy VL, Kwong R, Di Carli MF, et al. Presence of late gadolinium enhancement by cardiac magnetic resonance among patients with suspected cardiac sarcoidosis is associated with adverse cardiovascular prognosis: a systematic review and meta-analysis. *Circulation Cardiovascular imaging*. 2016;9(9):e005001.
34. Chan RH, Maron BJ, Olivotto I, Pencina MJ, Assenza GE, Haas T, Lesser JR, Gruner C, Crean AM, Rakowski H, et al. Prognostic value of quantitative contrast-enhanced cardiovascular magnetic resonance for the evaluation of sudden death risk in patients with hypertrophic cardiomyopathy. *Circulation*. 2014;130(6):484–95.
35. Grun S, Schumm J, Greulich S, Wagner A, Schneider S, Bruder O, Kispert EM, Hill S, Ong P, Klingel K, et al. Long-term follow-up of biopsy-proven viral myocarditis: predictors of mortality and incomplete recovery. *J Am Coll Cardiol*. 2012;59(18):1604–15.
36. Friedrich MG, Sechtem U, Schulz-Menger J, Holmvang G, Alakija P, Cooper LT, White JA, Abdel-Aty H, Gutberlet M, Prasad S, et al. Cardiovascular magnetic resonance in myocarditis: a JACC white paper. *J Am Coll Cardiol*. 2009;53(17):1475–87.
37. Knowles BR, Caulfield D, Cooklin M, Rinaldi CA, Gill J, Bostock J, Razavi R, Schaeffter T, Rhode KS. 3-D visualization of acute RF ablation lesions using MRI for the simultaneous determination of the patterns of necrosis and edema. *IEEE Trans Biomed Eng*. 2010;57(6):1467–75.
38. Weingartner S, Akcakaya M, Basha T, Kissinger KV, Goddu B, Berg S, Manning WJ, Nezafat R. Combined saturation/inversion recovery sequences for improved evaluation of scar and diffuse fibrosis in patients with arrhythmia or heart rate variability. *Magn Reson Med*. 2014;71(3):1024–34.
39. Rinck PA, Muller RN. Field strength and dose dependence of contrast enhancement by gadolinium-based MR contrast agents. *Eur Radiol*. 1999; 9(5):998–1004.
40. Kido T, Kido T, Nakamura M, Kawaguchi N, Nishiyama Y, Ogimoto A, Miyagawa M, Mochizuki T. Three-dimensional phase-sensitive inversion recovery sequencing in the evaluation of left ventricular myocardial scars in ischemic and non-ischemic cardiomyopathy: comparison to three-dimensional inversion recovery sequencing. *Eur J Radiol*. 2014;83(12):2159–66.
41. Morsbach F, Gordic S, Gruner C, Niemann M, Goetti R, Gotschy A, Kozerke S, Alkadhi H, Manka R. Quantitative comparison of 2D and 3D late gadolinium enhancement MR imaging in patients with Fabry disease and hypertrophic cardiomyopathy. *Int J Cardiol*. 2016;217:167–73.
42. Keegan J, Gatehouse PD, Haldar S, Wage R, Babu-Narayan SV, Firmin DN. Dynamic inversion time for improved 3D late gadolinium enhancement imaging in patients with atrial fibrillation. *Magnetic resonance in medicine : official journal of the Society of Magnetic Resonance in Medicine / Society of Magn Reson Med*. 2015;73(2):646–54.
43. Kellman P, Xue H, Olivier LJ, Cross RR, Grant EK, Fontana M, Ugander M, Moon JC, Hansen MS. Dark blood late enhancement imaging. *Journal of cardiovascular magnetic resonance : official journal of the Society for Cardiovascular Magnetic Resonance*. 2016;18(1):77.

Submit your next manuscript to BioMed Central and we will help you at every step:

- We accept pre-submission inquiries
- Our selector tool helps you to find the most relevant journal
- We provide round the clock customer support
- Convenient online submission
- Thorough peer review
- Inclusion in PubMed and all major indexing services
- Maximum visibility for your research

Submit your manuscript at
www.biomedcentral.com/submit



Lebenslauf

Mein Lebenslauf wird aus datenschutzrechtlichen Gründen in der elektronischen Version meiner Arbeit nicht veröffentlicht.

Publikationsliste

Artikel in wissenschaftlichen Fachzeitschriften (Peer-Review)

1. **Kermer J**, Traber J, Utz W, Hennig P, Menza M, Jung B, Greiser A, Barckow P, von Knobelsdorff-Brenkenhoff F, Töpper A, Blaszczyk E, Schulz-Menger J. Assessment of diastolic dysfunction: comparison of different cardiovascular magnetic resonance techniques. *ESC Heart Failure*. 2020;7(5):2637-49.
Journal Impactfactor 2019: 3,902
2. Funk S, **Kermer J**, Doganguezel S, Schwenke C, von Knobelsdorff-Brenkenhoff F, Schulz-Menger J. Quantification of the left atrium applying cardiovascular magnetic resonance in clinical routine. *Scandinavian cardiovascular journal : SCJ*. 2018;1-8.
Journal Impactfactor 2019: 1,084
3. Muehlberg F, Arnhold K, Fritschi S, Funk S, Prothmann M, **Kermer J**, Zange L, von Knobelsdorff-Brenkenhoff F, Schulz-Menger J. Comparison of fast multi-slice and standard segmented techniques for detection of late gadolinium enhancement in ischemic and non-ischemic cardiomyopathy – a prospective clinical cardiovascular magnetic resonance trial. *Journal of cardiovascular magnetic resonance : official journal of the Society for Cardiovascular Magnetic Resonance*. 2018;20.
Journal Impactfactor 2019: 5,361

Posterpräsentation (wissenschaftlicher Kongress)

Kermer J, Traber J, Utz W, Henning P, Menza M, Jung B, Greiser A, Kuijer J, Barckow P, von Knobelsdorff-Brenkenhoff F, Töpper A, Schulz-Menger J. Assessing diastolic function applying Cardiovascular Magnetic Resonance - comparison with the gold standard. Proc. 13th Annual CMR, Congress of the European Association of Cardiovascular Imaging (EACVI) of the ESC 2016, Florence, Italy

Danksagung

Als erstes möchte ich mich bei meiner Doktormutter Frau Prof. Dr. Jeanette Schulz-Menger bedanken, welche mir die Arbeit an diesem Forschungsprojekt ermöglicht hat. Ich danke ihr neben der verlässlichen und hervorragenden fachlichen Betreuung vor allem dafür, mich stets unterstützt, motiviert, gefördert und mit ihrer Neugier und Wissbegierde inspiriert zu haben.

Darüber hinaus geht ein ganz besonderer Dank an die Probandinnen und Probanden, ohne deren Teilnahme und Offenheit für die Forschung keine der vorliegenden Studien möglich gewesen wäre.

Sehr dankbar bin ich ebenso für all die Unterstützung und kritisch konstruktiven Diskussionen, welche ich durch die Koautorinnen und Koautoren sowie das gesamte Team der Arbeitsgruppe „Kardiale MRT“ erfahren durfte. Besonders möchte ich hierbei Dr. Julius Traber, Dr. Edyta Blaszczyk und Dr. Stephanie Wiesemann hervorheben, welche mir bei jeglicher Fragestellung zur Seite standen. Herzlich danke ich auch den medizinisch-technischen Radiologieassistentinnen Denise Kleindienst, Kerstin Kretschel und Evelyn Polzin, deren akkurate Bildakquise die Basis der erhobenen Daten darstellt und deren engagiertes Organisationsmanagement jegliche Untersuchungen auch bei noch so vollem Scanprogramm ermöglichte. Ich möchte mich zudem für die Hilfe und Anleitung durch die Studienschwestern Annette Köhler und Elke Nickel bedanken.

Vielen Dank auch an die Statistiker Susanne Schwenke und Dr. Carsten Schwenke, welche die statistischen Überlegungen und Auswertungen durch ihre geduldige und lehrreiche Art bereichert haben.

Ein großer Dank geht zu guter Letzt an meine Familie und Freunde, die stets hinter mir standen und auf deren Unterstützung ich jederzeit bauen konnte. Vor allem meinem guten Freund und treuen Wegbegleiter Maximilian Berger möchte ich dabei danken – er hat mich erst auf die Arbeitsgruppe der kardialen MRT aufmerksam gemacht, mit mir große und kleine Fragen rund um die Doktorarbeit diskutiert und mich jederzeit bestärkt, meine Ideen und Wünsche konsequent zu verfolgen.